

MICROCOPY RESOLUTION TEST CHART
NATIONAL BUREAU OF STANDARDS-1963-A

2

NAVAL POSTGRADUATE SCHOOL

Monterey, California

AD-A143 164



DTIC
ELECTE
JUL 18 1984
S B

THESIS

SUPERPLASTICITY IN THERMOMECHANICALLY
PROCESSED HIGH MAGNESIUM ALUMINUM-MAGNESIUM ALLOYS

by

John J. Becker

March 1984

Thesis Advisor:

T. R. McNeley

Approved for public release; distribution unlimited.

DTIC FILE COPY

84 07 11 027

Unclassified

SECURITY CLASSIFICATION OF THIS PAGE (When Data Entered)

REPORT DOCUMENTATION PAGE		READ INSTRUCTIONS BEFORE COMPLETING FORM	
1. REPORT NUMBER	2. GOVT ACCESSION NO. A163164	3. RECIPIENT'S CATALOG NUMBER	
4. TITLE (and Subtitle) Superplasticity in Thermomechanically Processed High Magnesium Aluminum- Magnesium Alloys		5. TYPE OF REPORT & PERIOD COVERED Master's Thesis; March 1984	
		6. PERFORMING ORG. REPORT NUMBER	
7. AUTHOR(s) John J. Becker		8. CONTRACT OR GRANT NUMBER(s)	
9. PERFORMING ORGANIZATION NAME AND ADDRESS Naval Postgraduate School Monterey, California 93943		10. PROGRAM ELEMENT, PROJECT, TASK AREA & WORK UNIT NUMBERS	
11. CONTROLLING OFFICE NAME AND ADDRESS Naval Postgraduate School Monterey, California 93943		12. REPORT DATE March 1984	
		13. NUMBER OF PAGES 98	
14. MONITORING AGENCY NAME & ADDRESS (if different from Controlling Office)		15. SECURITY CLASS. (of this report) Unclassified	
		15a. DECLASSIFICATION/DOWNGRADING SCHEDULE	
16. DISTRIBUTION STATEMENT (of this Report) Approved for public release; distribution unlimited.			
17. DISTRIBUTION STATEMENT (of the abstract entered in Block 20, if different from Report)			
18. SUPPLEMENTARY NOTES			
19. KEY WORDS (Continue on reverse side if necessary and identify by block number) Superplasticity; Aluminum; Aluminum-Magnesium; Thermomechanical Processing; Rolling; Annealing; Recrystallization; Grain Refinement.			
20. ABSTRACT (Continue on reverse side if necessary and identify by block number) — The elevated temperature deformation characteristics of two thermo- mechanically processed high magnesium, aluminum-magnesium alloys were investigated. The thermomechanical processing itself included warm rolling at 300°C to 94% reduction. Subsequent treatments included annealing after rolling for either one-half hour or ten hours at 300°C, or one half hour at 440°C. These annealing treatments resulted in — <i>one</i>			

DD FORM 1473
1 JAN 73

EDITION OF 1 NOV 68 IS OBSOLETE
S/N 0102-LF-014-6601

Unclassified
1 SECURITY CLASSIFICATION OF THIS PAGE (When Data Entered)

varying degrees of recrystallization and grain growth and facilitated examination of the effect of grain size on the superplastic deformation characteristics of these alloys. Tension testing was conducted at strain rates ranging from 5.3×10^{-5} to 5.3×10^{-4} S⁻¹ and temperatures varying from ambient to 300°C. Materials in the warm rolled condition exhibited the highest strength at ambient temperature and were generally most superplastic at elevated temperature. An Al 10%Mg-0.5%Mn alloy exhibited elongation of approximately 400% at 300°C.

053

Accession For	
NTIS GRA&I	<input checked="" type="checkbox"/>
DTIC TAB	<input type="checkbox"/>
Unannounced	<input type="checkbox"/>
Justification	
By	
Distribution/	
Availability Codes	
Dist	Avail and/or Special
A-1	



Approved for public release; distribution unlimited.

Superplasticity in Thermomechanically
Processed High Magnesium Aluminum-Magnesium Alloys

by

John J. Becker
Lieutenant Commander, United States Navy
B.S., University of North Dakota, 1971

Submitted in partial fulfillment of the
requirements for the degree of

MASTER OF SCIENCE IN MECHANICAL ENGINEERING

from the

NAVAL POSTGRADUATE SCHOOL
March 1984

Author



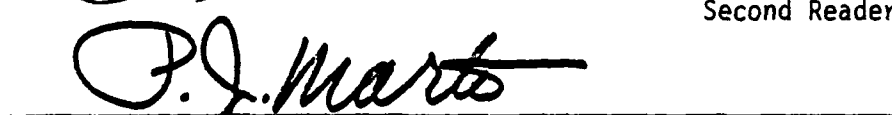
Approved by:



Thesis Advisor



Second Reader



Chairman, Department of Mechanical Engineering



Dean of Science and Engineering

ABSTRACT

The elevated temperature deformation characteristics of two thermo-mechanically processed high magnesium, aluminum-magnesium alloys were investigated. The thermomechanical processing itself included warm rolling at 300°C to 94% reduction. Subsequent treatments included annealing after rolling for either one-half hour or ten hours at 300°C, or one-half hour at 440°C. These annealing treatments resulted in varying degrees of recrystallization and grain growth and facilitated examination of the effect of grain size on the superplastic deformation characteristics of these alloys. Tension testing was conducted at strain rates ranging from 5.3×10^{-5} to 5.3×10^{-2} S⁻¹ and temperatures varying from ambient to 300°C. Materials in the warm rolled condition exhibited the highest strength at ambient temperature and were generally most superplastic at elevated temperature. An Al-10%Mg-0.5%Mn alloy exhibited elongation of approximately 400% at 300°C.

TABLE OF CONTENTS

I.	INTRODUCTION	10
II.	BACKGROUND	12
	A. ALUMINUM-MAGNESIUM ALLOYS	12
	B. PREVIOUS WORK	14
	C. SUPERPLASTIC BEHAVIOR	16
	1. Background and Scope	16
	2. Strain Rate Sensitivity	17
	3. Microstructural	19
	4. Stress Strain Relationships	20
	5. Mechanism of Deformation	23
III.	EXPERIMENTAL PROCEDURE	25
	A. MATERIAL PROCESSING	25
	B. TENSILE SPECIMEN FABRICATION	26
	C. ELEVATED TEMPERATURE TESTING	28
	D. DATA REDUCTION	30
	E. METALLOGRAPHY	30
IV.	RESULTS AND DISCUSSION	32
	A. OPTICAL MICROSCOPY	32
	1. As Rolled	32
	2. Annealed	33
	B. TEM MICROSCOPY	33
	C. MECHANICAL TEST RESULTS	36
	D. DEFORMED MICROSTRUCTURE	45

V. CONCLUSIONS AND RECOMMENDATIONS	52
LIST OF REFERENCES	53
APPENDIX A	55
APPENDIX B	68
APPENDIX C	84
INITIAL DISTRIBUTION LIST	101

LIST OF FIGURES

2.1	Partial Aluminum-Magnesium Phase Diagram.-----	13
2.2	Elongation Versus the Strain Rate Sensitivity Coefficient m for Sn-Pb Eutectic. Adopted from Avery and Backofen [Ref. 13].-----	18
2.3	Log Stress Versus Log Strain Rate for Aluminum Alloy. Data of Paton, et al., [Ref. 14].-----	20
2.4	Strain Rate Sensitivity Coefficient m Versus Log Strain Rate for 7475 Aluminum Alloy. Data of Paton, et al., [Ref 14].-----	21
2.5	Log Stress Versus Log Strain Rate Showing Region Two and Three Associated with Superplastic Materials.-----	22
3.1	Jig Utilized to Fabricate Tensile Specimens.-----	27
3.2	Test Specimen Geometry.-----	27
3.3	Placement of Thermocouples and Insulation.-----	29
3.4	Mounting of an Elongated Sample -----	31
4.1	Optical Micrographs of Al-8.14%Mg-0.4%Cu (a) and 10.2%Mg-0.52%Mn (b) in the Longitudinal Orientation Showing the As-Rolled Structure to be Banded in the 8%Mg Alloy at 200x -----	32
4.2	Optical Micrographs of Al-8.14%Mg-0.4%Cu Alloy in the Longitudinal Orientation Showing the Affects of Annealing; Reducing the Banding in the 300°C Annealed Condition and Fully Recrystallized Material for the 440°C Anneal at 200x.-----	34
4.3	Optical Micrographs of Al-10.2%Mg-0.52%Mn Alloy in the Longitudinal Orientation Showing the Affects of Annealing; Reducing the Banding in the 300°C Annealed Condition and Fully Recrystallized Material for the 440°C Anneal at 200x.-----	35
4.4	TEM Micrographs of Al-8.14%Mg-0.4%Cu Alloy for the As Rolled and Annealed at 300°C Showing the Coarsening of the Structure with Increasing Annealing Time at 10Kx.-----	37

4.5	TEM Micrographs of Al-10.2%Mg-0.52%Mn Alloy for the As Rolled and Annealed at 300°C Showing the Coarsening of the Structure with Increasing Annealing Time at 10kx.-----	38
4.6	Schematic Showing the Affects of Annealing on the Tensile Strength.-----	42
4.7	True Stress Versus True Strain for Al-8.14%Mg-0.4%Cu in an As Rolled Condition from Room Temperature to 150°C.-----	46
4.8	True Stress Versus True Strain for Al-8.14%Mg-0.4%Cu in an As Rolled Condition from 200-300°C.-----	47
4.9	Optical Micrographs of As Rolled Al-8.14%Mg-0.4%Cu Tested at 300°C and 5.3×10^{-5} (S-1) Strain Rate Taken at Various Positions Along the Specimen After Tensile Testing at 200x.-----	49
4.10	Optical Micrographs of As Rolled Al-10.29%Mg-0.52%Mn Tested at 300°C and 5.3×10^{-3} (S-1) Strain Rate Taken at Various Locations Along the Specimen After Tensile Testing at 200x.-----	50
4.11	Optical Micrographs of Al-10.2%Mg-0.52%Mn Annealed for 10 hrs. at 300°C and 5.3×10^{-3} (S-1) Strain Rate Taken at Various Locations Along the Specimen After Tensile Testing at 200x.-----	51

LIST OF TABLES

I.	Alloy Composition -----	25
II.	Test Data for Al-8.14%Mg-0.4%Cu -----	39
III.	Test Data for Al-10.2%Mg-0.52%Mn -----	40

I. INTRODUCTION

The purpose of this thesis was to investigate the elevated temperature deformation characteristic of two thermomechanically processed high magnesium aluminum-magnesium alloys. Particular attention was given to determine possible superplastic response and the extent and nature of this superplastic response. Previous research by Ness [Ref. 1], Bingay [Ref. 2], Glover [Ref. 3], Grandon [Ref. 4], Speed [Ref. 5], Chesterman [Ref. 6], Johnson [Ref. 7], and Shirah [Ref. 8] demonstrated that thermomechanically processed high-magnesium alloys are capable of high strength with good ductility. Both Ness [Ref. 1] and Glover [Ref. 3] found and reported in their research indications of superplasticity in the alloys they studied. McNelley and Garg [Ref. 9] in transmission microscopy studies have found that these alloys possess a fine microstructure, a prerequisite for superplastic behavior. The as-rolled structures were found by them to consist of fine, cellular structures or subgrain structures. Such microstructures were also found to recrystallize to submicron grain size with annealing, suggesting investigation of the annealed conditions may provide information on the contribution of fine subgrain structure as well as grain structure to elevated temperature strength and ductility.

This study utilizes Johnson's [Ref. 7] standardized processing technique as the basis for processing the materials for study. Two aluminum-magnesium alloys were chosen for the study, an 8.14% Mg 0.40% Cu alloy and 10.2% Mg 0.52% Mn alloy. The alloying additions to the

high magnesium aluminum-magnesium alloy were chosen based on previous observations of their effect in refining the microstructure, then hopefully leading to a more superplastic material. Mechanical testing was accomplished on an Instron test machine utilizing a Marshall three-zone furnace for elevated temperature control. Optical microscopy was done to characterize the as-rolled and annealed conditions and to examine for cavitation in the elongated samples. Transmission electron micrographs from McNelley and Garg [Ref. 9] were utilized for evaluation of the microstructure at higher magnification.

Data obtained from the mechanical testing, in conjunction with optical microscopy and previous TEM work is evaluated, compared and correlated with current theories of superplastic behavior. Review of this work and new questions are posed for subsequent investigation.

II. BACKGROUND

A. ALUMINUM-MAGNESIUM ALLOYS

Aluminum and its many alloys have been the subject of much investigation and study. A motivation for such study is to obtain an alloy that has a higher strength to weight ratio while maintaining corrosion resistance, machinability, ductility, toughness and an ability to be easily fabricated and possibly welded. Most of the higher strength aluminum alloys obtain their strength through precipitation and solid solution hardening. This involves the formation of discrete second phases to retard dislocation motion in the microstructure. Much of this research has been driven by the needs of the aerospace industry.

The magnesium addition to aluminum results in lower density and increased strength. Although precipitation does occur, most of the strength in aluminum-magnesium alloys is due to magnesium in solid solution. The strength can be increased by cold working. In conjunction with other alloying elements the aluminum-magnesium alloys are capable of obtaining good strength, corrosion resistance, toughness.

Commercially available aluminum-magnesium alloys, the 5xxx series, have long been available. They are lower in strength than the 2xxx and 7xxx precipitation hardened alloys. The high strength aluminum alloys do have some problems associated with them such as difficulty in attaining good fatigue resistance and stress corrosion cracking resistance at high strength levels. Interest in higher magnesium

aluminum-magnesium alloys stems in part from the desire to combine the good corrosion and fatigue characteristics of lower magnesium alloys with a high strength.

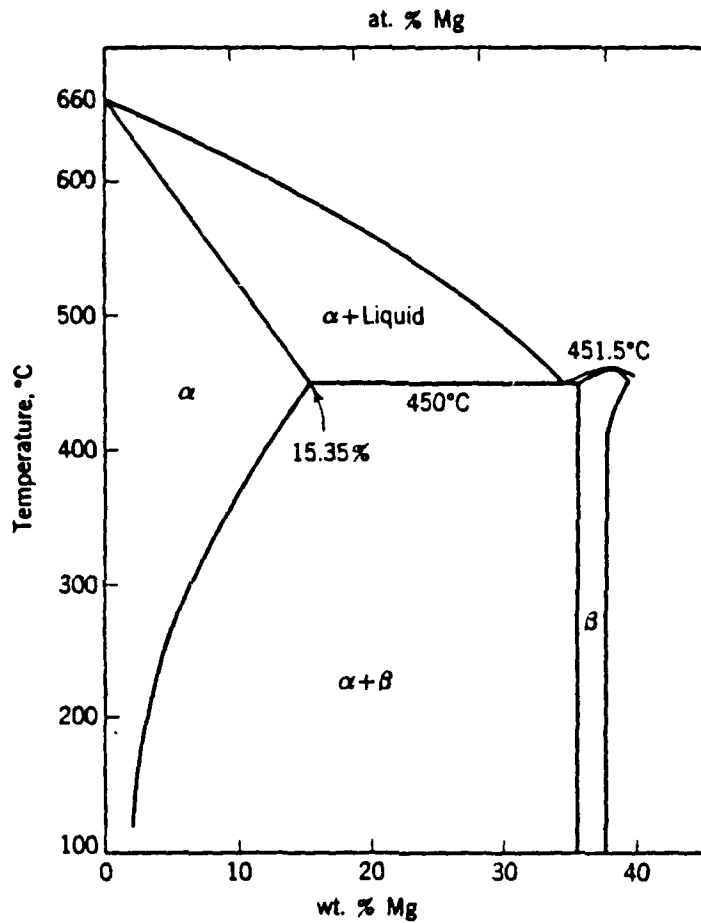


Figure 2.1 Partial Aluminum-Magnesium Phase Diagram.

The aluminum-magnesium phase diagram Figure 2.1 shows that the solubility of magnesium in aluminum varies from 0.8 weight percent at 100°C to a maximum at approximately 15 weight at the eutectic temperature of

451°C. This difference in solubility as a function of temperature provides a driving force for second phase particle formation when the temperature is reduced to a value below solvus for the amount of magnesium present in the alloy. The beta phase Al_8Mg_5 is the intermetallic that exists above 5 weight percent magnesium. Problems exist as this beta phase has a tendency to form at the grain boundaries. Strength increases and ductility decreases occur as the magnesium content is increased from 5 to 14 weight percent. Alloys above 14 weight percent have been found to be too brittle to determine tensile properties [Ref. 10]. For these reasons, commercially available aluminum-magnesium alloys, the 5xxx series, usually utilize weight percent magnesium of no more than 5 to 6 percent.

B. PREVIOUS WORK

Ness [Ref. 1] initiated the investigation of high magnesium alloys here. His work was conducted on an 18 percent magnesium, aluminum-magnesium alloy. His work attempted to parallel concepts developed by Bly, Sherby, and Young [Ref. 11] in work on high-carbon steel. They utilized mechanical working of a material in a two phase region to obtain microstructural refinement and an improvement in the mechanical properties. Ness [Ref. 1] reported that microstructural refinement could be obtained in an 18 percent alloy and a compression strength of 655 Mpa (99KSI) was reported.

As had been reported in Mondolfo [Ref. 10] and also found in this work, an alloy of this magnesium content is very brittle and cracks readily during rolling.

Bingay [Ref. 2] and Glover [Ref. 3] studied variations of this thermomechanical processing in an attempt to develop a processing method which would not have the material crack. Bingay [Ref. 2] introduced both isothermal and non-isothermal forging prior to rolling in an attempt to refine the microstructure of the alloys containing 15-19 weight percent magnesium. Those alloys above maximum solubility were suggested to be eliminated from further study and future work be concentrated on those alloys below 15 weight percent magnesium. Bingay [Ref. 2] also suggested that a solution treatment before deformation be introduced prior to deformation in the two phase region. Glover [Ref. 3] tested alloys varying from 7-9 weight percent magnesium and noted characteristics of superplastic behavior, especially in higher magnesium alloys.

Grandon [Ref. 4] extended the study into 7-10 percent magnesium alloys. Lower magnesium content alloys were chosen so that for some treatment temperature all the magnesium would be dissolved. He introduced a 24 hour solution treatment followed by a quench and then warm rolling at 300°C. The warm rolling was done to strengthen the material. His results show a doubling of strength compared to the 5xxx series alloys, while maintaining good ductility. Another important observation was that recrystallization apparently did not occur during warm rolling below the solvus for alloys of this magnesium content. Alloys with larger amounts of magnesium were investigated by Speed [Ref. 5].

Grandon [Ref. 4] posed several questions regarding the nature of precipitation and recrystallization in these alloys. These questions were investigated by Chesterman [Ref. 6]; based on optical microscopy

he concluded that recrystallization took place only at temperatures above the solvus for the 8-14 weight percent alloy. Cold working followed by annealing would not produce observable recrystallization if the annealing temperature was below the solvus. Even at annealing temperatures of $0.6T_m$ precipitation always replaced recrystallization as the method by which stored energy was released.

Johnson [Ref. 7] combined all the previous studies and standardized a thermomechanical process for high magnesium, aluminum-magnesium alloys. His work has examined six alloys, both binary and ternary, from 8.14% to 10% magnesium. His results also demonstrated material twice as strong as 5xxx alloys with good ductility. His process introduced a 10 hour solution treatment at 440°C with isothermal upset forging at the nine hour mark. After this, the material was quenched and warm rolled. The warm rolling was done at various temperatures between 200 and 340°C . His conclusion was that beta phase (Al_8Mg_5) intermetallic was the most significant factor in obtaining both high strength and good ductility.

Shirah [Ref. 8] in his work found that the microstructural homogeneity could be improved by extending the solution treatment time to 24 hours vice the 10 hours; this minimized banding of precipitate and still did not lead to grain growth. This 24 hour solution treatment was utilized in this thesis.

C. SUPERPLASTIC BEHAVIOR

1. Background and Scope

The term superplastic refers to extraordinary elongations in *tension testing*, generally in excess of 200 percent. Although recognized for many years, active reporting of research in the field of superplasticity

did not begin until Underwood's [Ref. 12] paper in 1962. Since that time considerable effort has been invested in studying and understanding the field of superplastic behavior.

Two primary approaches exist in analyzing superplastic behavior. Applied mechanics explains the phenomenon in terms of strain rate sensitivity of the material. On the other hand, material science attempts to understand superplasticity through an understanding of the microstructural characteristics.

2. Strain Rate Sensitivity

Superplastic deformation is a thermally activated process which occurs at elevated temperatures. At elevated temperatures, the power law equation 2.1 describes stress as a function of strain rate.

$$\sigma = k \dot{\epsilon}^m \quad (\text{eqn 2.1})$$

Where σ = stress, k is a constant and $\dot{\epsilon}$ is the strain rate. The m in the power law equation 2.1 is the strain rate sensitivity. The stress is still a function of strain at elevated temperatures, but more weakly. Stress-strain curves often tend to be flat (i.e., flow at constant stress) suggesting a steady state flow process is occurring. This m increases as a function of temperature until at temperatures above $0.5 T_m$ m becomes relatively constant with a value of about 0.2 to 0.25 for many metals and alloys. Studies of superplasticity have found that superplastic behavior occurs at m values of .3 to .8. It is found generally that superplastic ductility increases with increasing m and is a maximum at the highest m value. The value of

m can be found as the slope of a log stress vs log strain rate plot. Even though superplastic materials have in common a high strain rate sensitivity, high m values alone do not necessarily lead to superplastic behavior due to microstructural changes which can occur during plastic flow. These may be changes such as internal or inter-phase boundary cracking, or cavitation or grain boundary separation and these may intervene and limit deformation. This high strain rate sensitivity confers resistance to localized deformation.

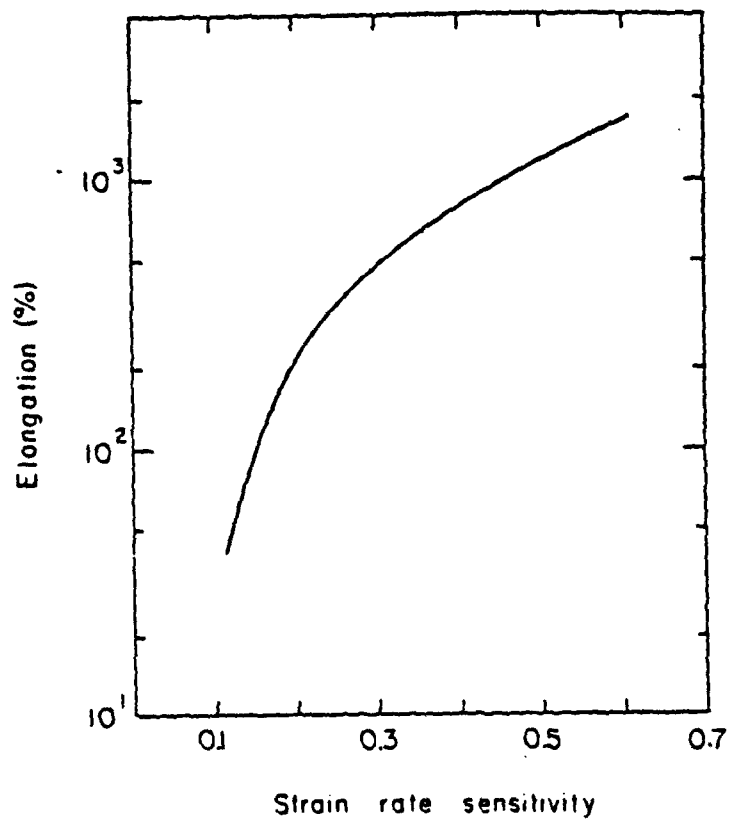


Figure 2.2 Elongation Versus the Strain Rate Sensitivity Coefficient m for Sn-Pb Eutectic. Adopted from Avery and Backofen [Ref. 13].

Figure 2.2 shows results reported by Avery and Backofen [Ref.13] in their study of superplasticity in Sn-Pb alloys. This result, increased elongations with increasing values of m , is generally observed for other superplastic materials as well.

3. Microstructural

Fine grain size is characteristic of superplastic materials, and superplasticity is enhanced by a homogeneous, fine grain size. Many ways have been found to provide this fine grain size. Most of these methods involve controlled mechanical working of the material or the use of a phase transformation to refine the grain size. Stabilization of fine grains is often accomplished by the use of second phases. It is very important that these second phases be deformable along with the matrix.

Because superplasticity is observed at elevated temperatures and over perhaps lengthy test times, grain growth must be considered. Growth may occur at an elevated rate during deformation. Tests usually are conducted at temperatures of 0.4 to 0.7 T_m to minimize grain growth as such relatively lower temperatures assist in maintaining a stable grain size. Also, alloying agents may be added to retard grain growth in superplastic materials.

Not only are the grains required to be fine for superplastic behavior but they must also be equiaxed and have smooth and curved grain boundaries. This reflects the contribution of grain boundary sliding to the process of deformation under superplastic conditions. If grain growth does occur, the alloy will strain harden. This is readily seen in the Nabarro-Herring diffusion creep model, equation

$$\dot{\epsilon} = \frac{7 b \sigma D}{k T d^2} \quad (\text{eqn 2.2})$$

2.2 where $\dot{\epsilon}$ equals the strain rate, σ equals the stress, b is the Burgers vector, d is the grain size, D is the diffusion coefficient and T is the temperature. In this relation, an increase in d will require an increase in σ if $\dot{\epsilon}$ is to be maintained as a constant, i.e., the material would strain harden in a stress-strain test. The Nabarro-Herring model is not thought to be a completely accurate model for superplastic deformation but is used here to illustrate the importance of grain size.

4. Stress Strain Relationships

It is convenient to express this stress-strain rate relationship on a log stress vs log strain rate axes. The power law equation 2.1

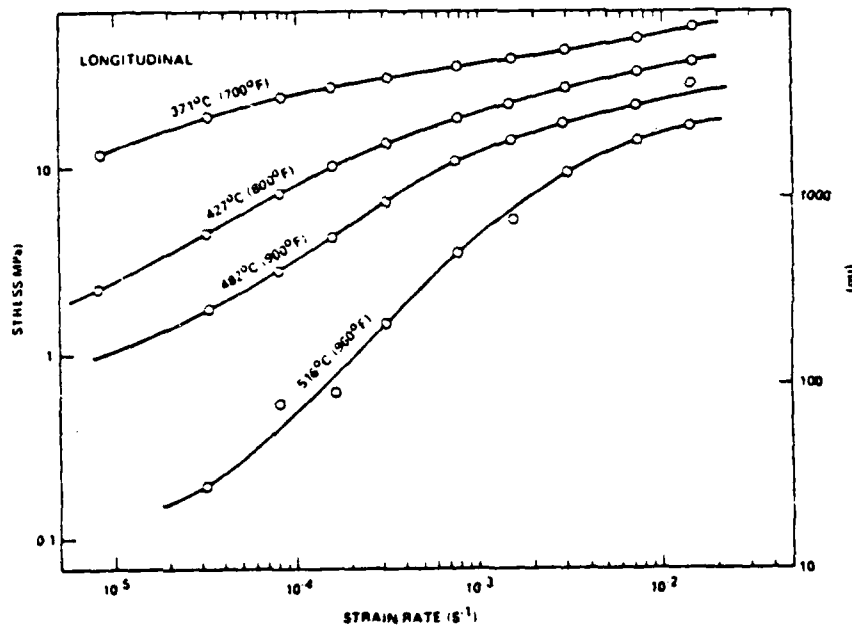


Figure 2.3 Log Stress Versus Log Strain Rate for Aluminum Alloy. Data of Paton, et al., [Ref. 14].

suggests that log stress vs log strain rate data would fall on a straight line. Figure 2.3 clearly shows a sigmoidal curve on such axes for data on 7475 aluminum alloy. In fact, this clearly suggests that the power law must be modified to be a completely accurate description of behavior. Nonetheless, the "instantaneous" value of m may be inferred from such data and used to interpret data. Maximum superplastic behavior was found to be at 516°C , the lower curve on the plot in Figure 2.3.

Maximum ductility is usually found at the point of greatest m .

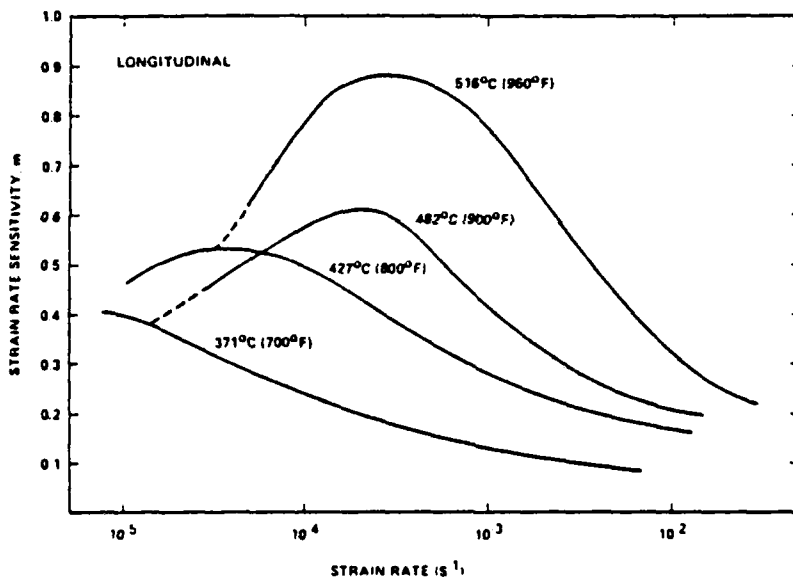


Figure 2.4 Strain Rate Sensitivity Coefficient m Versus Log Strain Rate for 7475 Aluminum Alloy. Data of Paton, et al., [Ref. 14].

Figure 2.4 shows the results from Paton, Hamilton, Wert and Mahoney [Ref. 14] for a superplastic 7475 aluminum alloy. Also notable on this curve is that the region of maximum superplastic behavior occurs at a strain rate between 10^{-4} and 10^{-3} (S-1).

The curve of log stress vs log strain rate for most superplastic materials is usually S shaped having three distinct regions. Stress rises steadily with strain rate but first with an lesser slope and limited ductility (region 1), through a region of higher slope with a maximum m and maximum ductility (region 2) before the slope and the ductility decrease in region 3. In some alloys, such as nickel-chromium, a two segment curve is observed. A schematic of these two types of curves is shown on Figure 2.5. Ductility would be a maximum at strain rates where the slope is a maximum. This is reported, e.g., by Paton, et al., [Ref. 14].

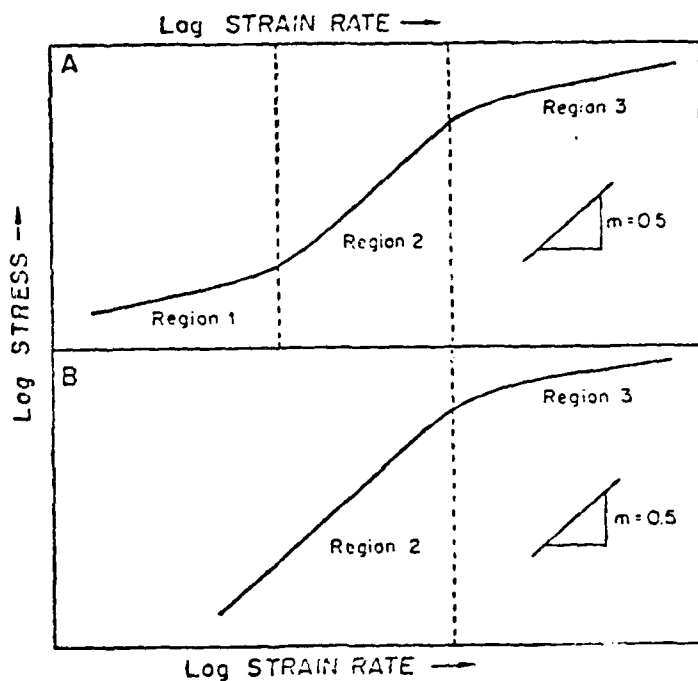


Figure 2.5 Log Stress Versus Log Strain Rate Showing Region Two and Three Associated with Superplastic Materials.

5. Mechanism of Deformation

Two distinct observations distinguish deformation mechanisms for superplastic behavior. These are first, a strong inverse dependence of strain rate on grain size, usually expressed as strain rate being proportional to the inverse third power of grain size. Secondly, little grain elongation occurs; rather, grains tend to remain equiaxed. These imply the existence of grain boundary sliding during deformation.

Ashby and Verrall [Ref. 15] explain this change in the shape of the deformed specimen with respect to the original not in terms of change of shape of grains but in terms of change of place of grains, i.e., grains change neighbors by sliding. Grain boundary sliding with accommodation by diffusion, either in the boundary or in the lattice, is the predominant mechanism of deformation in region 2, the region of maximum superplastic behavior. Ashby and Verrall [Ref. 15] concluded that the strain rate is about seven times faster than Nabarro or Coble creep for such a diffusion accommodated sliding process where grains will change their neighbors.

Coble creep is the mechanism of deformation in region 1. Coble creep is a diffusional process involving atomic or ionic diffusion along grain boundaries. Coble creep is very sensitive to grain size due to the increase in the amount of grain boundary with smaller grain size.

In region 3 the deformation mechanism is assumed to be dislocation creep. Diffusional movements of dislocation form the backbone of this mechanism. Paton, et al., [Ref. 14] suggests that edge dislocation

climb away from dislocation barriers is the predominant mechanism in region 3. This dislocation process is accelerated by the creation of excess vacancies brought about by dislocation-dislocation interactions.

III. EXPERIMENTAL PROCEDURE

A. MATERIAL PROCESSING

The alloys selected for study were Al-10.2 weight percent Mg-0.52 weight percent Mn and 8.14 weight percent Mg-0.40 weight percent Cu. These alloys were obtained as direct chill cast ingots, 127mm (5 in) in diameter by 1016mm (40 in) in length. The ingots were produced at the Alcoa Technical Center, Alcoa Center, Pennsylvania, utilizing 99.99% pure Al as a base metal and were alloyed using commercially pure copper, magnesium, 5% beryllium-aluminum master alloy and 5% titanium - 0.2% boron-aluminum masteralloy [Ref. 7]. The details of the compositions of the alloys are given below in weight percent [Ref. 7].

Table I
Alloy Composition

<u>Serial Number</u>	<u>Si</u>	<u>Fe</u>	<u>Cu</u>	<u>Mn</u>	<u>Mg</u>	<u>Ti</u>	<u>Be</u>
501300A	0.01	0.03	0.00	0.52	10.2	0.01	0.0002
501303A	0.01	0.03	0.40	0.00	8.14	0.01	0.0002

The as-received ingots were sectioned to produce billets of 96mm (3.75 in) length by a 32mm (1.25 in) by 32mm (1.25 in) cross section to facilitate subsequent thermomechanical processing.

The thermomechanical processing scheme was similar to that developed by Johnson [Ref. 7]. The essential difference was that the solution treating at 440°C of the billets was done for 24 hours as recommended

by Shirah [Ref. 8]. The billets were isothermally upset forged at 440°C on heated platens to a height of approximately 28mm (1.1 in), requiring a maximum force of approximately 125,000 N (28,000 lbf). The billets were then annealed at 440°C for one hour followed by an oil quench.

The billets were further deformed following the warm rolling procedure developed by Johnson [Ref. 7]. Temperature was measured by placing the billets against a monitoring thermocouple. When the thermocouple indicated the desired temperature (300°C) the rolling commenced. Prior to the initial pass this heating time was approximately 10 minutes. In order to maintain isothermal conditions, the billets were reheated between passes and in the later stages of rolling reheating times were typically four minutes. Due to the fact that the rolls are not heated time during the rolling sequence was held under 15 seconds for each pass. Final thickness of approximately 1.8mm (0.07 in) was sought, giving a final reduction of approximately 94%.

B. TENSILE SPECIMEN FABRICATION

Each billet resulted in a sheet of approximately 1.8mm (0.07 in) thickness and of 75mm (3.0 in) width of 550mm (22 in) length. This sheet of material was sectioned into 63.5mm ± 0.127mm (2.5 ± 0.005 in) by 14.2mm ± 0.127mm (0.56 ± 0.005 in) blanks. These blanks were cut on a bandsaw by first removing the forward 25mm (1 in) of the sheet. The sides of the blanks were then trimmed into 14.2mm (0.56 in) widths. A holder as shown in Figure 3.1 was fabricated and used as a jig to hold the blanks while cutting the gage section on a Tensilkut (R) machine. The test sample design is shown in Figure 3.2. The relatively small

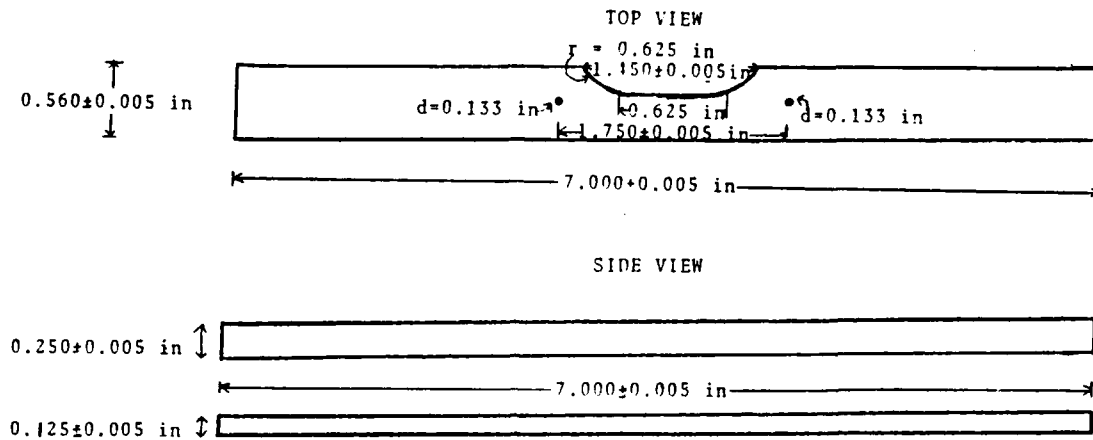


Figure 3.1 Jig Utilized to Fabricate Tensile Specimens.

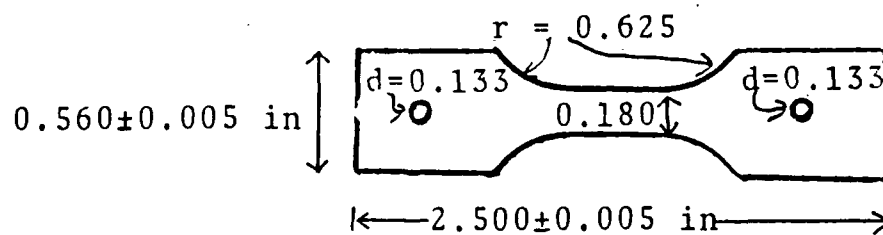


Figure 3.2 Test Specimen Geometry.

size was dictated by the available furnace and grip assembly size and the expectation of substantial elevated temperature ductility.

C. ELEVATED TEMPERATURE TESTING

Wedge-type grips manufactured by ATS, Inc., Butler, Pennsylvania, were utilized for conducting all the testing including that at elevated temperatures. These grips were Model #713C and were fabricated of Inconel 718 specifically for use at elevated temperatures.

A Marshall model #2232 three-zone clamshell furnace was used for maintaining the elevated temperatures. The temperature in the furnace was controlled by three separate controllers, one for each zone. The thermocouples for the furnace controllers were passed into the furnace utilizing a ceramic thermocouple sheath. The controller thermocouple for the upper zone of the furnace was located six inches above the thermocouple entrance port and approximately one inch in from the furnace elements. The controller thermocouple for the bottom furnace was located in a corresponding location below the thermocouple entrance. The center controller was one inch directly inside the furnace at the thermocouple entrance. Insulation was installed at several locations both inside and outside of the furnace. Glass insulation of one inch thickness was utilized for the insulation. Two hollow circular disks were employed to reduce the flue effect of the furnace. These were placed around the pull rods at both the top and bottom of the furnace. Thin strips of insulation were placed on the closing surfaces of the furnace. These strips were found to be especially important in obtaining and maintaining uniformity of temperature in the test zone. A

thermal pad was placed over the top of the furnace. Each of the pull rods were wrapped with insulation in the areas external to the furnace.

The temperature in the furnace was monitored by installing five measuring thermocouples. A thermocouple was placed on the top pull rod, four inches above the bottom of it and on the back side of the furnace. Another thermocouple was placed in contact with the specimen and just inside of the upper wedge. A thermocouple was also placed on the middle of the specimen at the start of the test. Two additional thermocouples were placed at corresponding positions on the lower pull rod. During the test, set temperature was held to within two degrees of the desired temperature as a function of time. At a set point of 300°C the following would be representative temperatures as noted from top to bottom: 285°C, 300°C, 300°C, 300°C, and 285°C. Placement of the thermocouples and insulation utilized for the test can be seen in Figure 3.3.

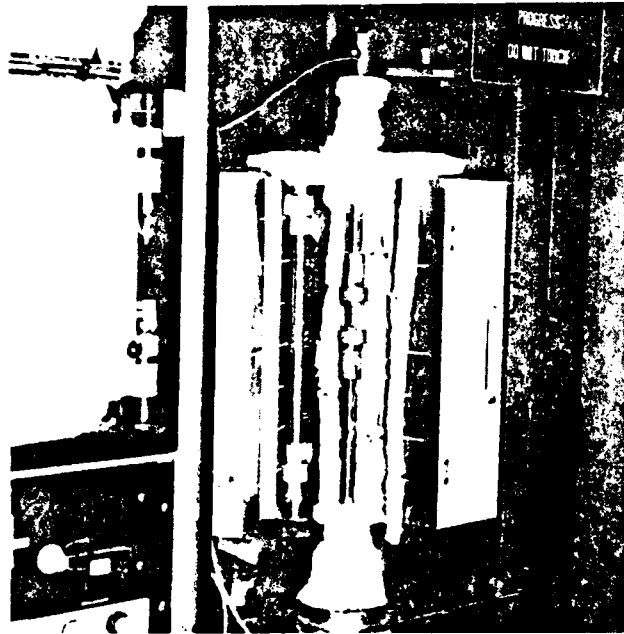


Figure 3.3 Placement of Thermocouples and Insulation.

An Instron machine was utilized to conduct the stress-strain testing. The crosshead speed for the test ranged 0.002 in/min to 2 in/min (0.05mm/min to 50mm/min). Except for 0.002 inch per minute speed the magnification ratio for the autographic chart was 10; for the 0.002 in/min speed, the magnification ratio was 100.

D. DATA REDUCTION

Elongation was computed both by measuring the length of the deformed and fractured specimen and by utilizing the data from the strip-chart recorder of the Instron machine. The yield strength was computed utilizing a 1% offset on all tests except for the 0.002 in/min strain rates. This was done because of the magnification ratio of 10 was too small for reliable readings of the 0.2% offset. For the 0.002 in/min tests, both a 0.2 and a 1% offset were calculated. Therefore, all yield strength data presented represent the stress at a 1% offset unless otherwise noted.

E. METALLOGRAPHY

Samples of as-rolled or annealed material were mounted in standard molds with cold mounting compound. The elongated test samples were mounted by fabricating a rectangular mold just larger than the specimen using a sheet of glass as a base. Figure 3.4 shows the mounting of an elongated-sample. All of the optical microscopy specimens were polished first utilizing 240 to 600 grit papers and then polishing on wheels utilizing magnesium oxide abrasive. Etching was accomplished utilizing Barkers reagent at 20 volts d.c. and for times varying from 60 to 75 seconds. The specimens were placed in a beaker containing approximately

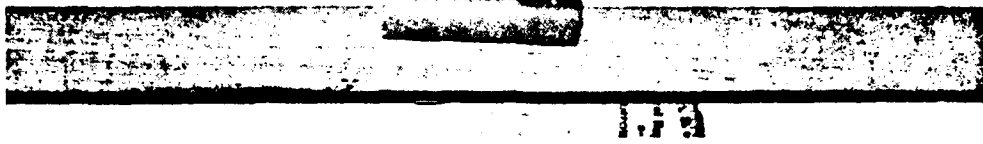


Figure 3.4 Mounting of an Elongated Sample.

25mm (1 in) of reagent. The specimen was immersed to a level of approximately 6mm (0.25 in). Examination and photographic work was done with a Zeiss Universal microscope, Polarized light and strain-free optics were used. Panatomic X 35mm film was used for photographic recording.

IV. RESULTS AND DISCUSSION

A. OPTICAL MICROSCOPY

1. As Rolled

Optical micrographs of these materials show an elongated, banded grain structure, often obscured by the precipitated intermetallic.



a) Al-8.14%Mg-0.4%Cu



b) Al-10.2%Mg-0.52%Mn

Figure 4.1 Optical Micrographs of Al-8.14%Mg-0.4%Cu (a) and 10.2%Mg-0.52%Mn (b) in the Longitudinal Orientation Showing the As-Rolled Structure to be Banded in the 8%Mg Alloy at 200x.

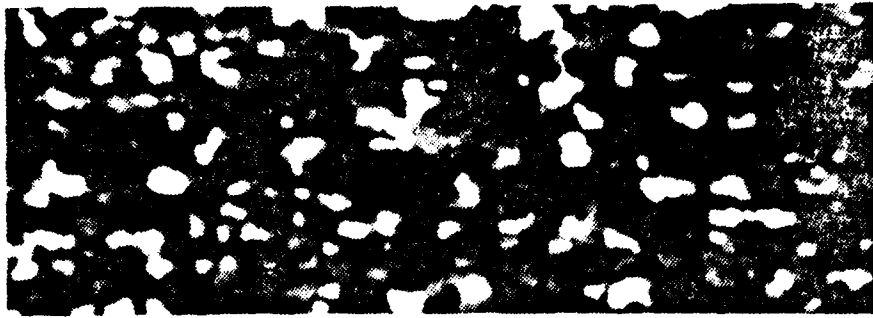
Banding with an elongated structure is clearly evident in Figure 4.1 for the 8%Mg, 0.4%Cu alloy and less so but still visible in the 10%Mg 0.52%Mn alloy. Intermetallic beta phase (Al_8Mg_5) is dispersed in both alloys, however is more evident in the 10%Mg-0.52%Mn alloy. The greater amount of dispersion of beta in the higher percent magnesium alloy is expected due to the larger amounts of magnesium present.

2. Annealed

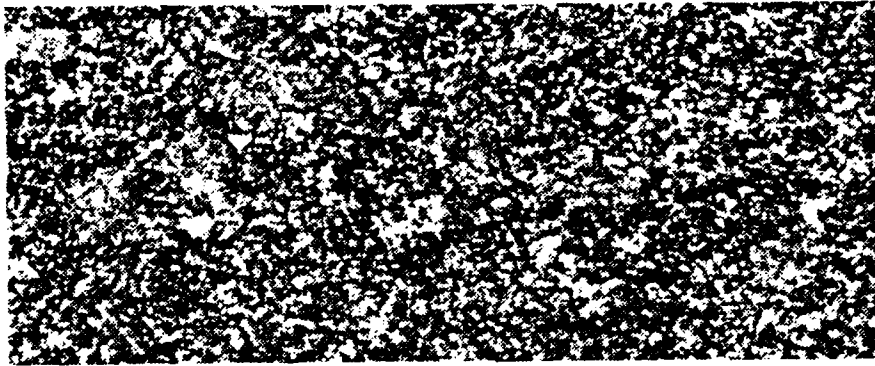
Figure 4.2 and 4.3 show the effect of annealing on the microstructures. There are two annealing temperatures. At 440°C (above the solvus), annealing for 1/2 half hour leads to complete recrystallization and a single-phase material. The size of grains in the fully recrystallized material is 10-20 microns. For the 300°C (below the solvus) annealing conditions microstructural banding becomes less marked and precipitation becomes more apparent, and these lead to more uniformity in the microstructure. At 10 hours annealing, growth has caused a coarsening of the precipitate and possibly a grain structure is becoming apparent, suggesting recrystallization may have taken place. Annealing above the solvus leads to recrystallization with little beta evident.

B. TEM MICROSCOPY

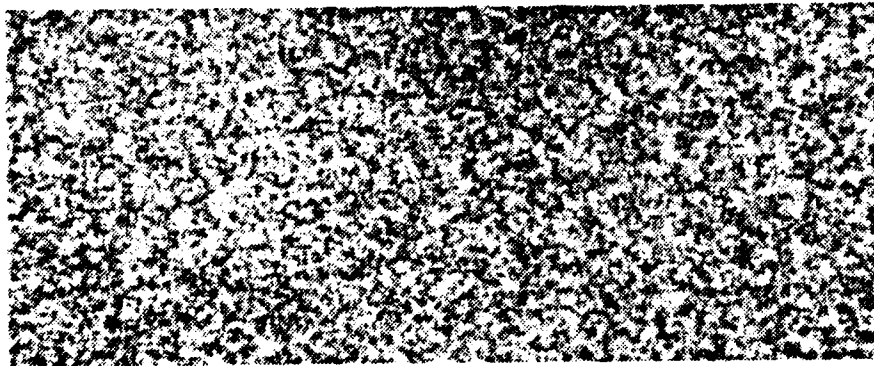
The TEM micrographs from the work of McNelley and Garg are included to assist in the evaluation of the substructure in these alloys for processing by warm rolling and annealing at 300°C. The banded structure in the 8%Mg 0.4%Cu alloy, observed optically Figure 4.1 is more easily seen in the TEM. The structure further is revealed to be a cellular substructure as can be seen in the TEM micrograph (Figure 4.4). The



1/2 Hr @ 440°C

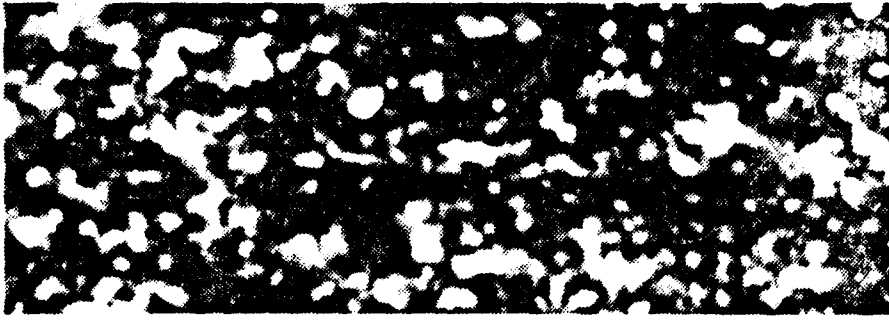


10 Hr @ 300°C

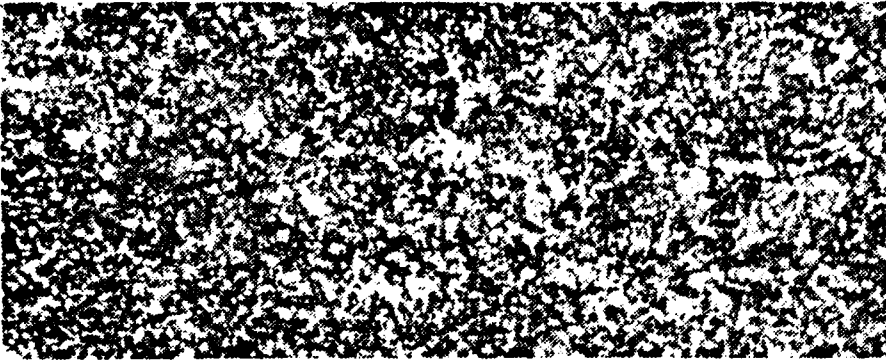


1/2 Hr @ 300°C

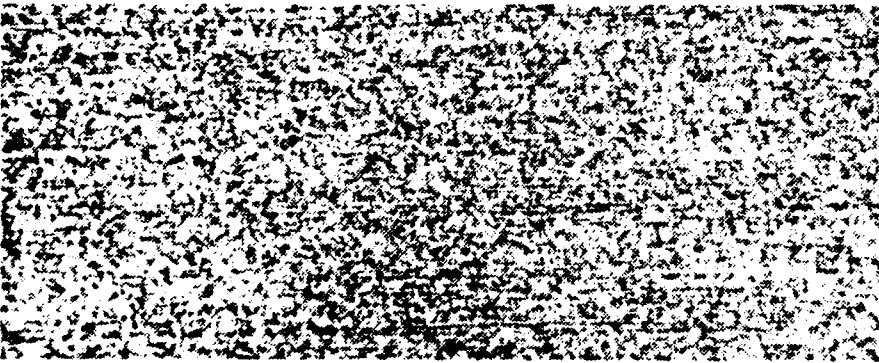
Figure 4.2 Optical Micrographs of Al-8.14%Mg-0.4%Cu Alloy in the Longitudinal Orientation Showing the Affects of Annealing; Reducing the Banding in the 300°C Annealed Condition and Fully Recrystallized Material for the 440°C Anneal at 200x.



1/2 Hr @ 440°C



10 Hr @ 300°C



1/2 Hr @ 300°C

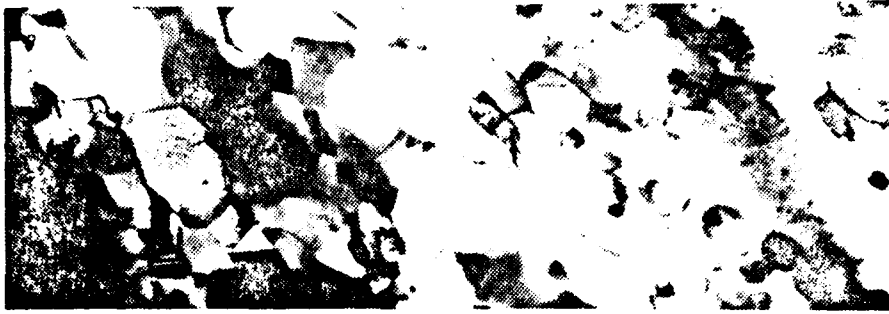
Figure 4.3 Optical Micrographs of Al-10.2%Mg-0.52%Mn Alloy in the Longitudinal Orientation Showing the Affects of Annealing; Reducing the Banding in the 300°C Annealed Condition and Fully Recrystallized Material for the 440°C Anneal at 200x.

precipitated beta is not obvious in the as rolled TEM micrograph. The 8%Mg-0.4%Cu alloy, annealed 1/2 hour at 300°C, shows a decrease in the amount of banding (similar to the optical micrograph). At 1/2 hour annealing the precipitated beta still is not evident. The most significant change is a "cleaning up" of the cellular structure. A dislocation subgrain structure is now apparent. At 10 hours of annealing at 300°C what appears to be a fully recrystallized grain structure appears. The beta precipitate is now apparent at the grain boundary junctions. The grain size is now on the order of one micron. The 10%Mg-0.52%Mn alloy (Figure 4.5) in the as rolled condition exhibits less evidence of banding. The substructure is finer and better organized than in the 8%Mg alloy. When the 10%Mg alloy is annealed the subgrain size increases and the dislocation density decreases.

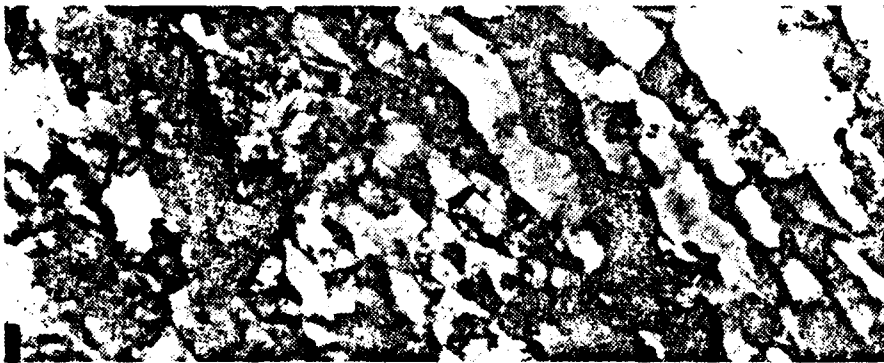
Comparison of the optical micrographs to the TEM micrographs suggest that the optical microscope is unable to resolve the structure. This appears to be the result of the manner in which the etchant works and with the presence of the beta. The optical micrographs, especially in the as rolled condition, do not accurately represent the precipitated intermetallic and are unable to reveal the grain structure.

C. MECHANICAL TEST RESULTS

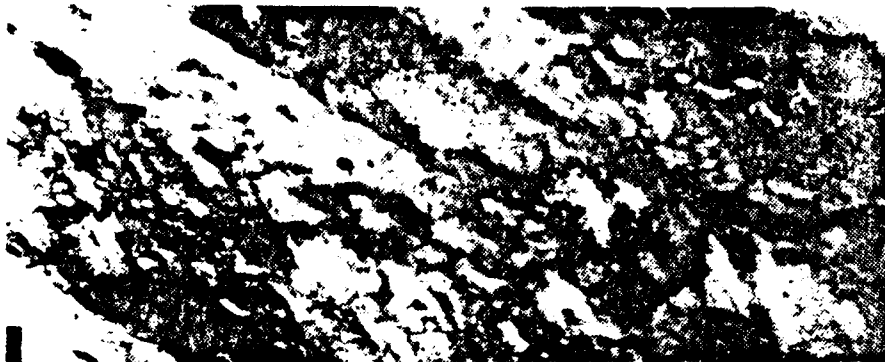
Stress-strain data was obtained as described in the experimental section for the Al-8.14%-0.4%Cu and Al-10.2%Mg-0.52%Mn aluminum-magnesium alloys. The test data is summarized in Tables II and III. Plots of this data appear in the Appendices. Appendix A contains the plots of ultimate tensile strength (UTS), yield strength and elongation



10 Hr @ 300°C

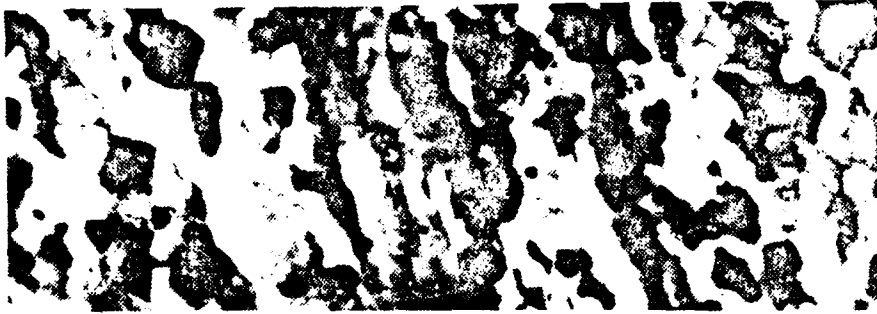


1/2 Hr @ 300°C

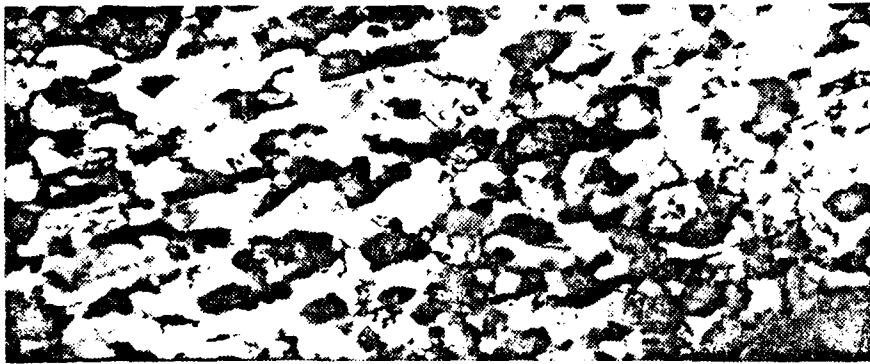


As Rolled

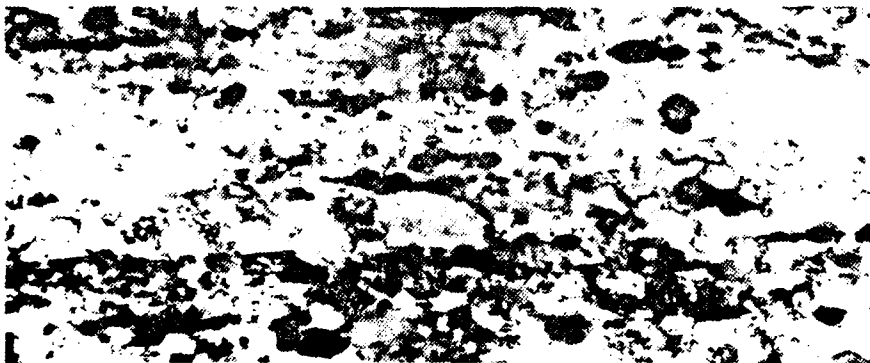
Figure 4.4 TEM Micrographs of Al-8.14%Mg-0.4%Cu Alloy for the As Rolled and Annealed at 300°C Showing the Coarsening of the Structure with Increasing Annealing Time at 10kx.



10 Hr @ 300°C



1/2 Hr @ 300°C



As Rolled

Figure 4.5 TEM Micrographs of Al-10.2%Mg-0.52%Mn Alloy for the As Rolled and Annealed at 300°C Showing the Coarsening of the Structure with Increasing Annealing Time at 10kx.

Table II

Test Data for Al-8.14%Mg-0.4%Cu

TEMPERATURE (C) STRAIN RATE (S-1)	YIELD (Mpa)				UTS (Mpa)				ELONGATION (%)			
	As Rolled	1/2 Hr @ 300°C	10 Hr @ 300°C	1/2 Hr @ 440°C	As Rolled	1/2 Hr @ 300°C	10 Hr @ 300°C	1/2 Hr @ 440°C	As Rolled	1/2 Hr @ 300°C	10 Hr @ 300°C	1/2 Hr @ 440°C
300 5.3x10-3	63	75	86	117	75	80	86	118	152	136	168	80
5.3x10-4	30	30	39	69	40	39	40	70	224	267	213	133
5.3x10-5	22	19	15	37	26	21	17	37	210	211	198	136
0.2% Offset	19	17	15	37								
250 5.3x10-3	119	153	141	146	122	154	142	146	123	72	104	40
5.3x10-4	66	77	75	149	84	87	91	150	130	144	134	61
5.3x10-5	35	41	44	91	38	74	45	93	312	224	150	112
0.2% Offset	28	30	40	90								
200 5.3x10-3	201	210	181	154	217	213	191	185	51	48	56	48
5.3x10-4	171	157	172	181	180	160	171	199	96	50	54	45
5.3x10-5	108	113	110	208	109	116	112	233	83	109	59	59
0.2% Offset	100	109	103	196								
150 5.3x10-3	308	265	246	211	311	292	287	267	29	51	50	50
5.3x10-4	246	282	233	223	252	285	245	253	39	38	51	61
5.3x10-5	216	231	198	220	217	235	199	272	46	42	48	40
0.2% Offset	207	221	195	199								
100 5.3x10-3	393	267	243	227	406	360	340	305	13	24	27	46
5.3x10-4	407	315	282	243	416	349	344	311	22	43	44	48
5.3x10-5	378	299	270	275	379	317	299	283	27	34	56	53
0.2% Offset	369	294	247	255								
50 5.3x10-3	456	287	284	209	479	383	374	338	13	26	22	34
5.3x10-4	446	301	260	223	473	398	372	311	13	22	24	46
5.3x10-5	428	270	272	211	475	348	392	313	16	29	30	48
0.2% Offset	402	226	260	169								
RM 5.3x10-3	451	278	283	219	487	393	371	346	8	16	21	32
5.3x10-4	463	307	296	210	493	426	352	341	11	19	18	32
5.3x10-5	453	318	295	195	470	388	389	326	13	22	24	35
0.2% Offset	420	276	252	163								

Table III

Test Data for Al-10.2%Mg-0.52%Mn

		YIELD (Mpa)				UTS (Mpa)				ELONGATION (%)			
TEMPERATURE (C)	STRAIN RATE (S-1)	As Rolled	300°C			As Rolled	300°C			As Rolled	300°C		
			1/2 Hr	10 Hr	1/2 Hr		1/2 Hr	10 Hr	1/2 Hr		1/2 Hr	10 Hr	1/2 Hr
300	5.3x10-2	77				91				144			
	1.3x10-2	52				61				214			
	5.3x10-3	28	26	32	79	34	32	39	84	384	432	240	138
	5.3x10-4	18				20				262			
	5.3x10-5	8				10				144			
	0.2% Offset	8											
200	5.3x10-3	170	156	185	183	181	160	187	212	75	91	56	35
	5.3x10-4	110				122				102			
	5.3x10-5	59				66				117			
	0.2% Offset	54											
100	5.3x10-3	452	322	333	228	457	356	381	335	32	27	29	48
	5.3x10-4	418				420				34			
	5.3x10-5	376				378				54			
	0.2% Offset	362											
RM	5.3x10-3	477	317	320	217	522	376	413	390	8	6	6	32
	5.3x10-4	534				538				11			
	5.3x10-5	521				543				6			
	0.2% Offset	508											

vs temperature at a given strain rate for each of the alloys. All four testing conditions are compared on each graph. Appendix B contains plots of UTS, yield and elongation vs temperature for a given processing condition. All the strain rates used for the testing are compared. Appendix C contains the plots of log stress and elongation vs log strain rate of 250°C and 300°C for each of the conditions. The values of m are given on the plots of log stress vs log strain rate.

Examination of the graphical or tabular data reveals the trends illustrated in Figure 4.6. Annealing either of the alloys results in softening at ambient temperature but strengthening at temperatures of 200°C to 300°C. The softening at low temperatures may be understood in terms of the effect of annealing on grain or substructure size and also the dislocation density. The Hall-Petch equation 4.1, where σ_y

$$\sigma_y = \sigma_0 + Ky(d)^{-\frac{1}{2}} \quad (\text{eqn 4.1})$$

is the yield strength, σ_0 is the lattice resistance to dislocation motion resulting from the effect of Mg in solution, strain hardening and other short ranged effects, Ky is a constant and d is the grain size. This expression includes the dislocation density in the σ_0 term and the grain size in d . The annealing reduces the dislocation density and hence the σ_0 term while increased d also results in a reduction of σ_y and this is the low temperature response observed in Figure 4.4, namely that the as rolled material with its finer structure and higher dislocation density is stronger than those materials annealed either at 300°C or 440°C.

SCHEMATIC EFFECTS OF ANNEALING

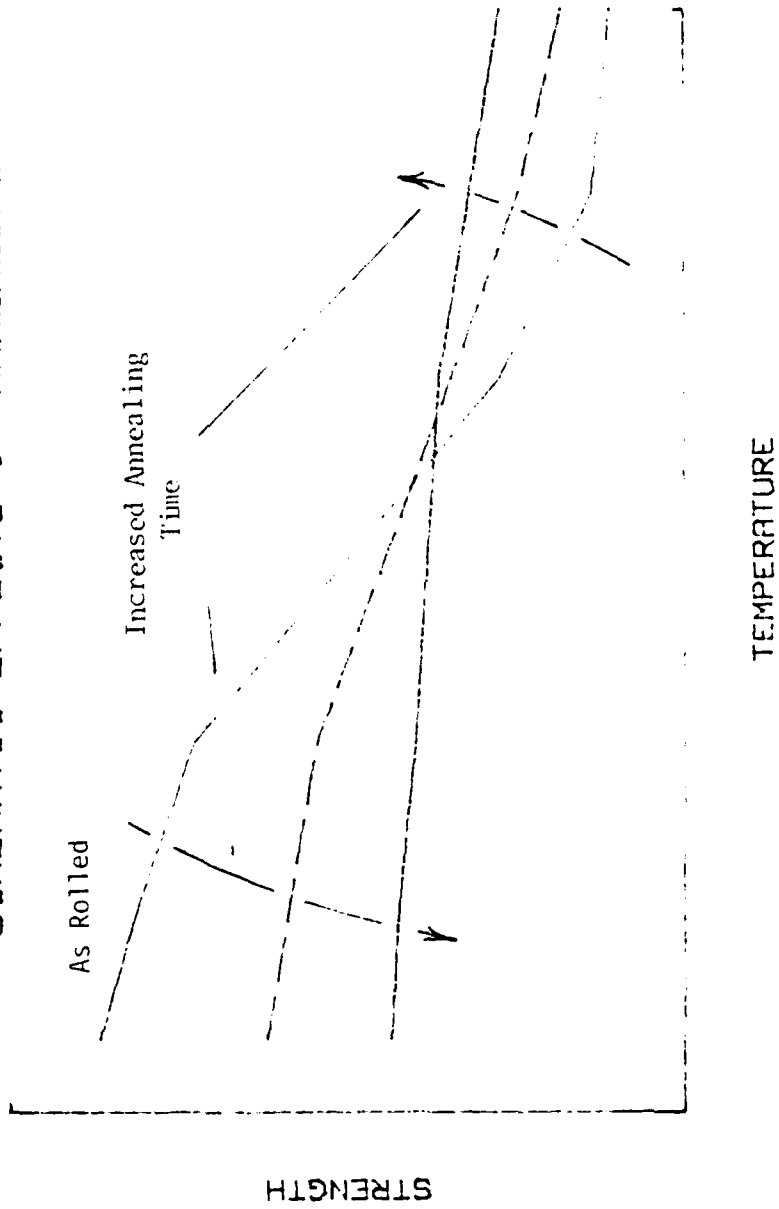


Figure 4.6 Schematic Showing the Affects of Annealing on the Tensile Strength.

As the temperature increases other deformation mechanisms gain increasing significance. Dislocation creep, Coble creep and grain boundary sliding start to be important in the middle range test temperatures. For test temperature in the upper portion of test range (300°C), grain boundary sliding likely starts to be the dominant mechanism. Due to the finer structure in the as rolled material, this condition exhibits the least strength at the elevated temperature. As temperature increases grain boundary sliding gains significance and the finer grain sized, as rolled condition becomes the lowest strength material.

Whereas annealing resulted in increased low temperature ductility as strength decreased, the effects of prior annealing on the elevated temperature ductility are more complex. An important factor appears to be grain growth during the course of the test, and increase in grain size will suppress grain boundary sliding and result in dislocation creep processes dominating with a reduced ductility.

To reach 100% elongation at strain rates of $5.3 \times 10^{-3} \text{ S}^{-1}$, $5.3 \times 10^{-4} \text{ S}^{-1}$ and $5.3 \times 10^{-5} \text{ S}^{-1}$ require approximately 3 minutes, 30 minutes and 5 hours, respectively. The latter times are comparable to the annealing treatments employed prior to elevated temperature testing for those materials annealed at 300°C . The 8% Mg alloy exhibits its most superplastic behavior at a strain rate of $5.3 \times 10^{-5} \text{ S}^{-1}$ and at a temperature of 250°C . At the 300°C temperature and the $5.3 \times 10^{-5} \text{ S}^{-1}$ strain rate, the effects of grain growth likely have overtaken the effects of grain boundary sliding and result in the non-recrystallized samples all coming to about the same structure and elongation. At 300°C , the 8% Mg alloy is near the solvus for Mg in the alloy and hence the Mg is tending to

go into the solid solution. A result would be a relatively small volume fraction of beta to retard grain growth. Applying the lever rule at 300°C, the beta content is calculated to be about 3 weight percent, while the equilibrium beta content at 250°C is higher, 8 weight percent.

For the 10% Mg alloy the most superplastic behavior was observed in testing at 300°C, also the annealing temperature and at a strain rate of 5.3×10^{-3} S-1. This was in a sample with an annealing time of approximately 30 minutes. Both alloys at temperatures above 150°C have decreased yield and UTS with decreasing strain rate for all processing conditions. In the 8% Mg alloy, the elongation at elevated temperature increases with decreasing strain rate throughout the range investigated in these tests. However, the 10% Mg alloy has a maximum elongation at the 5.3×10^{-3} S-1 strain rate and lesser elongations for both faster and slower strain rates. It is notable that this peak elongation, more than 400%, is observed at this relatively high strain rate and at this relatively low temperature. As noted previously, Paton, Hamilton, Wert and Mahoney [Ref. 14], in their work on high strength 7475 aluminum alloy, report similar elongation but at 516°C and at a strain rate of approximately 10^{-4} S-1, 50 times slower a strain rate. The observation here of a higher rate for maximum elongation is of considerable technological importance in that superplastic forming is of limited application often because of the slow forming rate required to achieve the highest ductilities.

As only three strain rates were utilized for the testing of the 8% Mg alloy, it is difficult to generalize from the appearances of these curves. However it is interesting to note that the highest elongation

did not coincide with the greatest m value. Because no TEM work on deformed samples has been done it is difficult to explain this at present time.

For the 10% Mg alloy, 5 strain rates at 300°C were utilized. The maximum m value does occur at the region of maximum superplastic elongation, however the data on the log stress vs log strain rate plot do not suggest clearly the typical sigmodal behavior. In fact, these data are readily fit by a straight line. This could be a result of a sampling error or grain growth could be occurring for the longer test times at strain rate less than $5.3 \times 10^{-3} \text{ S}^{-1}$, causing a decreasing in elongation and strength. It should be noted that the m value is obtained from data at relatively small strains (20%) whereas fracture occurs at strains of 100-400%. Further microscopy of samples in various stages of deformation will be required to develop data on the effect of grain size and changes in grain size during deformation.

Figure 4.7 and Figure 4.8 show a series of stress-strain curves for the 8% Mg alloy in an as rolled condition for a strain rate of $5.3 \times 10^{-3} \text{ S}^{-1}$. The flat nature of the curves for elevated temperatures indicate little grain growth during deformation, at least to the extent to which these curves can be analyzed. At larger strains, necking becomes appreciable and affects the reduction of the data to true stress vs true strain.

D. DEFORMED MICROSTRUCTURE

One of the important problems found in superplastic materials is the tendency to cavitate during deformation. This cavitation is often evident even at a low magnification in optical microscopy. Figures 4.9, 4.10 and

Al-8.14%Mg-0.4%Cu AS ROLLED 5.3x10-3

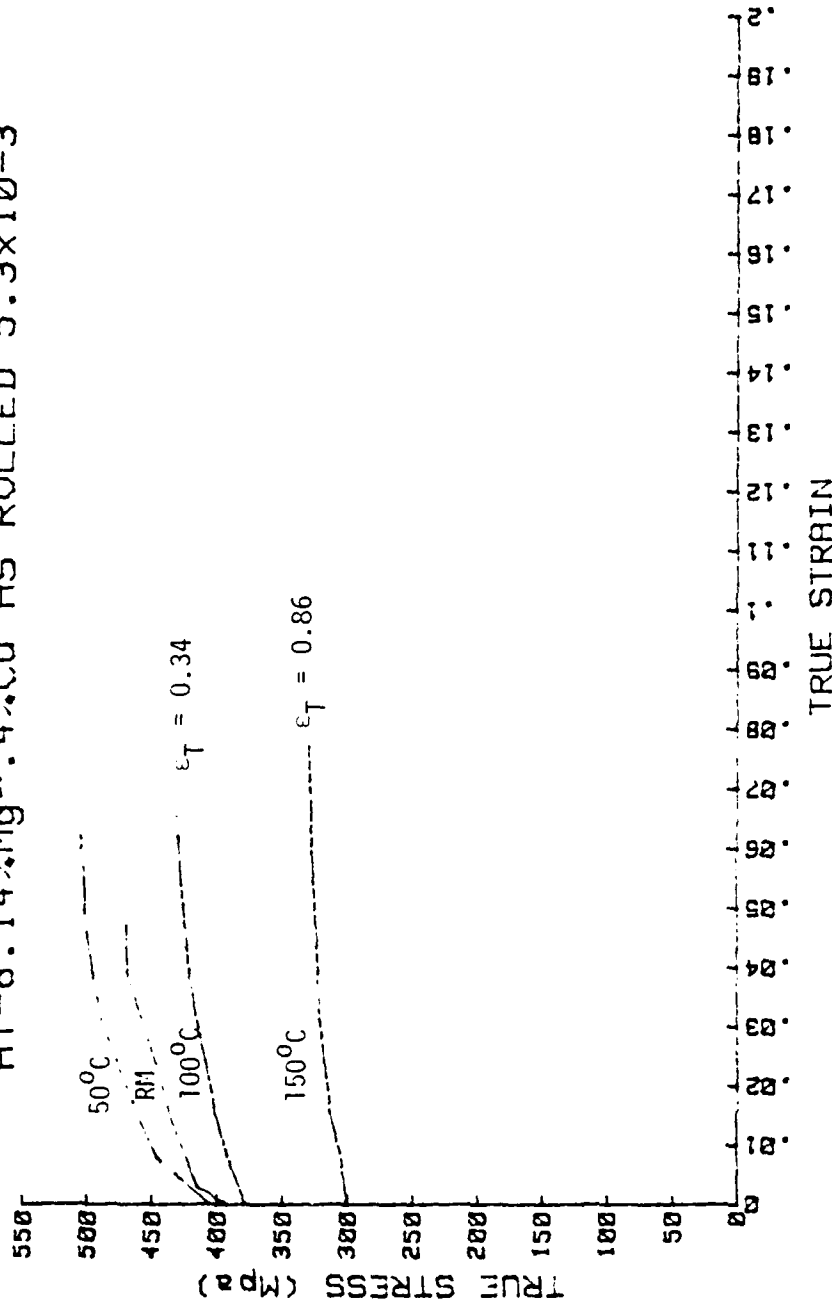


Figure 4.7 True Stress Versus True Strain for Al-8.14%Mg-0.4%Cu in an As Rolled Condition from Room Temperature to 150°C.

Al-8.14%Mg-0.4%Cu AS ROLLED 5.3x10⁻³

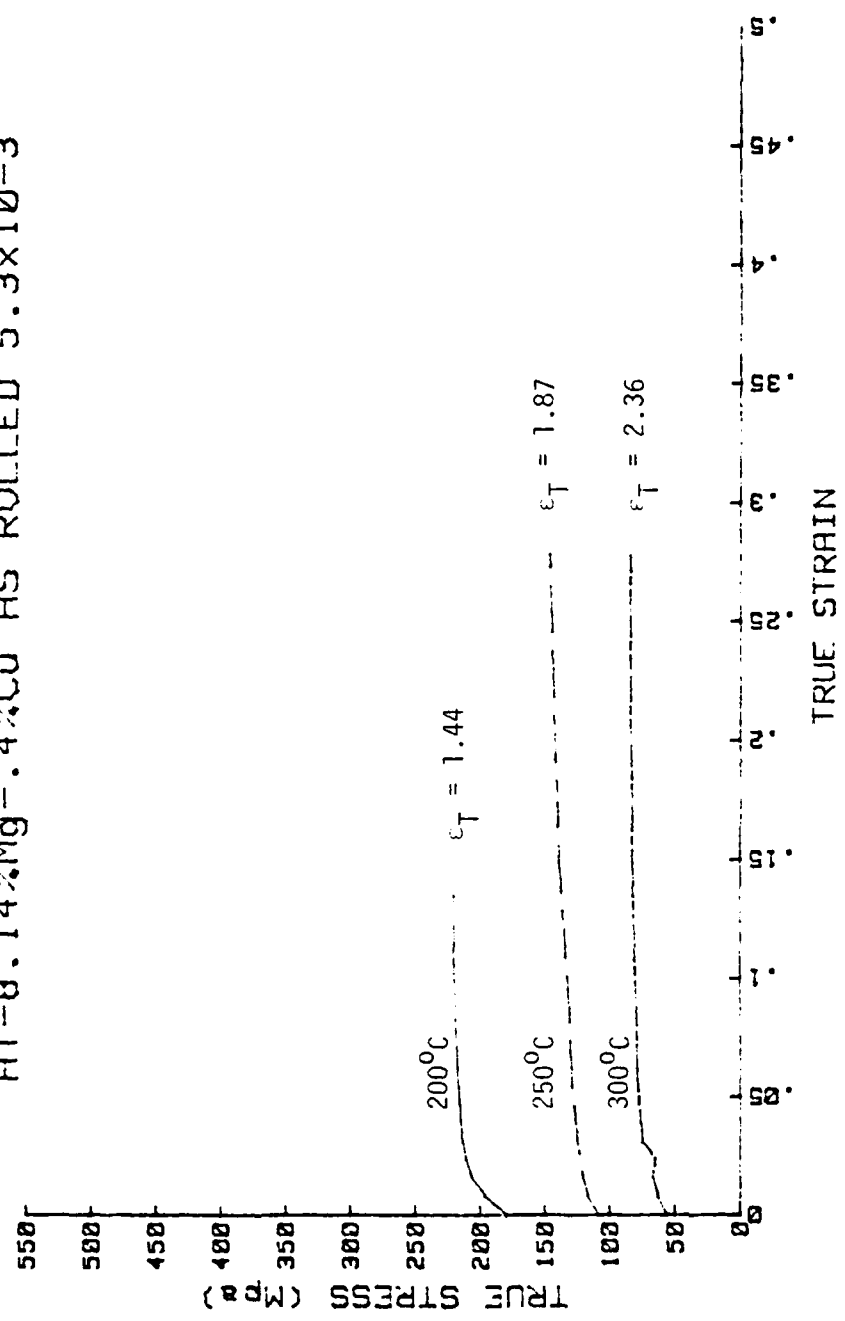
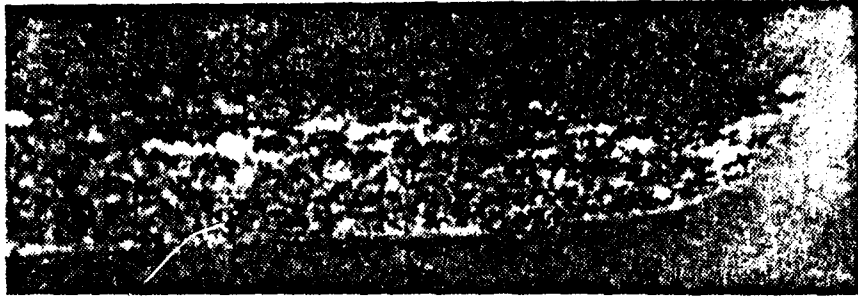
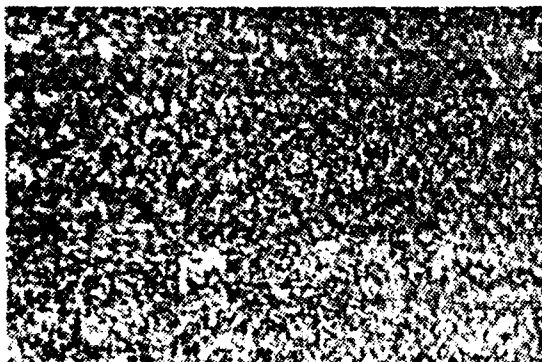


Figure 4.8 True Stress Versus True Strain for Al-8.14%Mg-0.4%Cu in an As Rolled Condition from 200-300°C.

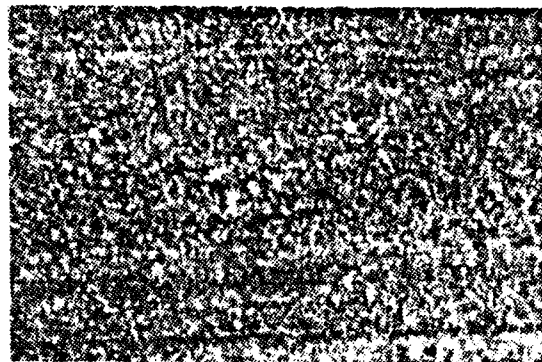
4.11 show the microstructures of deformed gage sections of three samples. The micrographs are taken at various locations along the length of the deformed specimens. Locations are at the fracture point, 1/4 the way from the fracture to the specimen grip section, 1/2 the way from the fracture, 3/4 the way from the fracture and at the undeformed grip section. No cavitation was noted in this specimen. It can be seen that a fine structure is maintained, beta is well dispersed in all the locations and the banding seen in the initial as rolled condition is not seen here.



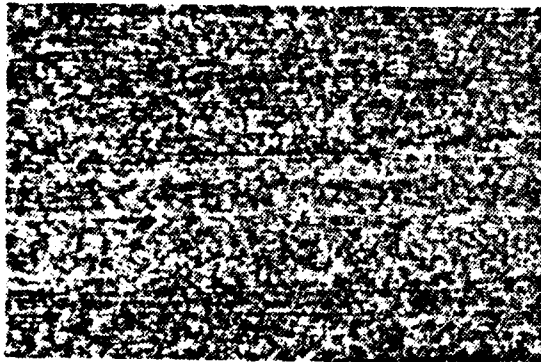
FRACTURE POINT



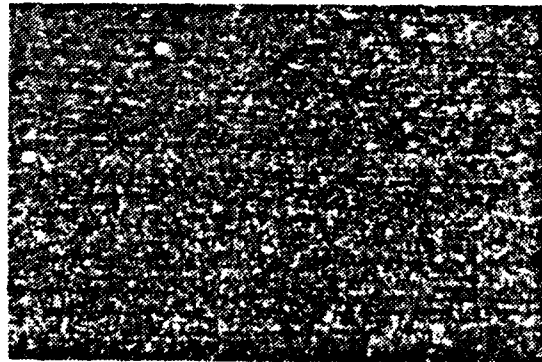
1/4 FROM FRACTURE



1/2 FROM FRACTURE

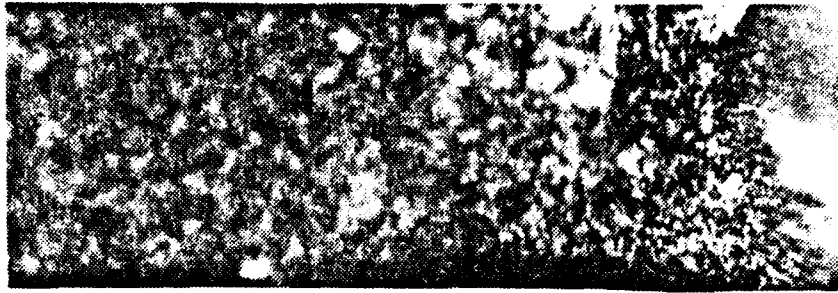


3/4 FROM FRACTURE

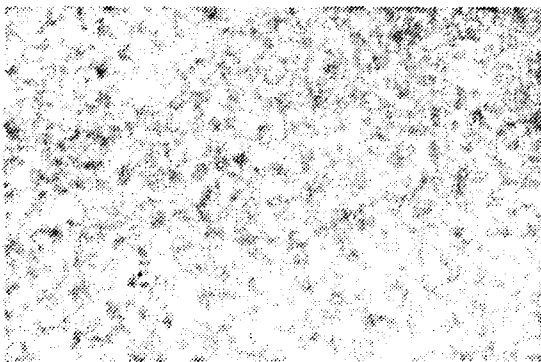


UNDEFORMED END

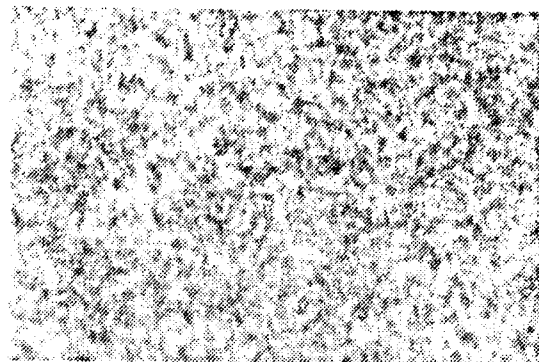
Figure 4.9 Optical Micrographs of As Polled Al-8.14%Mg-0.4%Cu Tested at 300°C and 5.3×10^{-9} (S-1) Strain Rate Taken at Various Positions Along the Specimen After Tensile Testing at 200x.



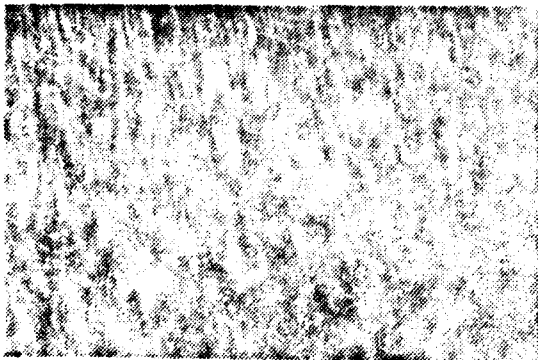
FRACTURE POINT



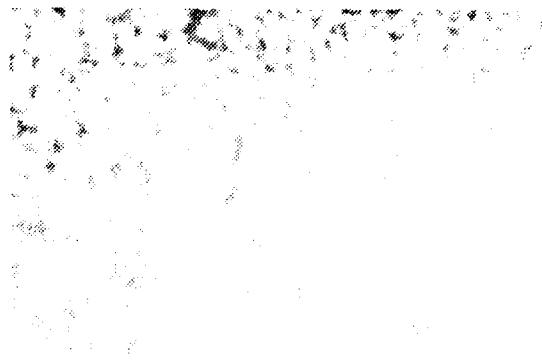
1/4 FROM FRACTURE



1/2 FROM FRACTURE

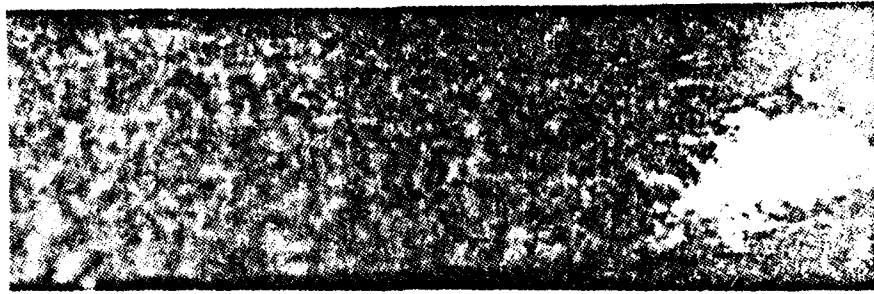


3/4 FROM FRACTURE

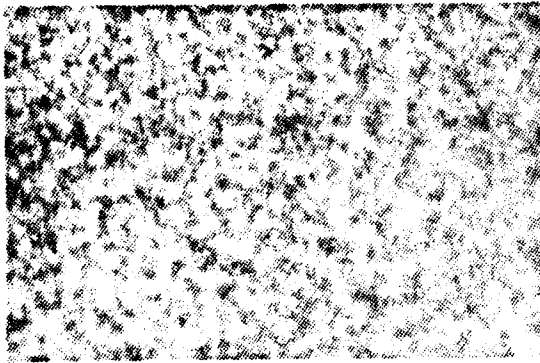


UNDEFORMED END

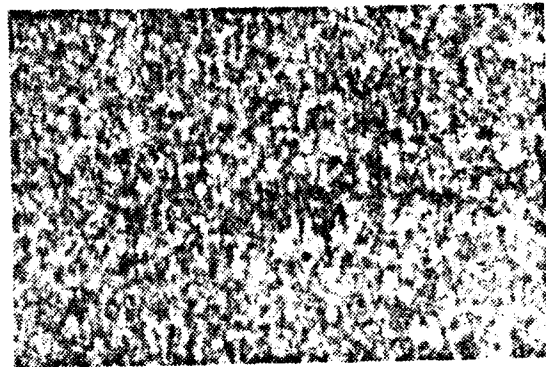
Figure 4.10 Optical Micrographs of As Rolled Al-10.29%Mg-0.52%Mn Tested at 300°C and 5.3×10^{-3} (S-1) Strain Rate Taken at Various Locations Along the Specimen After Tensile Testing at 200x.



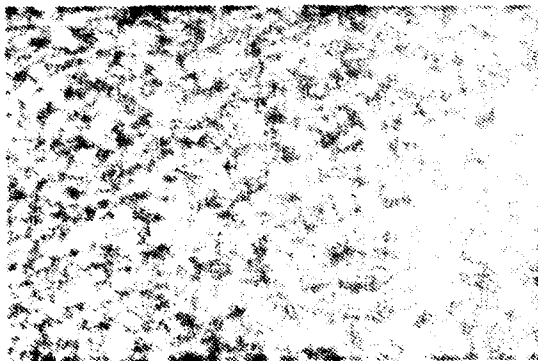
FRACTURE POINT



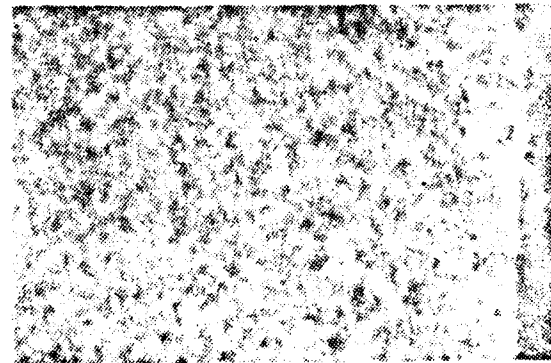
1/4 FROM FRACTURE



1/2 FROM FRACTURE



3/4 FROM FRACTURE



UNDEFORMED END

Figure 4.11 Optical Micrographs of Al-10.2%Mg-0.52%Mn Annealed for 10 hrs. at 300°C and 5.3×10^{-3} (S-1) Strain Rate Taken at Various Locations Along the Specimen After Tensile Testing at 200x.

V. CONCLUSIONS AND RECOMMENDATIONS

The following conclusions are drawn from this research: 1) Optical microscopy does not reveal the grain structure of these alloys; rather, TEM is required to reveal grain and subgrain structures as well as the details of the dispersion of the intermetallic beta; 2) superplastic elongations up to 400% are attainable in high-magnesium, aluminum-magnesium alloys at temperatures of 200-300°C, and in the 10.2%Mg-0.52%Mn alloy, at strain rates up to about 5×10^{-3} S⁻¹; 3) warm rolled materials tend to exhibit the greatest degree of superplasticity; the beta phase tends to stabilize grain structures and when the solvus temperature is approached, resolutioning of the beta leads to grain growth and loss of superplastic characteristics, as observed in the 8.14%Mg-0.4%Cu alloy; 4) the higher magnesium content of the 10.2%Mg-0.52%Mn alloy likely stabilizes grain size and extends the range of superplastic behavior to higher temperatures in this alloy. The following recommendations for further study are made: 1) study by TEM of the microstructure of deformation be conducted to ascertain the extent of grain growth during deformation; 2) study of the deformation characteristics especially of the 10.2%Mg-0.52%Mn alloy be conducted with more closely spaced strain rates and temperatures to better define the rate and temperature dependence in these alloys; 3) additional alloy compositions be study to delineate the effects separately of the Mg, Mn, Cu, and other possible alloy additions such as Zr and Zn.

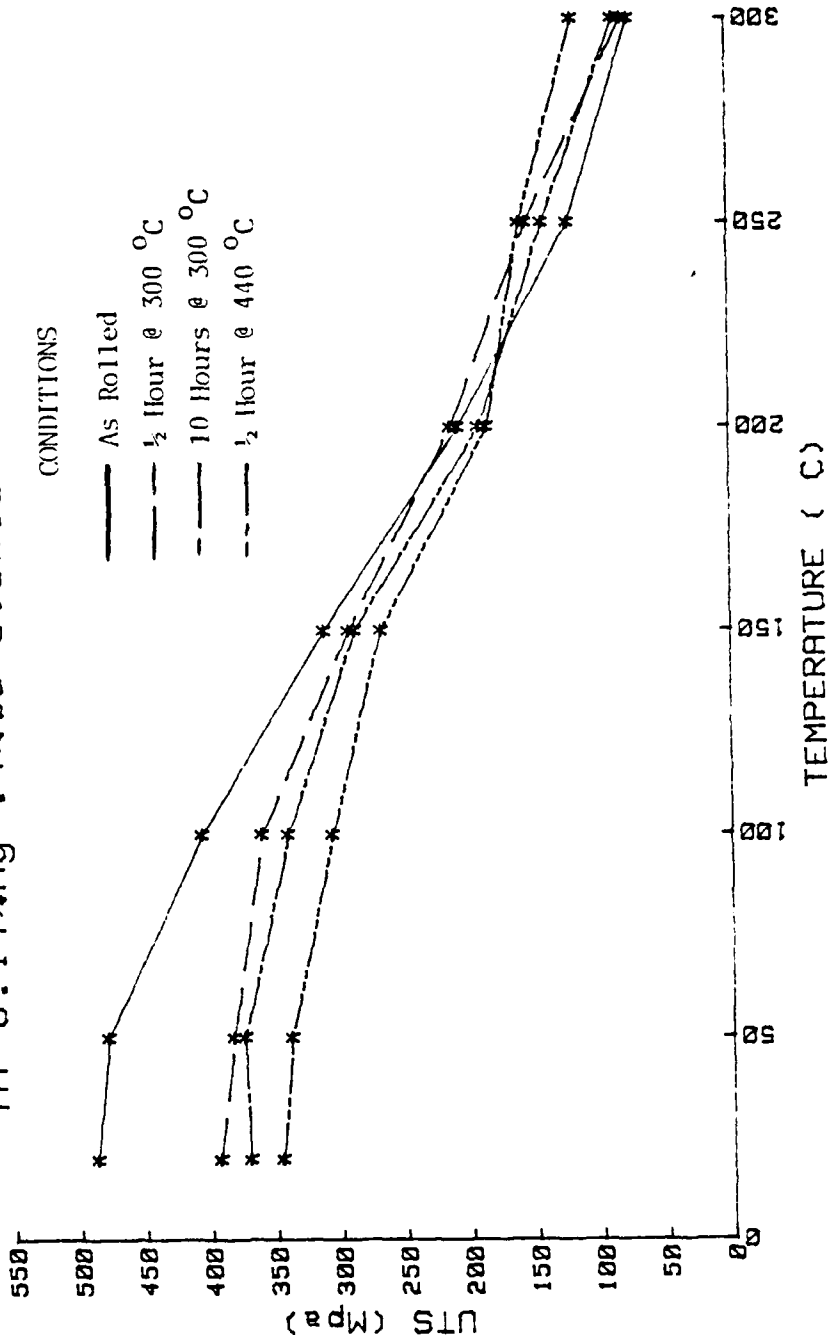
LIST OF REFERENCES

1. Ness, F. G., Jr., High Strength to Weight Aluminum-18 Weight Percent Magnesium Alloy Through Thermomechanical Processing, M.S. Thesis, Naval Postgraduate School, Monterey, California, December 1976.
2. Bingay, C. P., Microstructural Response of Aluminum-Magnesium Alloys to Thermalmechanical Processing, M.S. Thesis, Naval Postgraduate School, Monterey, California, December 1977.
3. Glover, T. L., Effects of Thermomechanical Processing on Aluminum-Magnesium Alloys Containing High Weight Percent Magnesium, M.S. Thesis, Naval Postgraduate School, Monterey, California, December 1977.
4. Grandon, R. A., High Strength Aluminum-Magnesium Alloys: Thermo-mechanical Processing, Microstructure and Tensile Mechanical Properties, M.S. Thesis, Naval Postgraduate School, Monterey, California, December 1976.
5. Speed, W. G., An Investigation into the Influence of Thermomechanical Processing on Microstructure and Mechanical Properties of High Strength Aluminum-Magnesium Alloys, M.S. Thesis, Naval Postgraduate School, Monterey, California, December 1977.
6. Chesterman, C. W., Jr., Precipitation, Recovery and Recrystallization Under Static and Dynamic Conditions for High Magnesium Aluminum-Magnesium Alloys, M.S. Thesis, Naval Postgraduate School, Monterey, California, March 1980.
7. Johnson, R. B., The Influence of Alloy Composition and Thermomechanical Processing Procedure on Microstructural and Mechanical Properties of High-Magnesium Aluminum Magnesium Alloys, M.S. Thesis, Naval Postgraduate School, Monterey, California, June 1980.
8. Shirah, R. H., The Influence of Solution Time and Quench Rate on the Microstructure and Mechanical Properties of High Magnesium Aluminum-Magnesium Alloys, M.S. Thesis, Naval Postgraduate School, Monterey, California, December 1981.
9. McNelley, T. and Garg, A., "Development of Structure and Mechanical Properties in Al-10.2%Mg by Thermomechanical Processing," unpublished research, Naval Postgraduate School, Monterey, California.
10. Mondolfo, L. F., Aluminum Alloys: Structure and Properties, Butterfield and Co. (Publishers) 1976.

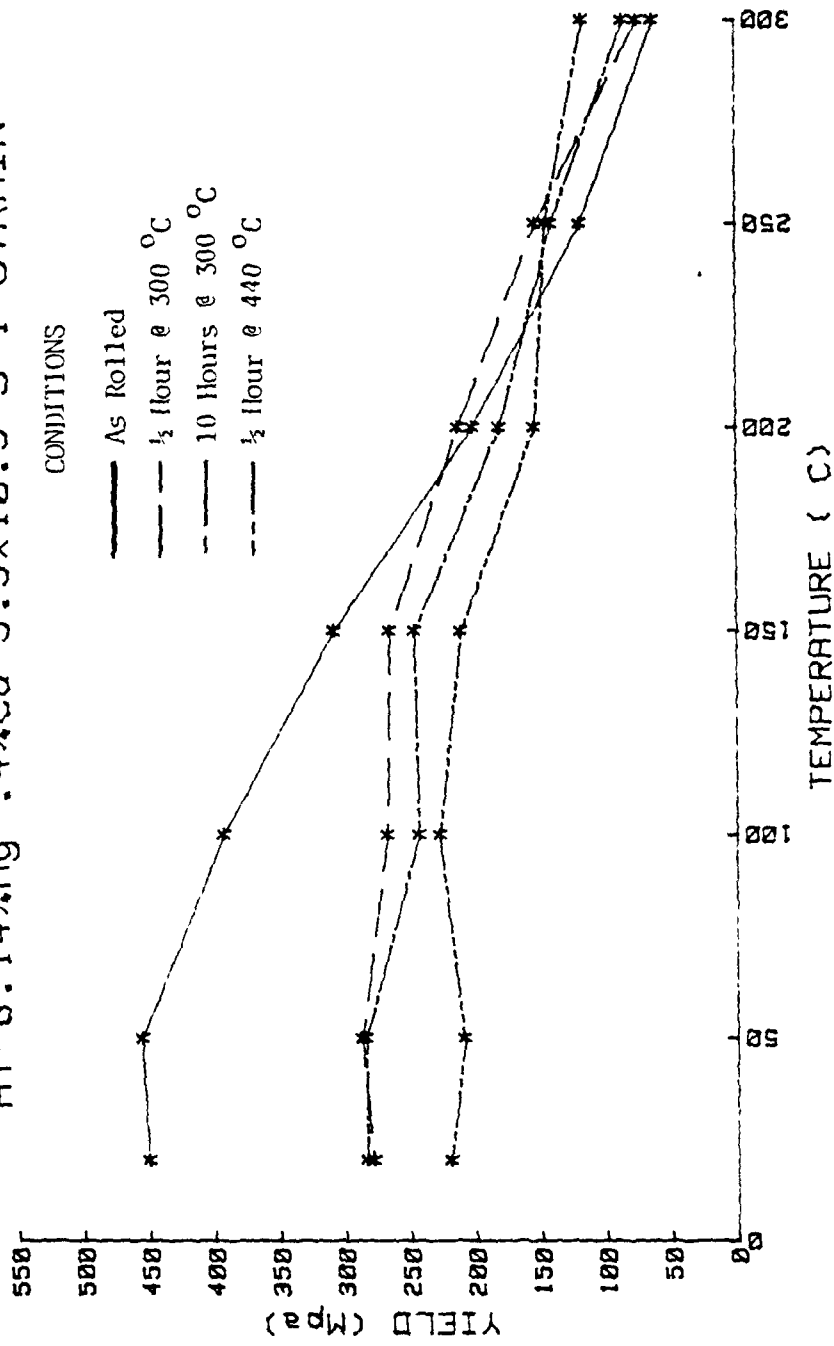
11. Bly, D. C., Sherby, O. D. and Young, C. M., "Influence of Thermal Mechanical Treatments on the Mechanical Properties of a Finely Spheroidized Eutectic Composition Steel," Material Science and Engineering, V. 12, pp. 41-46, 1973.
12. Underwood, L. F., Journal of Metals, pp. 914-919, 1962.
13. Avery, D. H. and Backofen, W. A., American Society of Metals Transmission Quarterly, V. 58, pp. 551-562, 1965.
14. Paton, N. E., Hamilton, C. H., Wert, J., and Mahoney, M., "Characterization of Fine-Grained Superplastic Aluminum Alloys," Journal of Metals, pp. 21-27, August 1982.
15. Ashby, M. F., and Verrall, R. A., Acta Metallography, Volume 21, pp. 149-163, 1973.

APPENDIX A

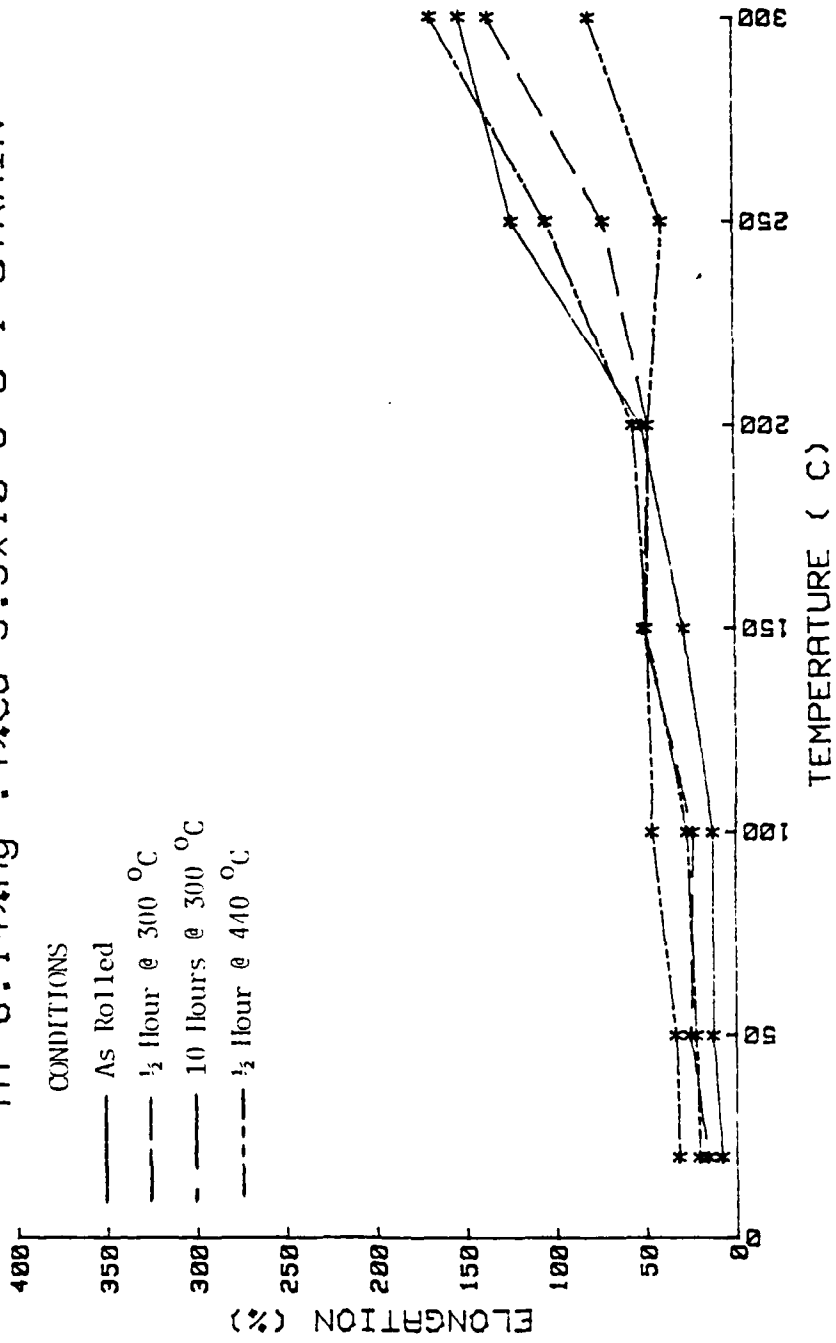
Al-8.14%Mg-.4%Cu 5.3x10⁻³ S-1 STRAIN



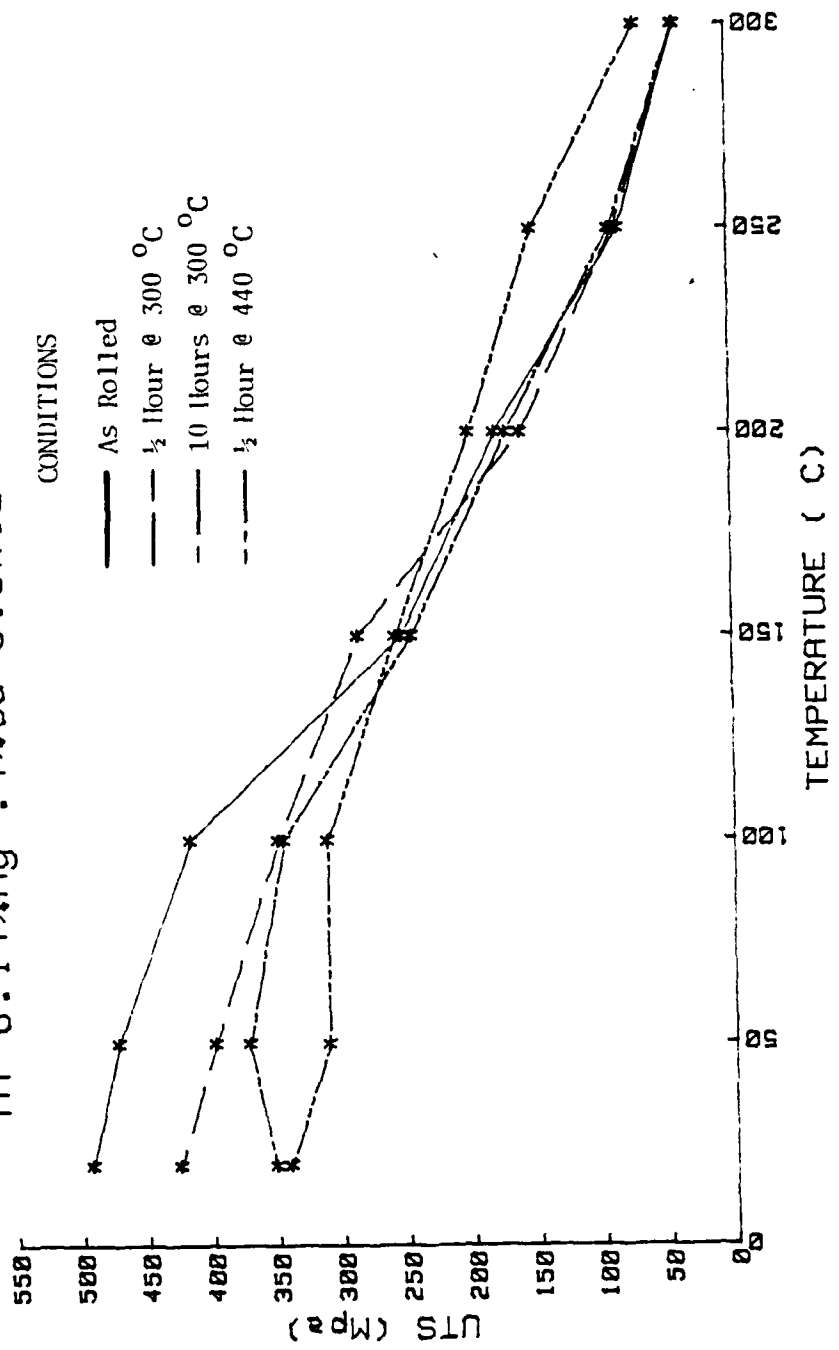
Al-8.14%Mg-.4%Cu 5.3x10.3 S-1 STRAIN



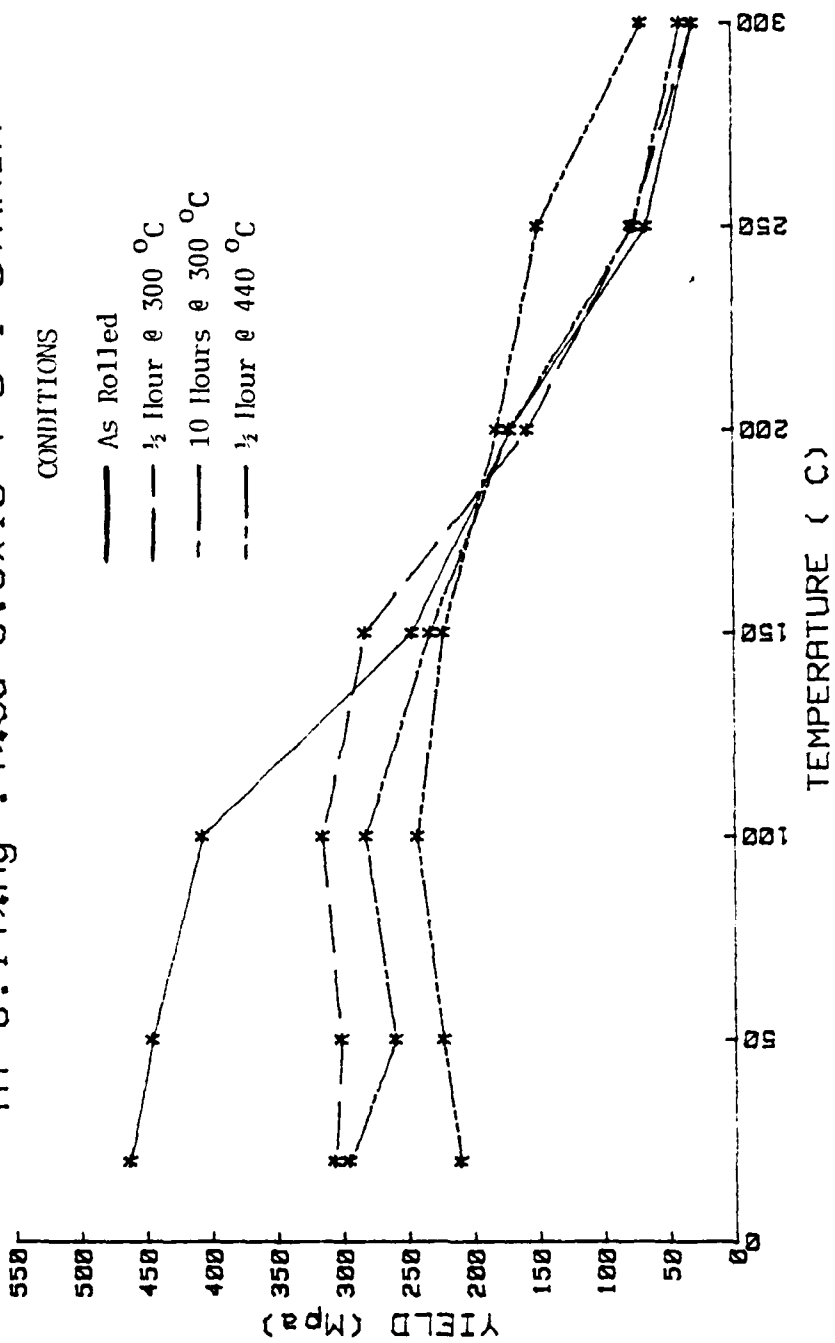
Al-8.14%Mg-.4%Cu 5.3x10⁻³ S-1 STRAIN



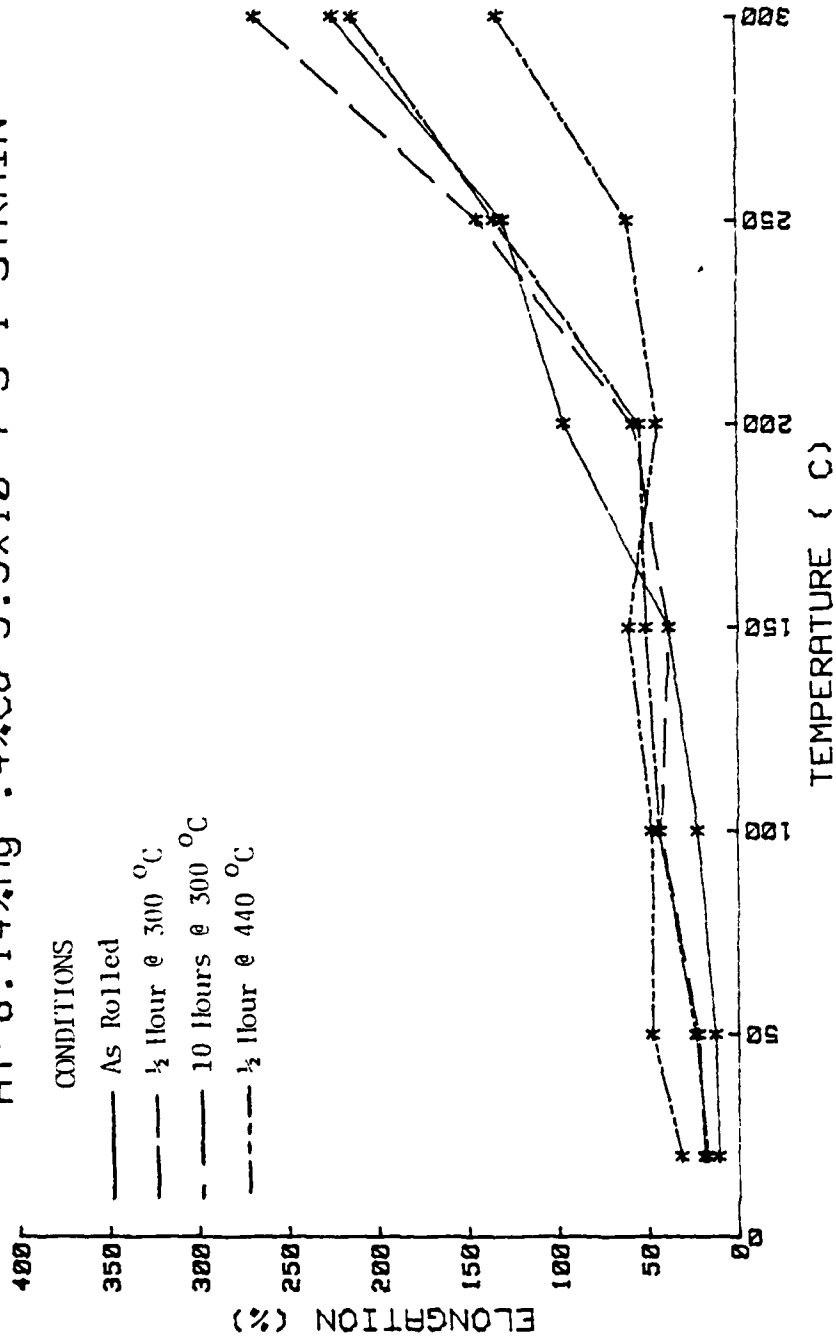
Al-8.14%Mg-.4%Cu 5.3x10⁻⁴ S-1 STRAIN



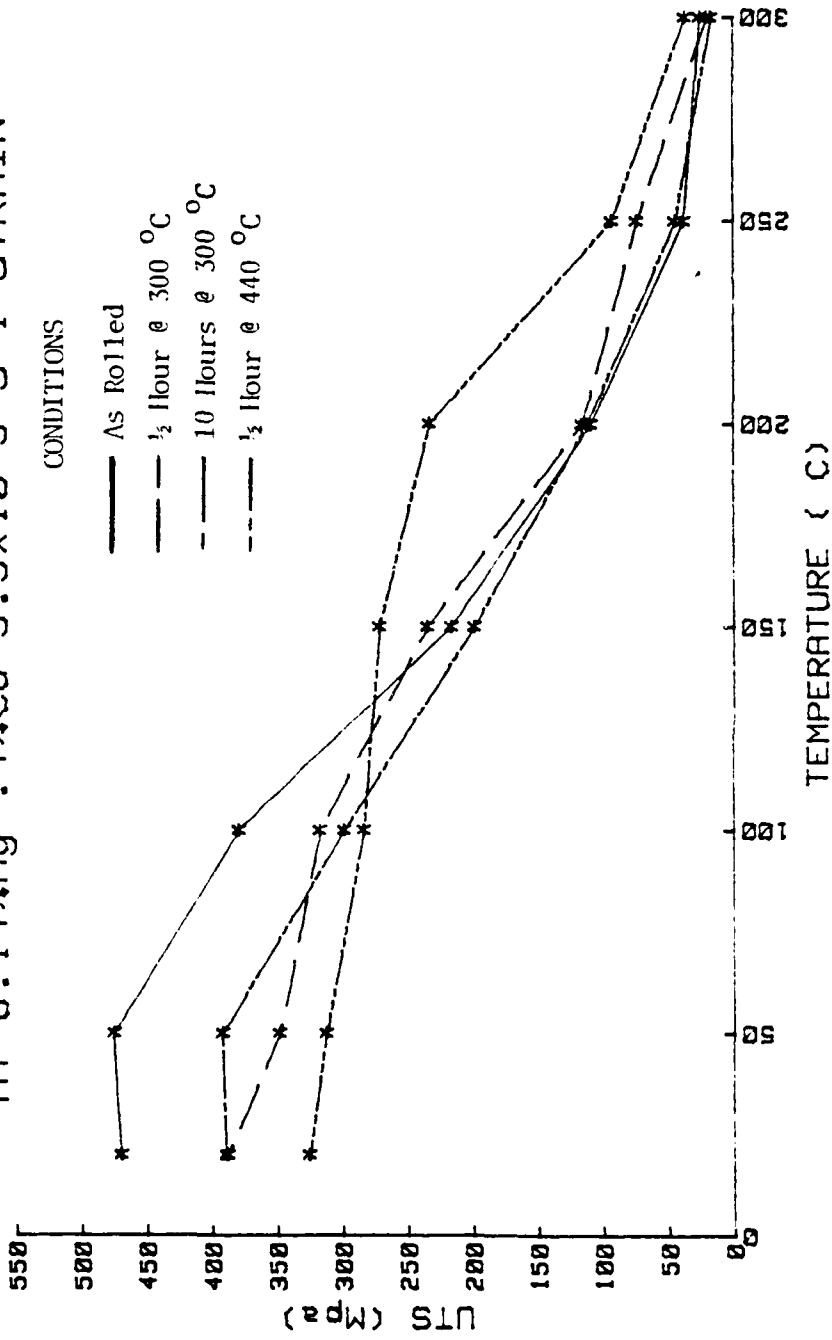
Al-8.14%Mg-.4%Cu 5.3×10^{-4} S-1 STRAIN



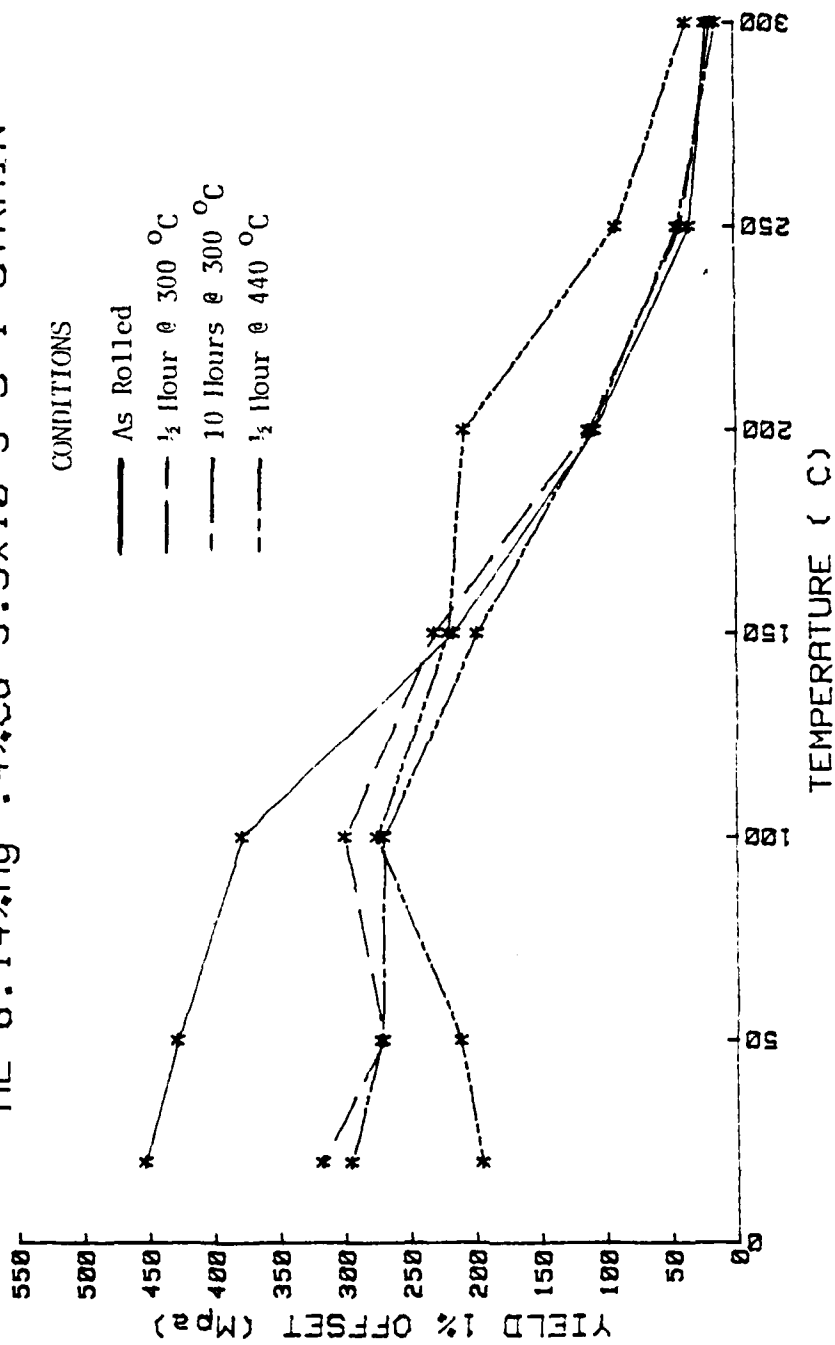
Al-8.14%Mg-.4%Cu 5.3x10⁻⁴ S-1 STRAIN



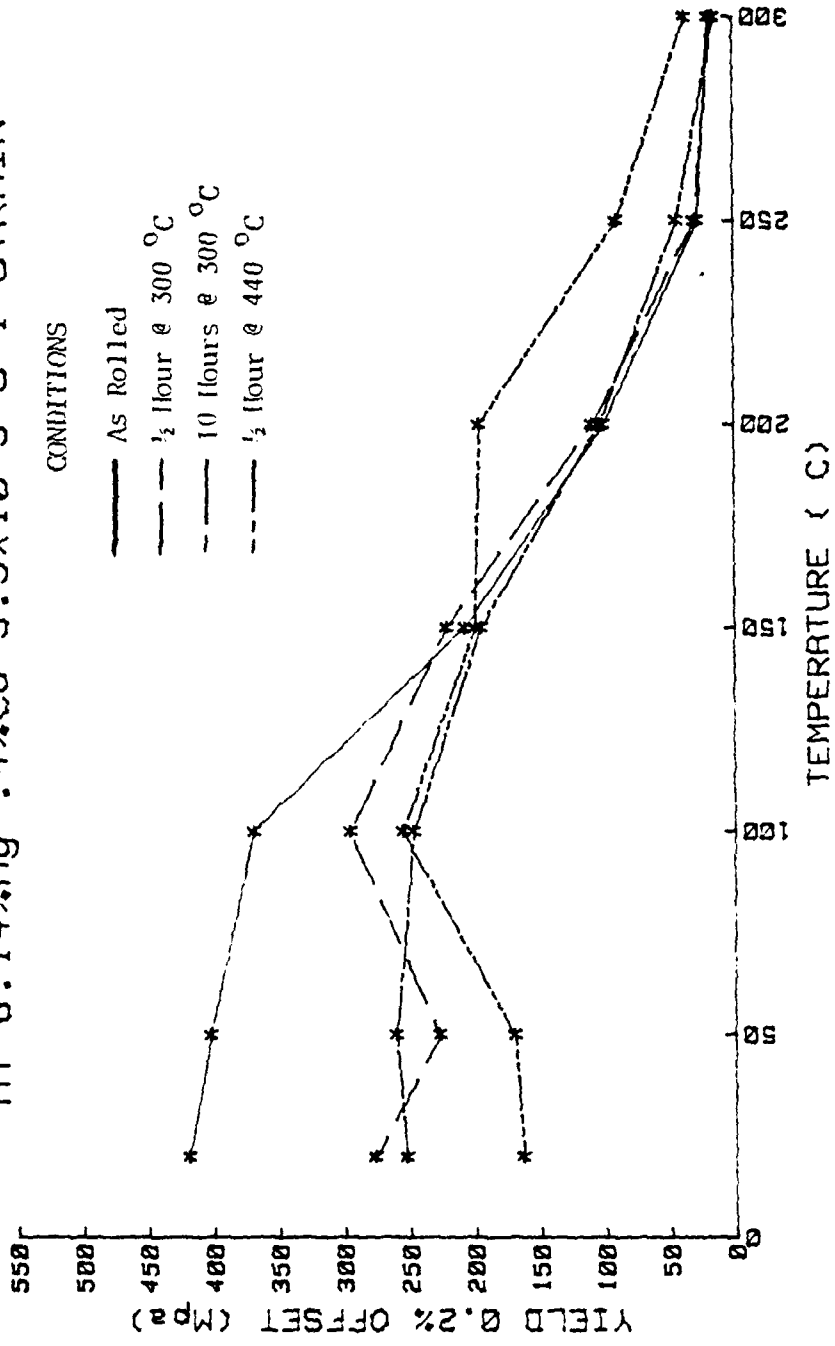
Al-8.14%Mg-.4%Cu 5.3x10⁻⁵ S-1 STRAIN



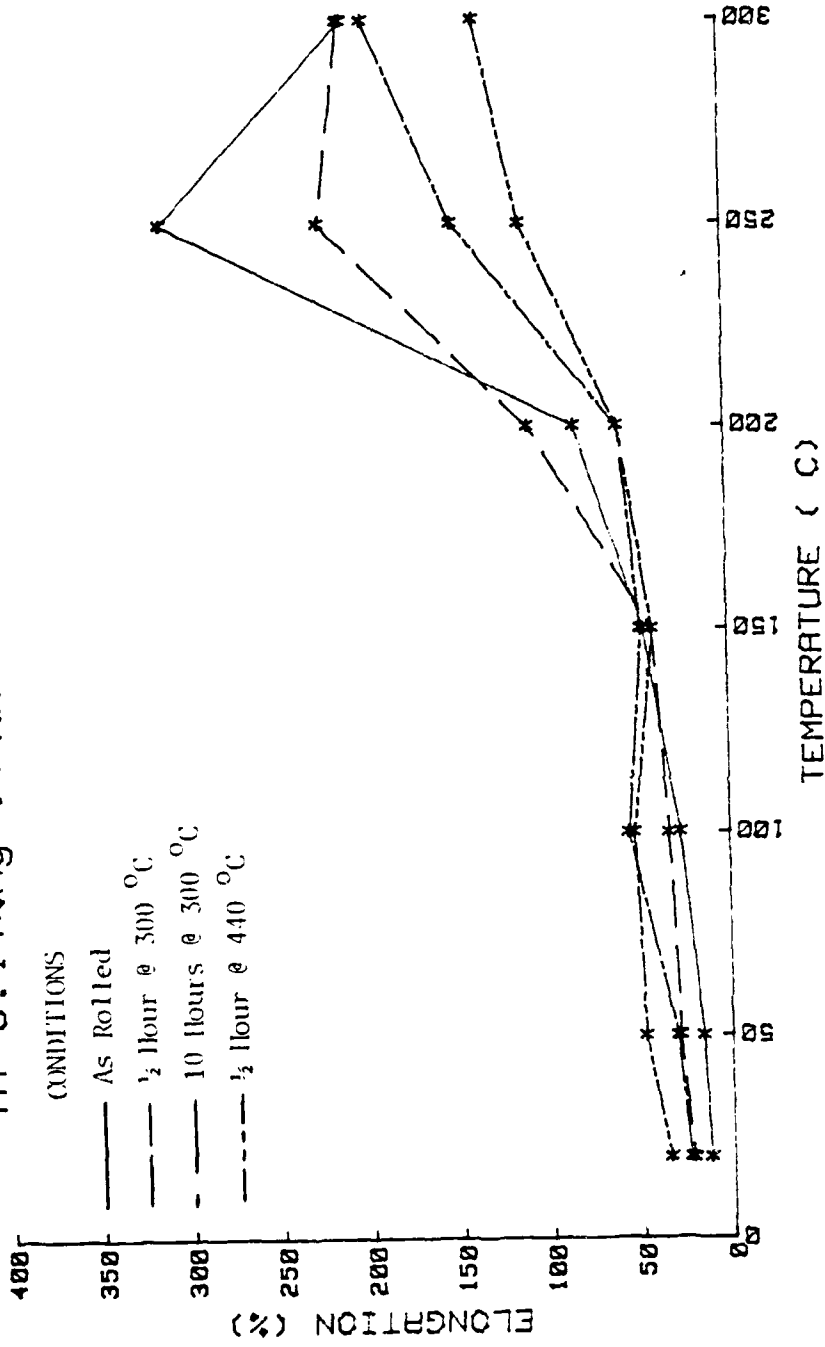
AL-8.14%Mg-.4%Cu 5.3x10⁻⁵ S-1 STRAIN



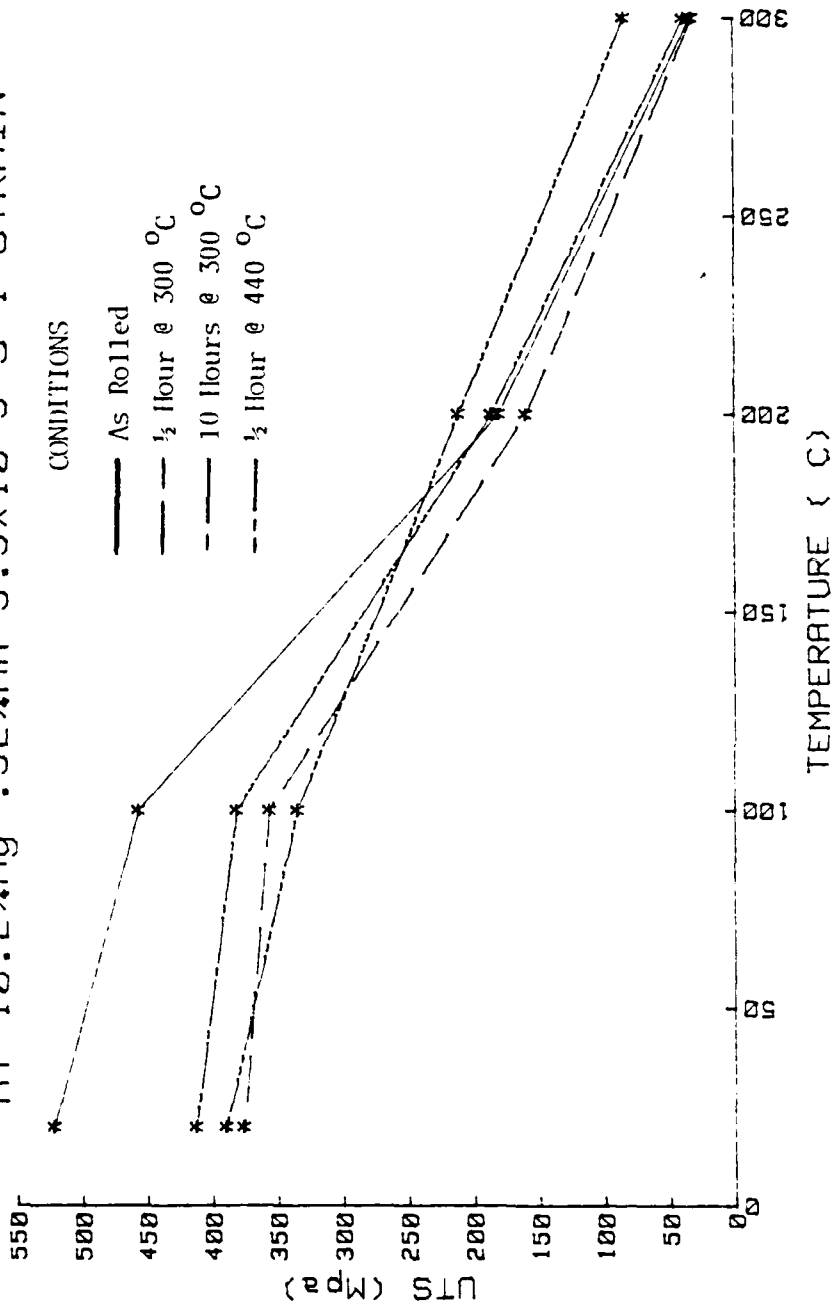
Al-8.14%Mg-.4%Cu 5.3x10⁻⁵ S-1 STRAIN



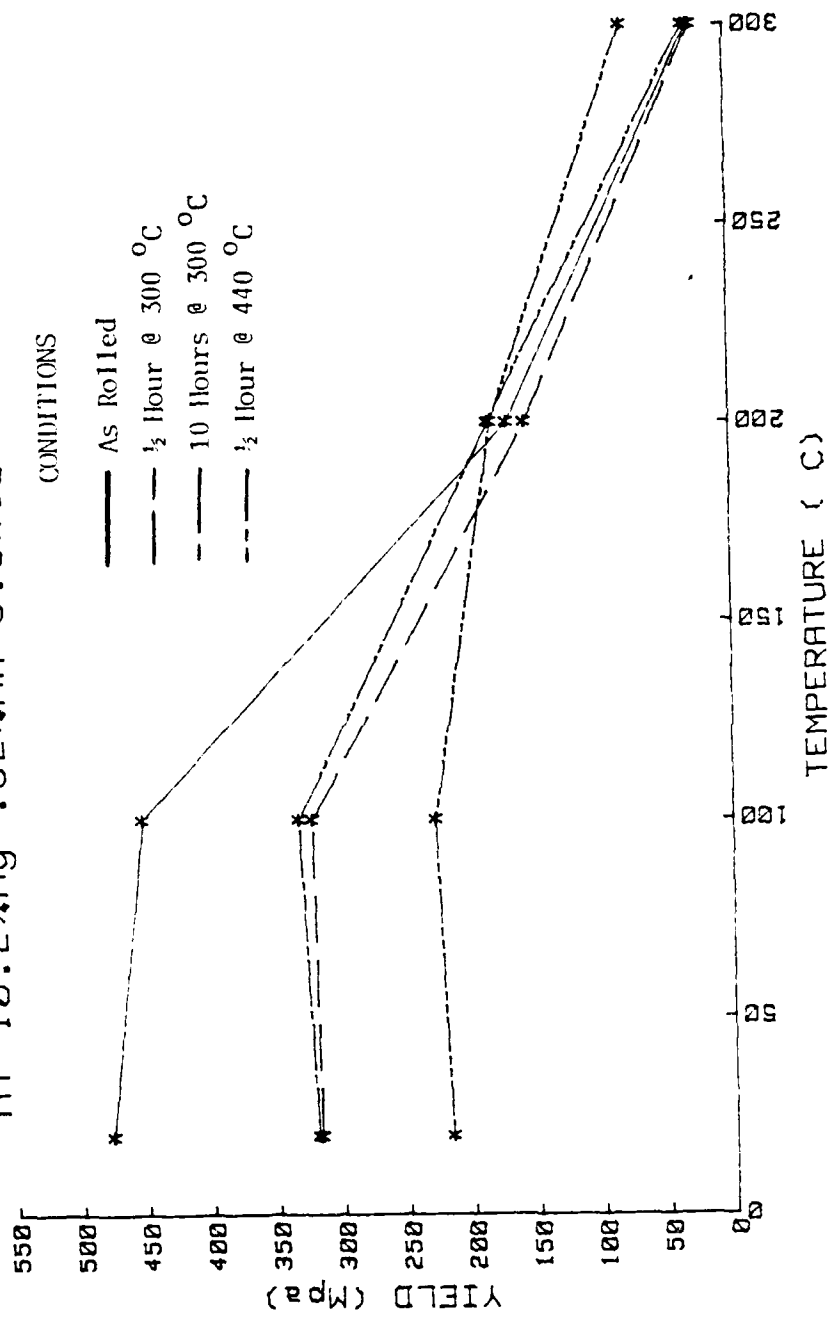
Al-8.14%Mg-.4%Cu 5.3x10⁻⁵ S-1 STRAIN



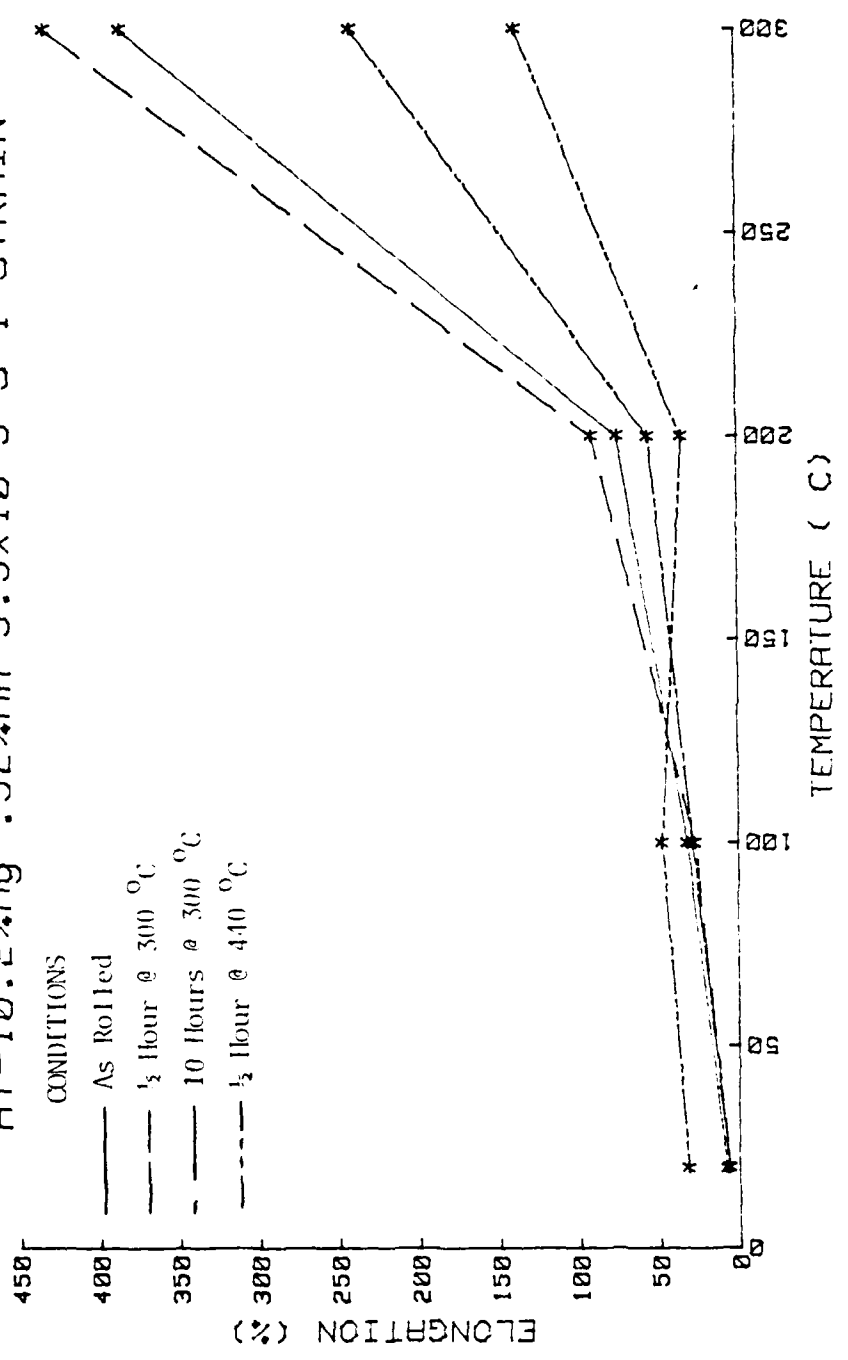
Al-10.2%Mg-.52%Mn 5.3x10⁻³ S-1 STRAIN



Al-10.2%Mg-.52%Mn 5.3x10⁻³ S-1 STRAIN

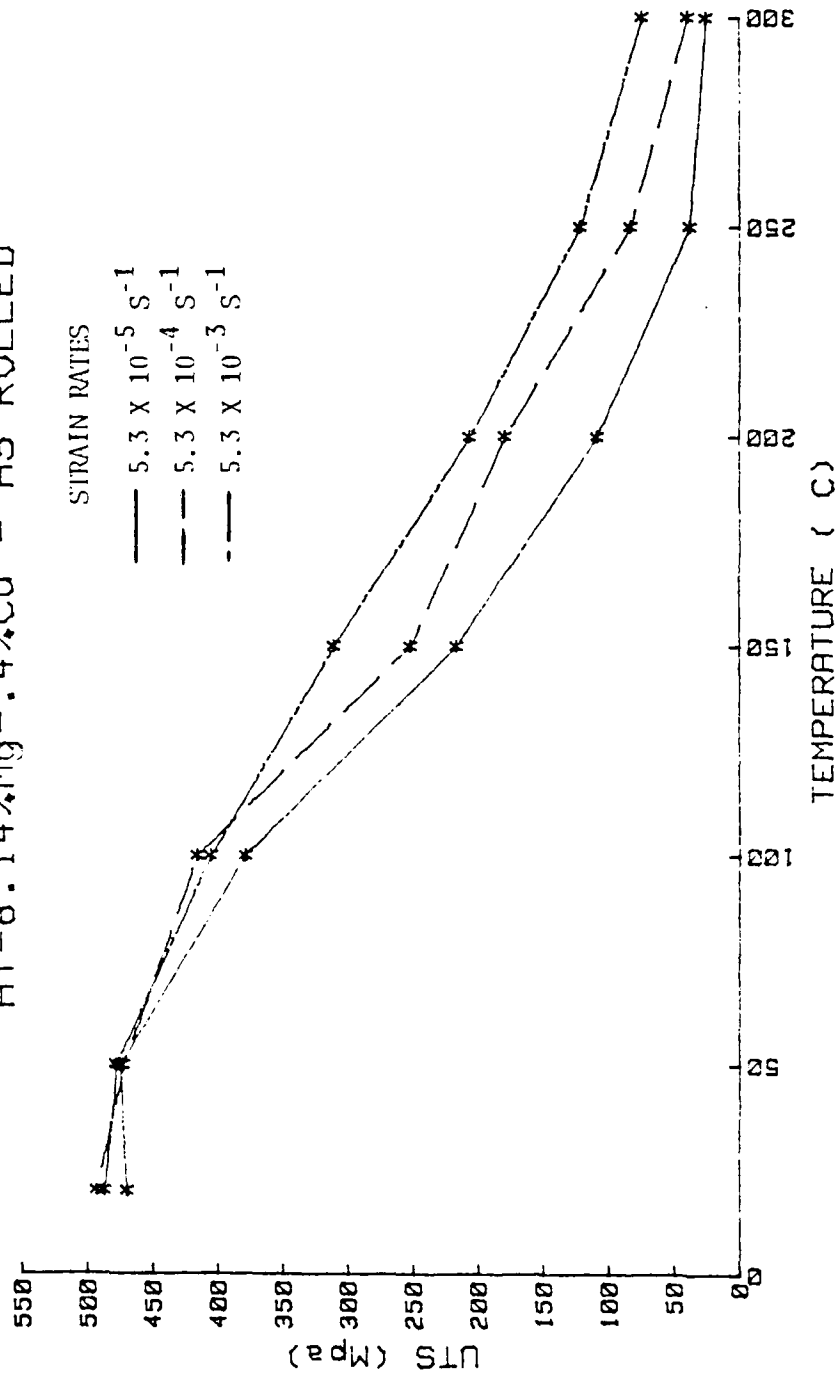


Al-10.2%Mg-.52%Mn 5.3x10⁻³ S-1 STRAIN

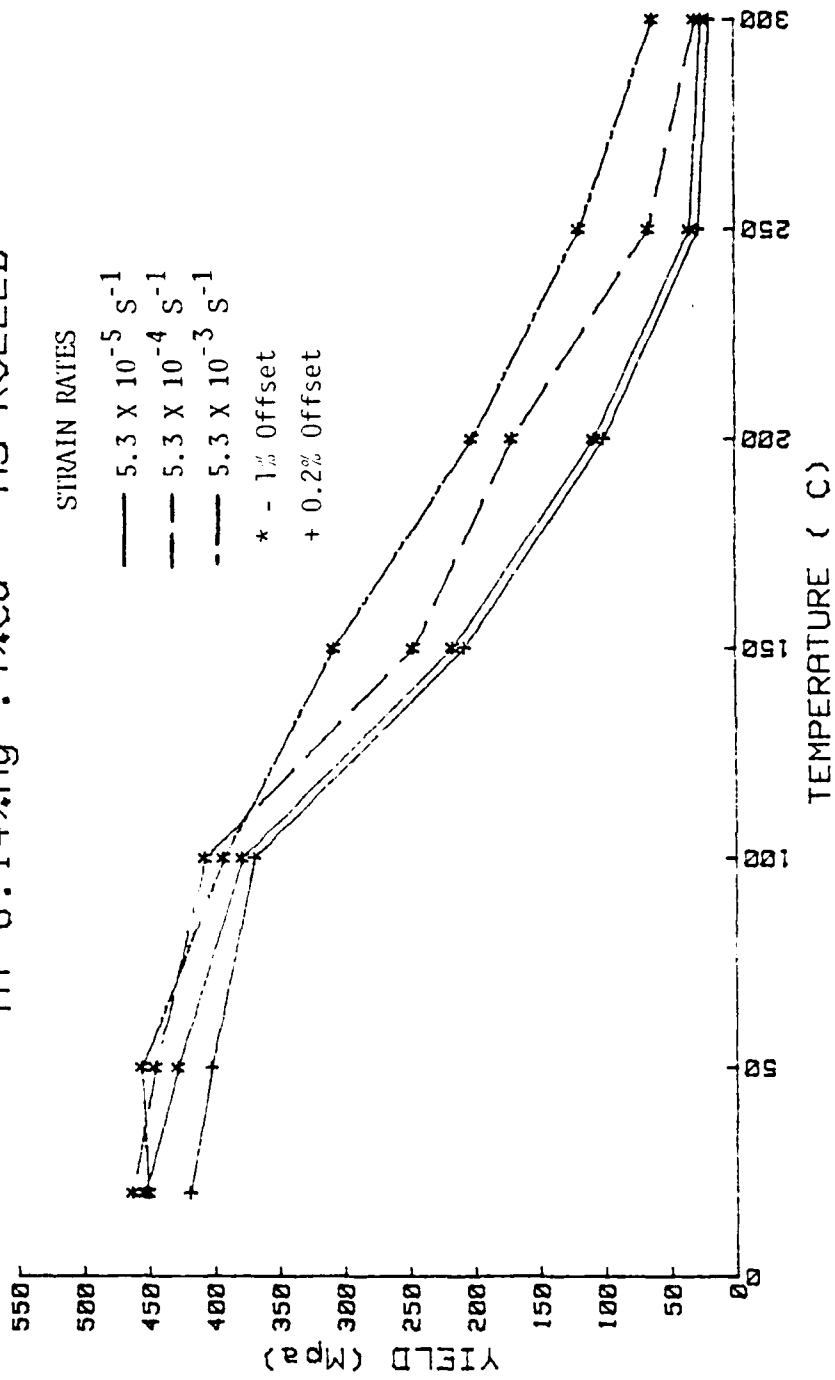


APPENDIX B

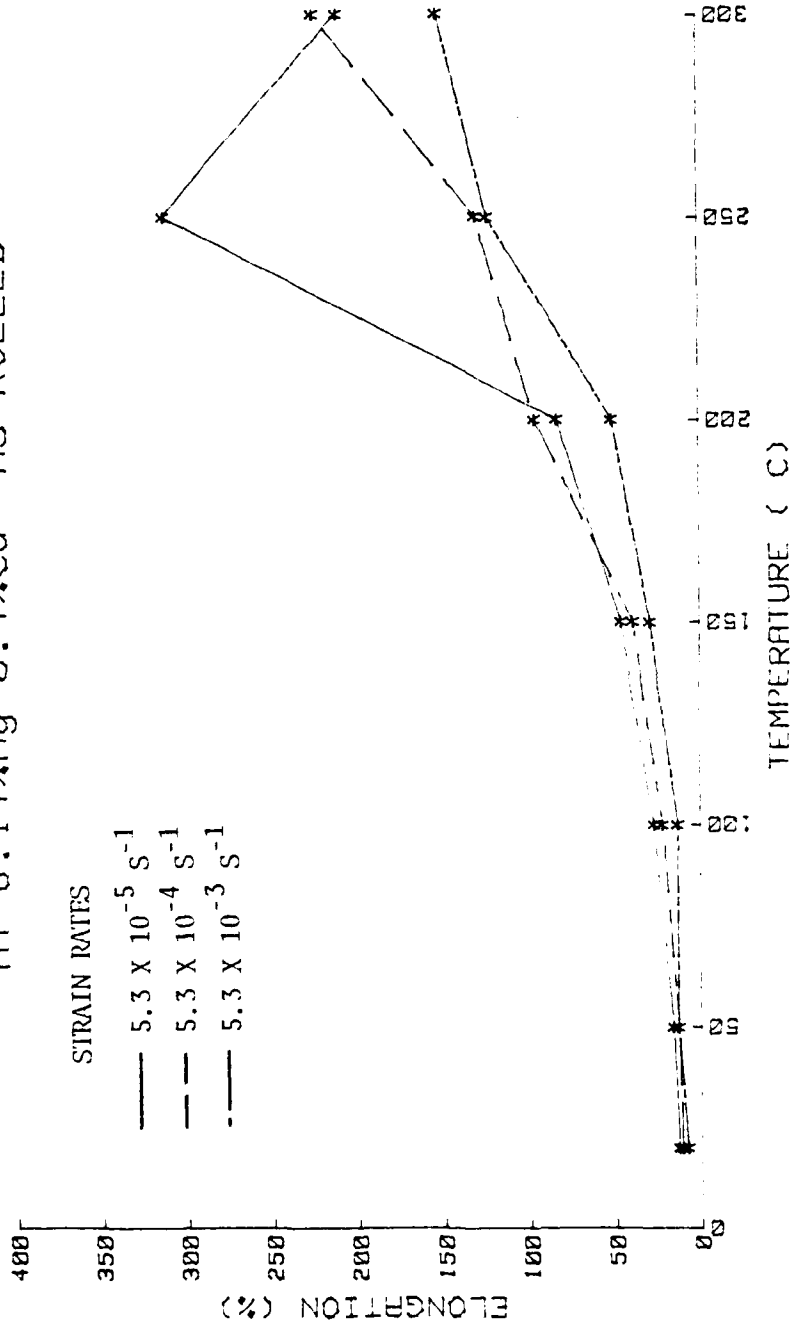
Al-8.14%Mg-.4%Cu - AS ROLLED



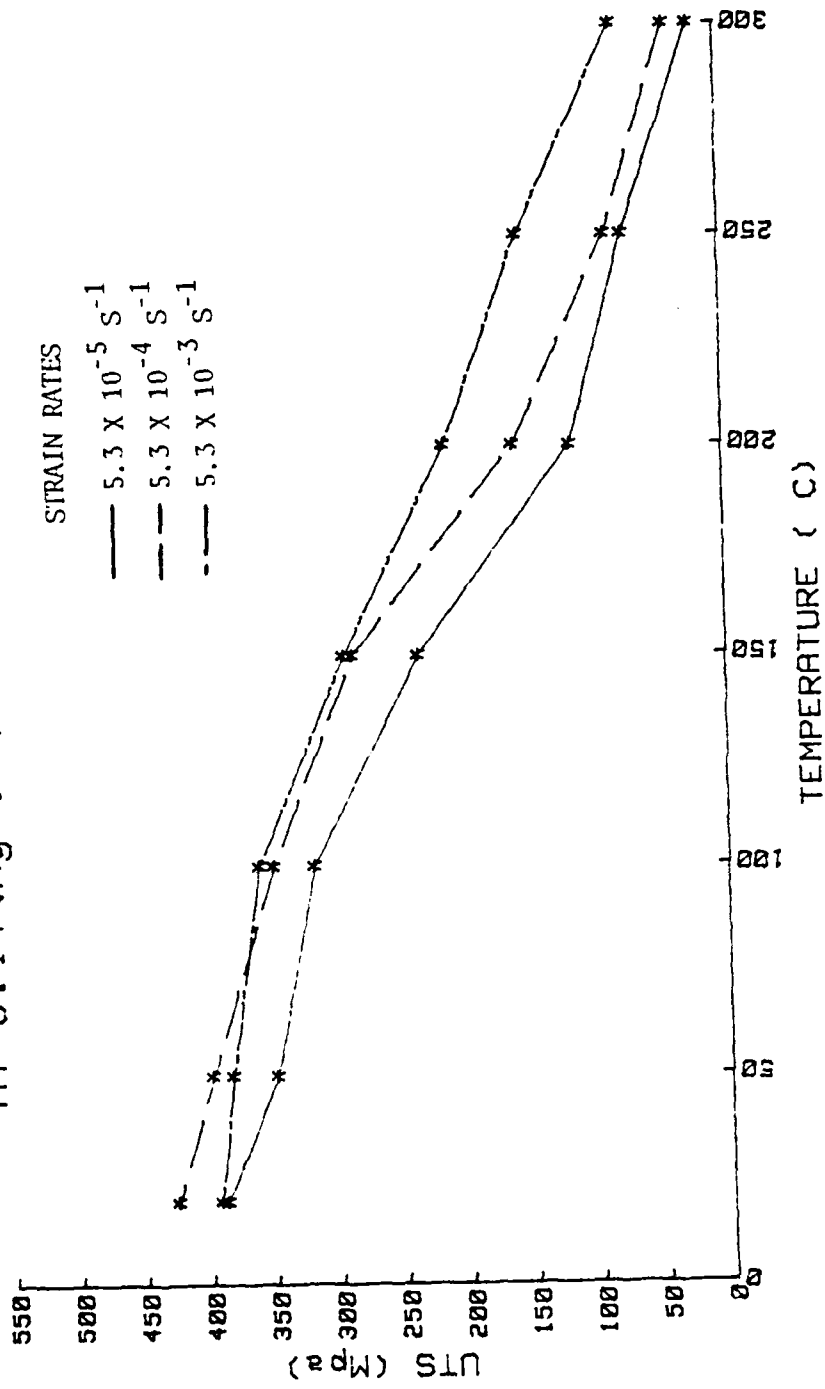
Al-8.14%Mg-.4%Cu - AS ROLLED



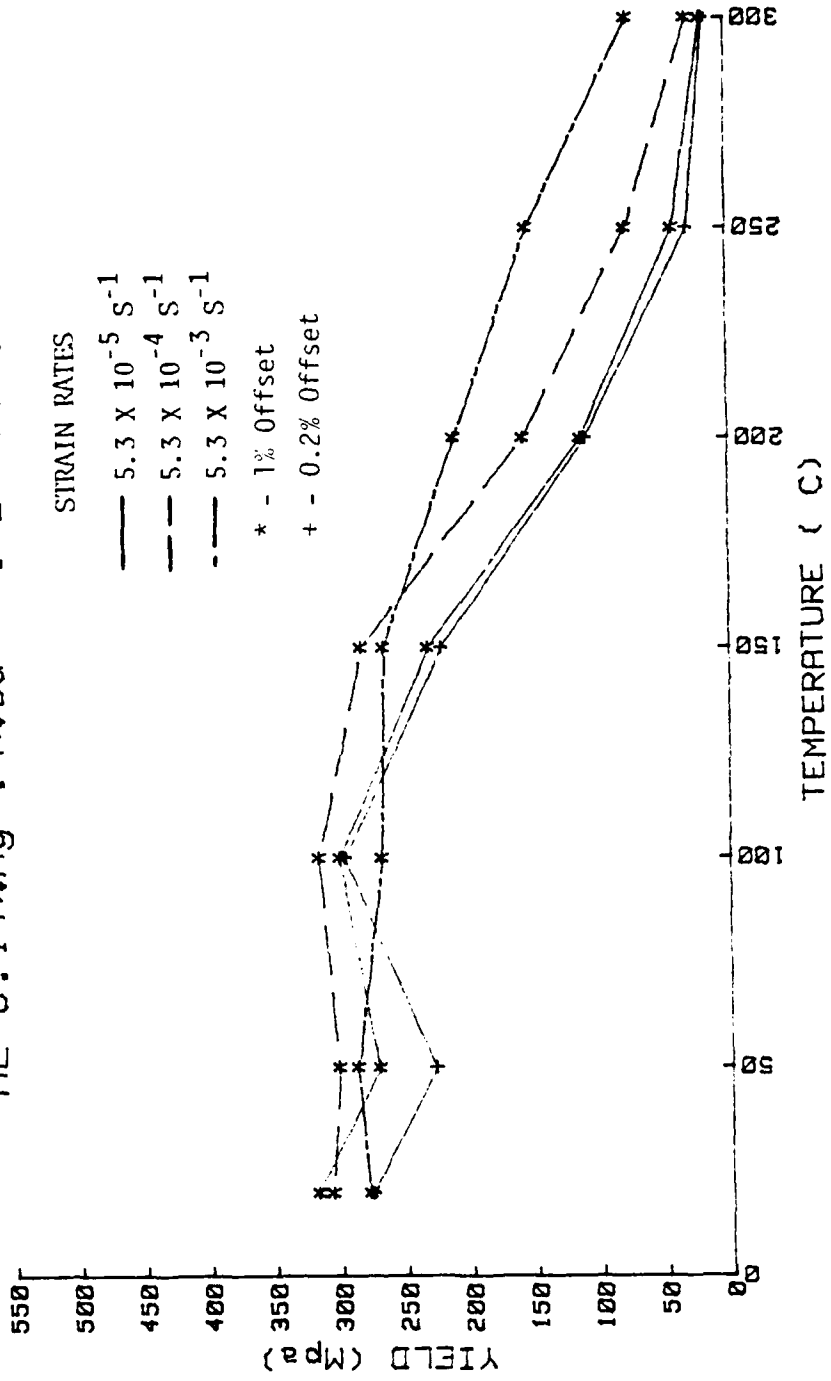
Al-8.14%Mg-0.4%Cu HS ROLLED



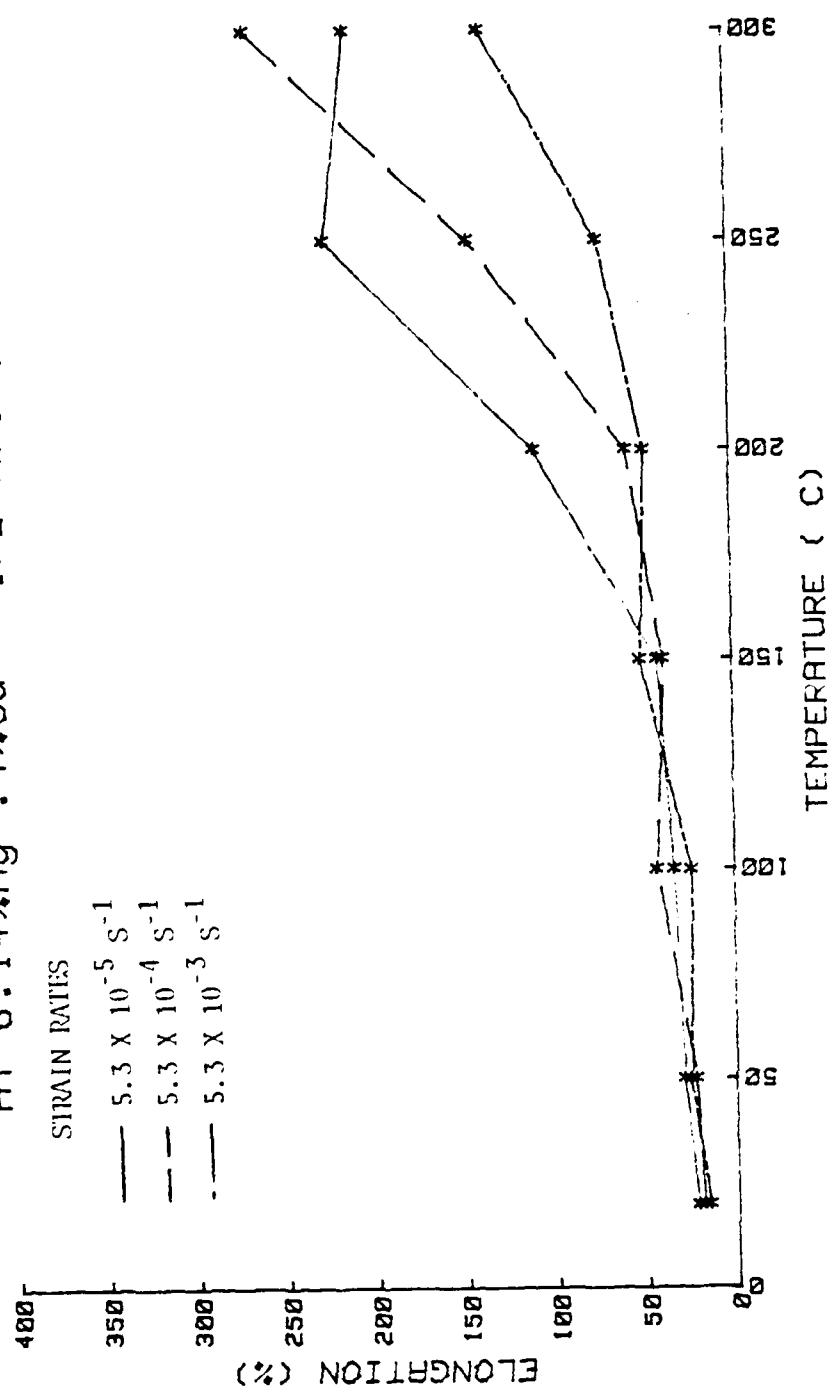
Al-8.14%Mg-.4%Cu - 1/2 Hr. @ 300 C



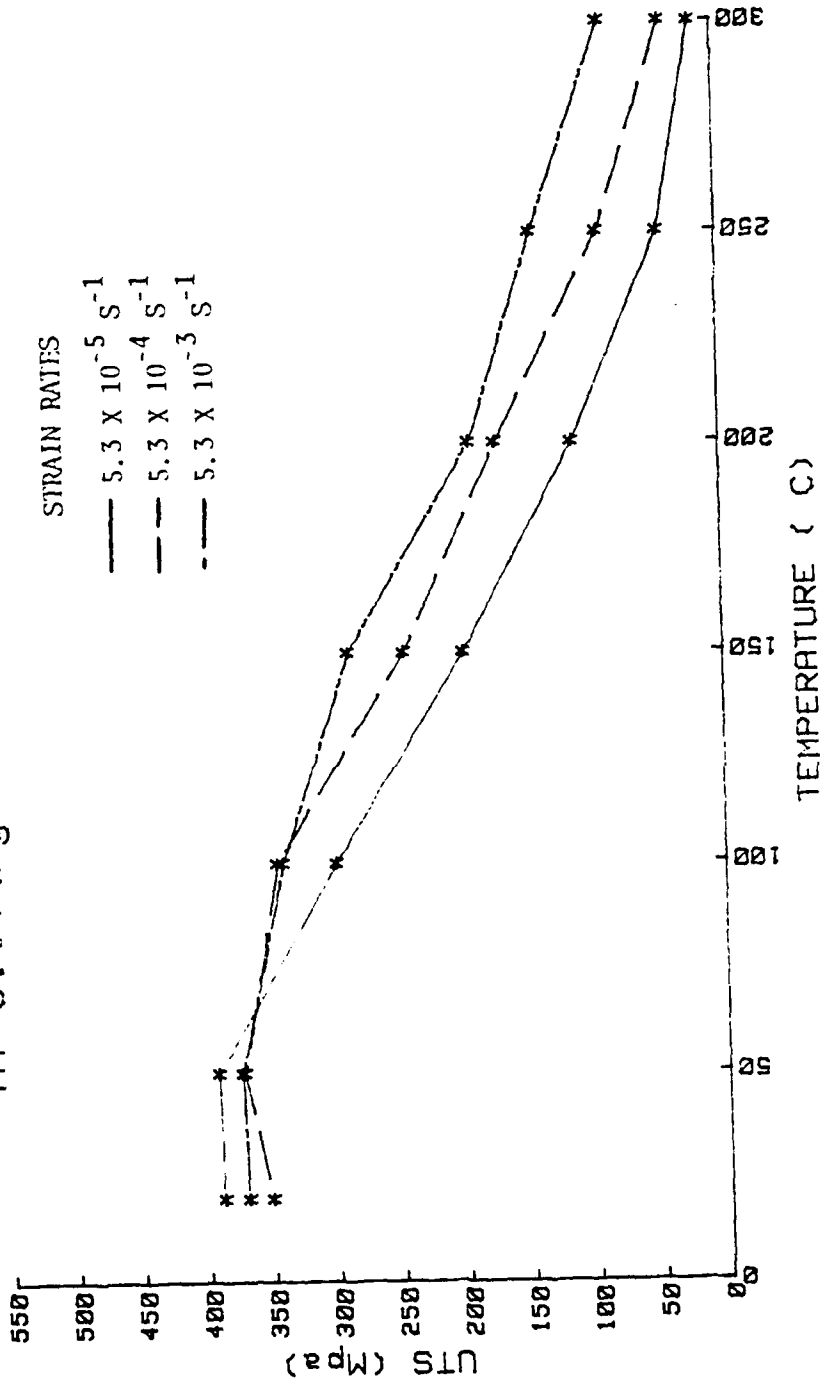
AL-8.14%Mg-.4%Cu - 1/2 Hr. @ 300 C



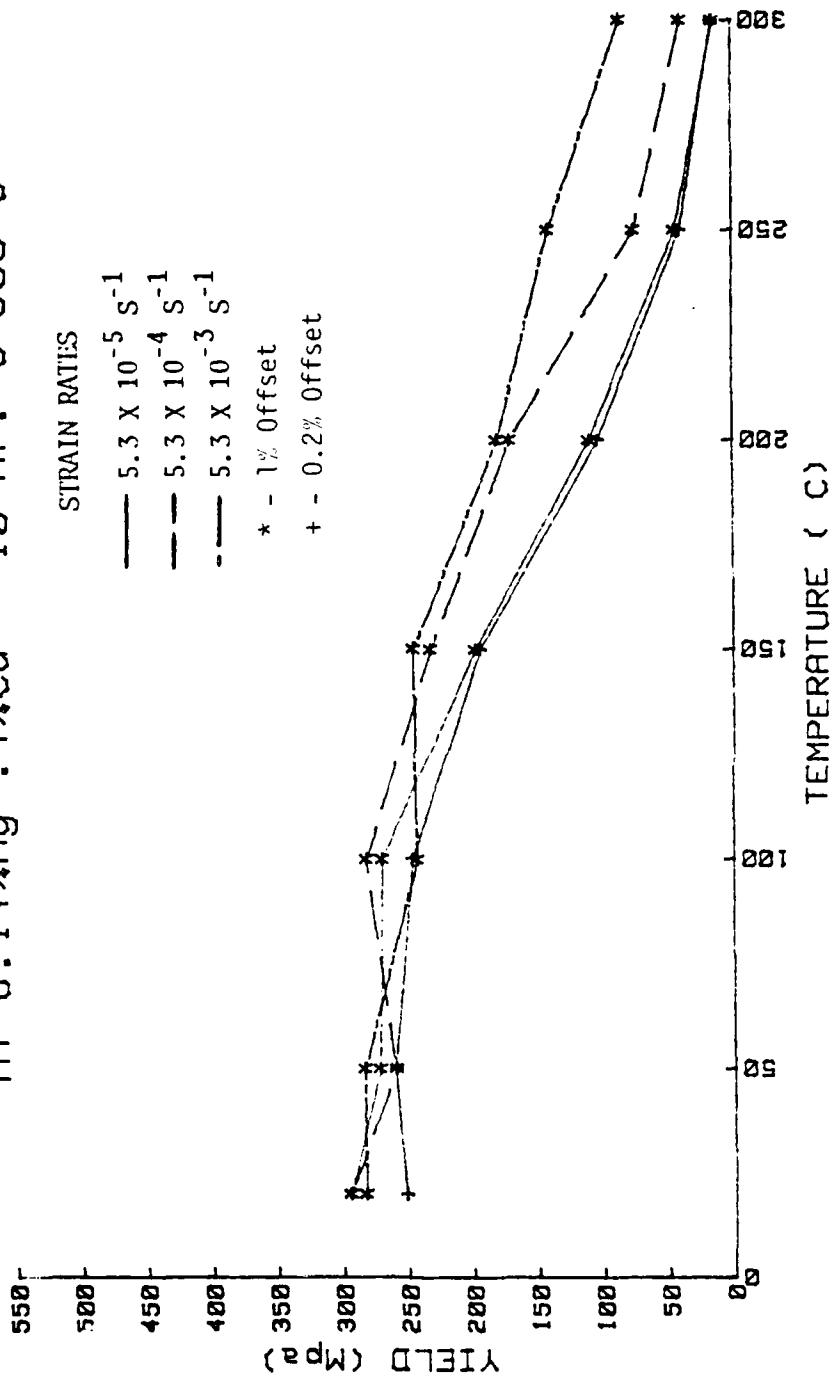
Al-8.14%Mg-.4%Cu - 1/2 Hr. @ 300 C



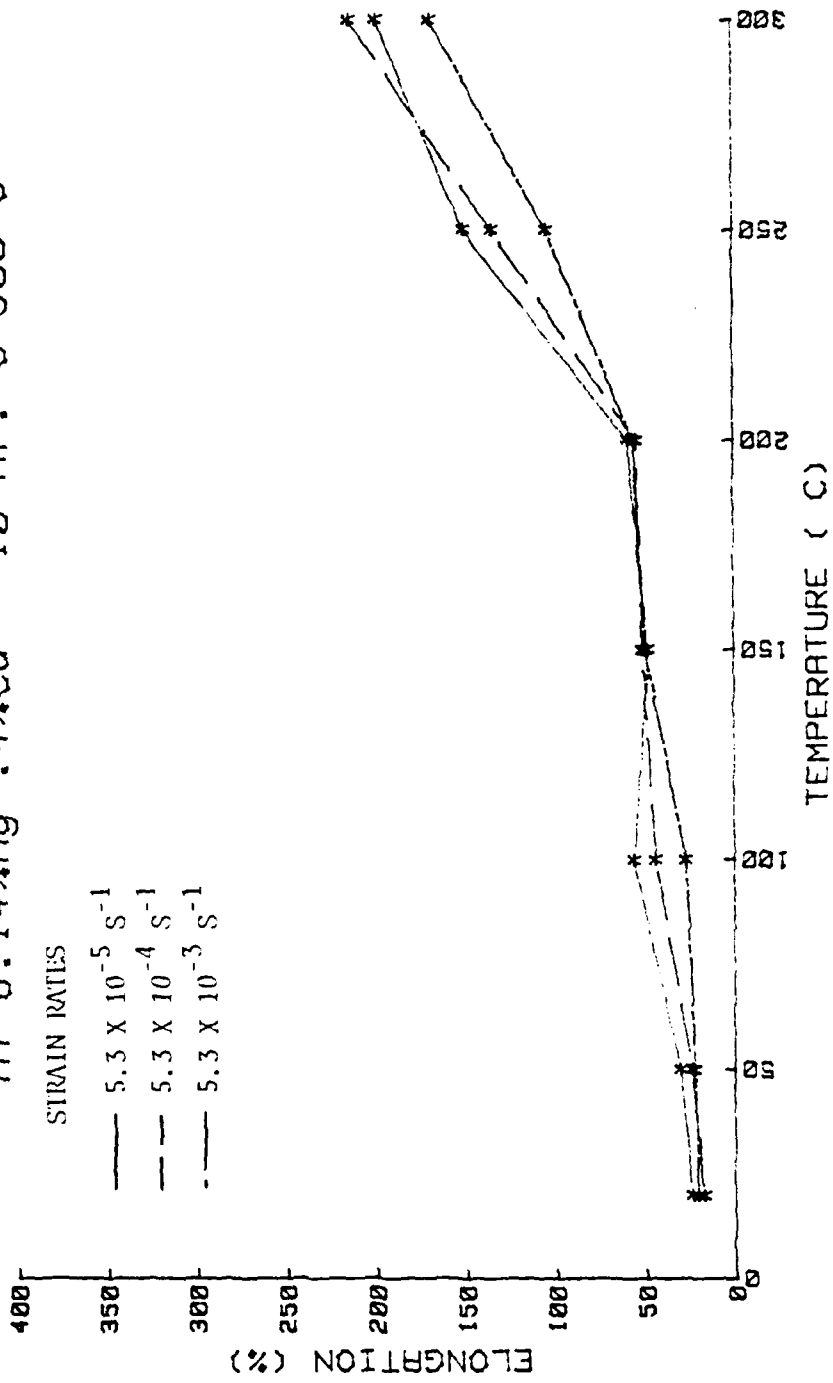
Al-8.14%Mg-4%Cu - 10 Hr. @ 300 C



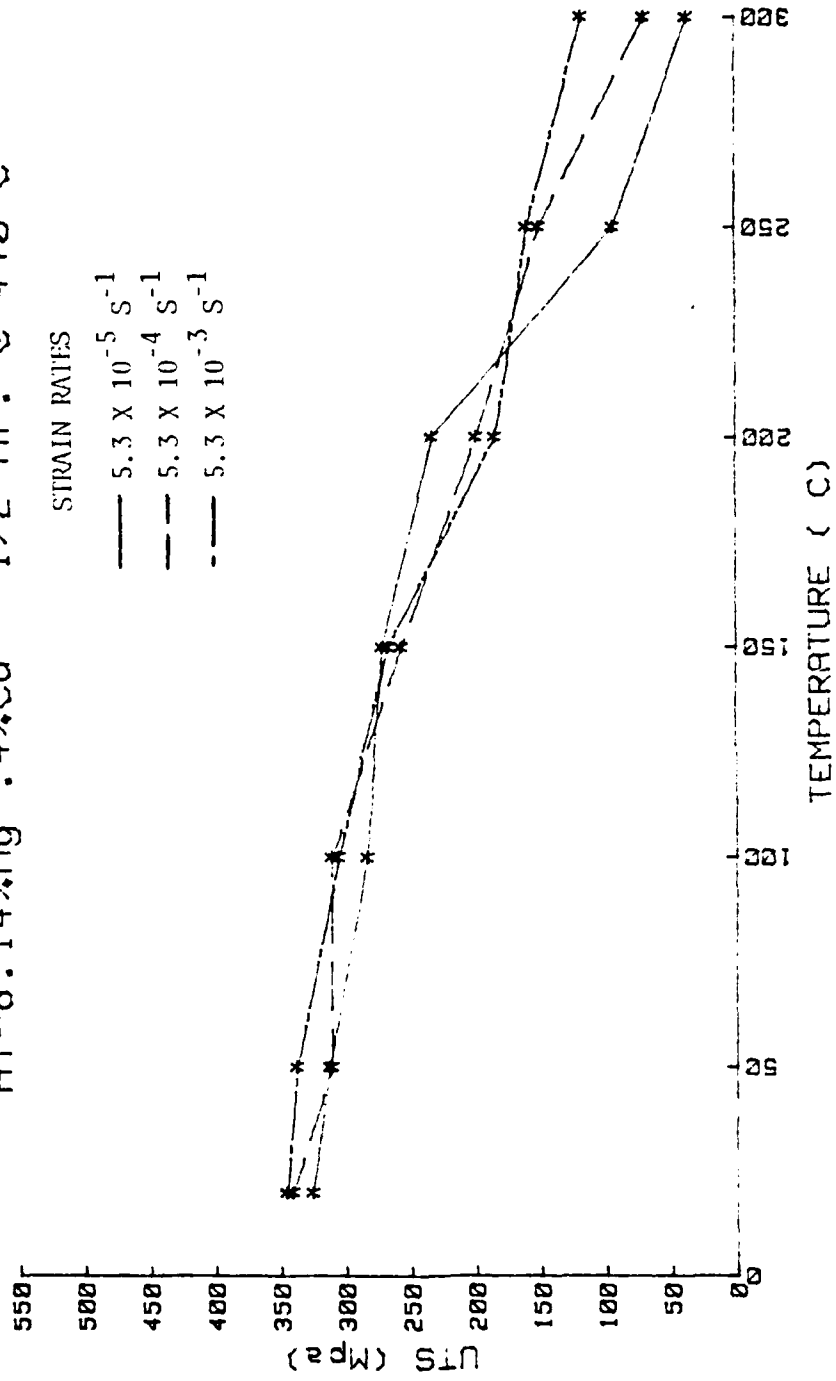
Al-8.14%Mg-.4%Cu - 10 Hr. @ 300 C



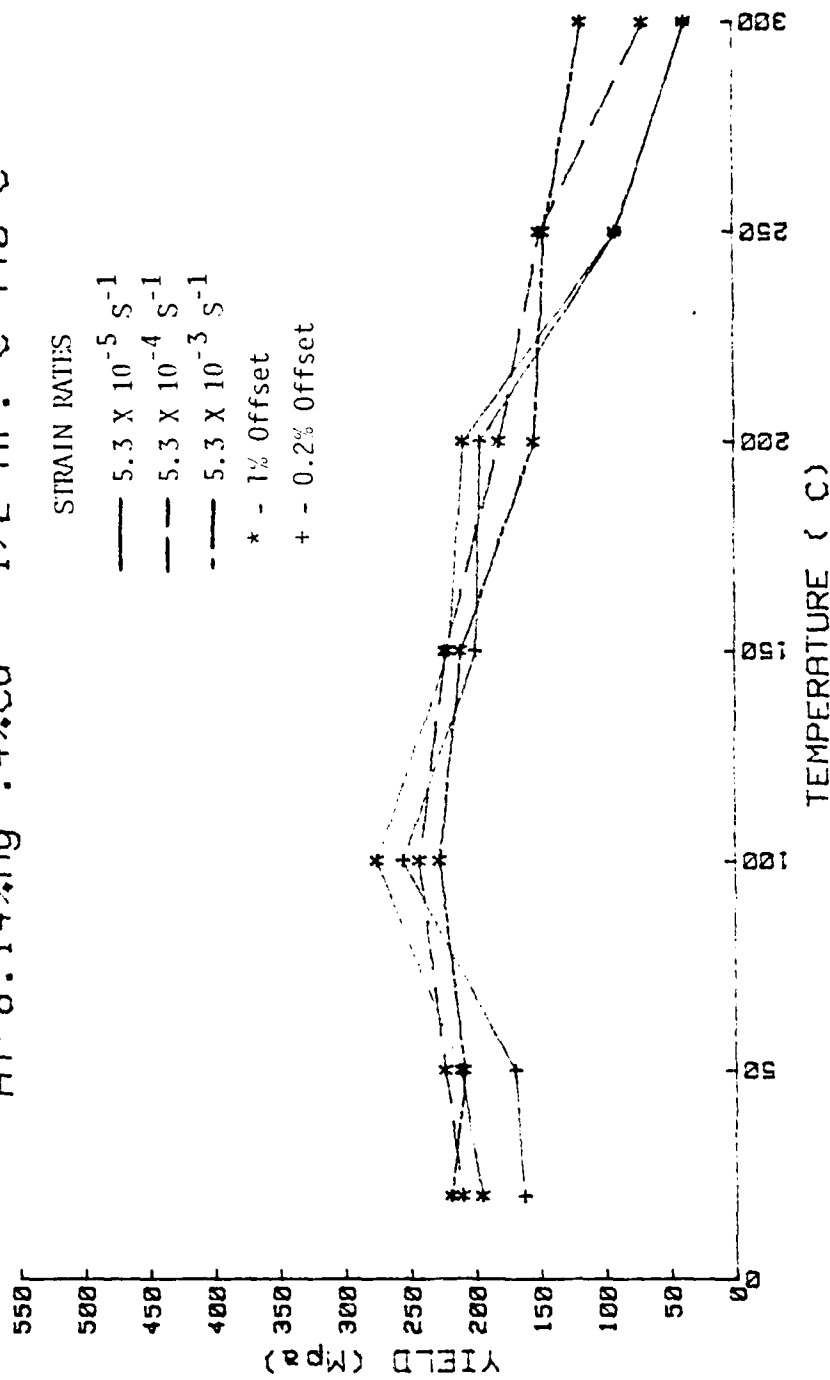
Al-8.14%Mg-.4%Cu - 10 Hr. @ 300 C



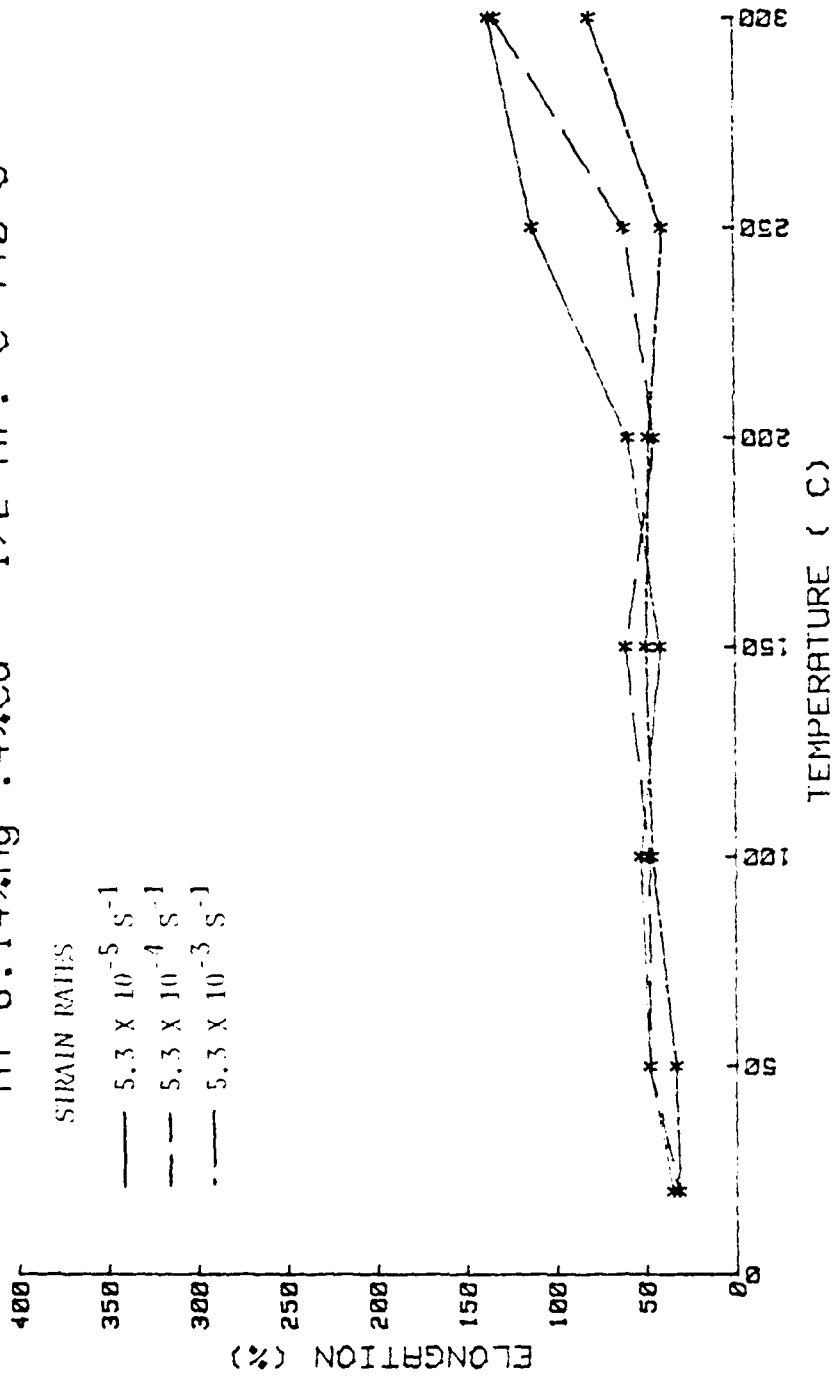
Al-8.14%Mg-.4%Cu - 1/2 Hr. @ 440 C



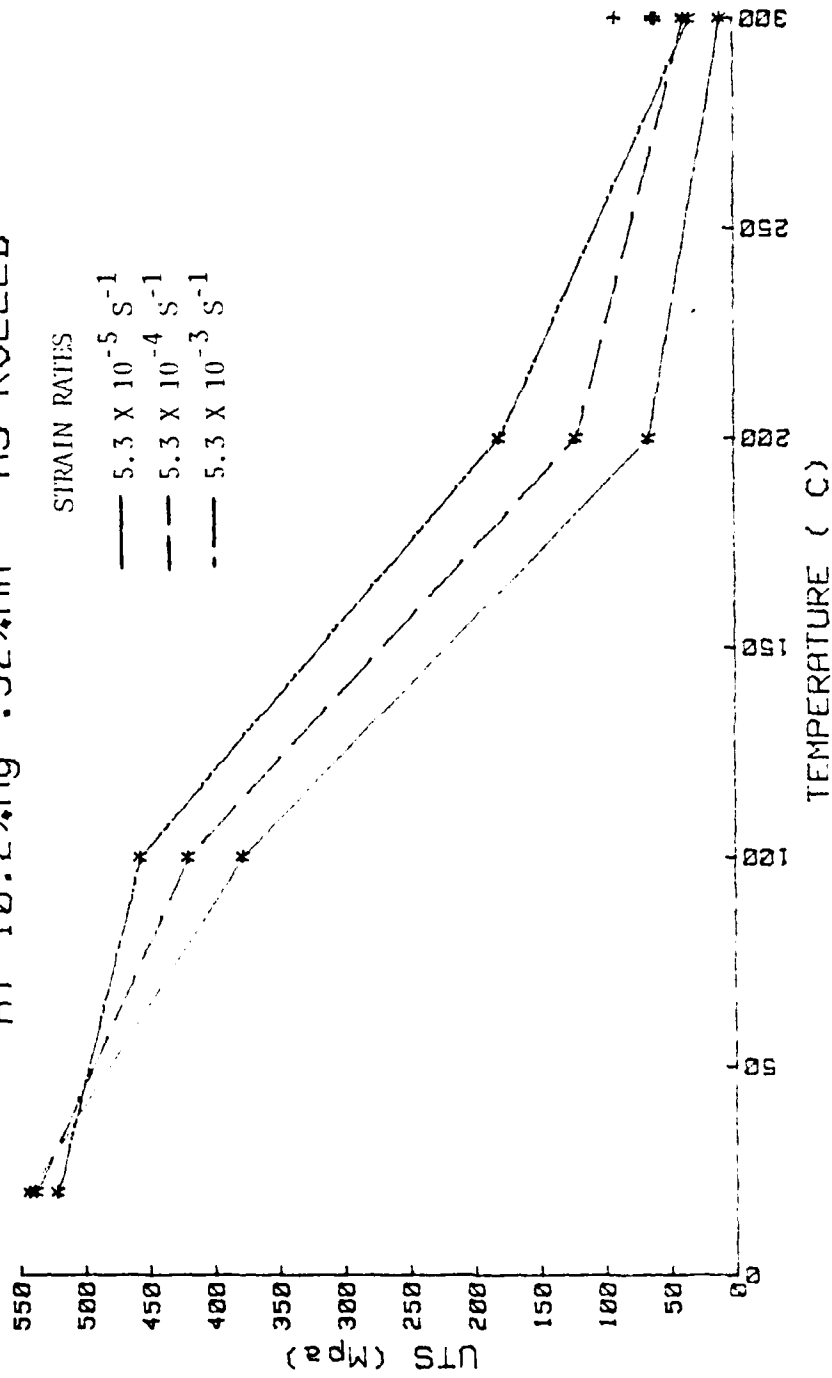
Al-8.14%Mg-.4%Cu - 1/2 Hr. @ 440 C



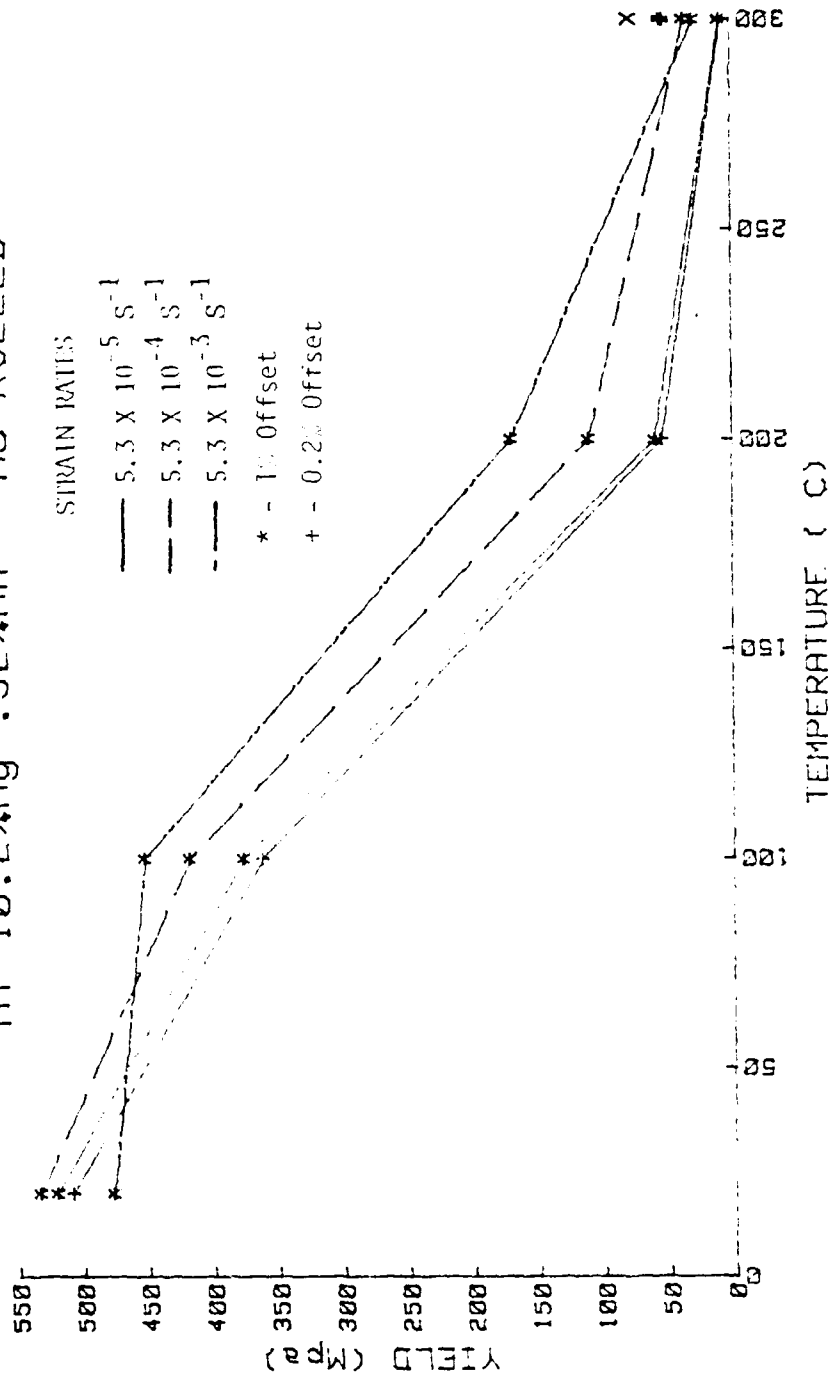
Al-8.14%Mg-0.4%Cu - 1/2 Hr. @ 440 C



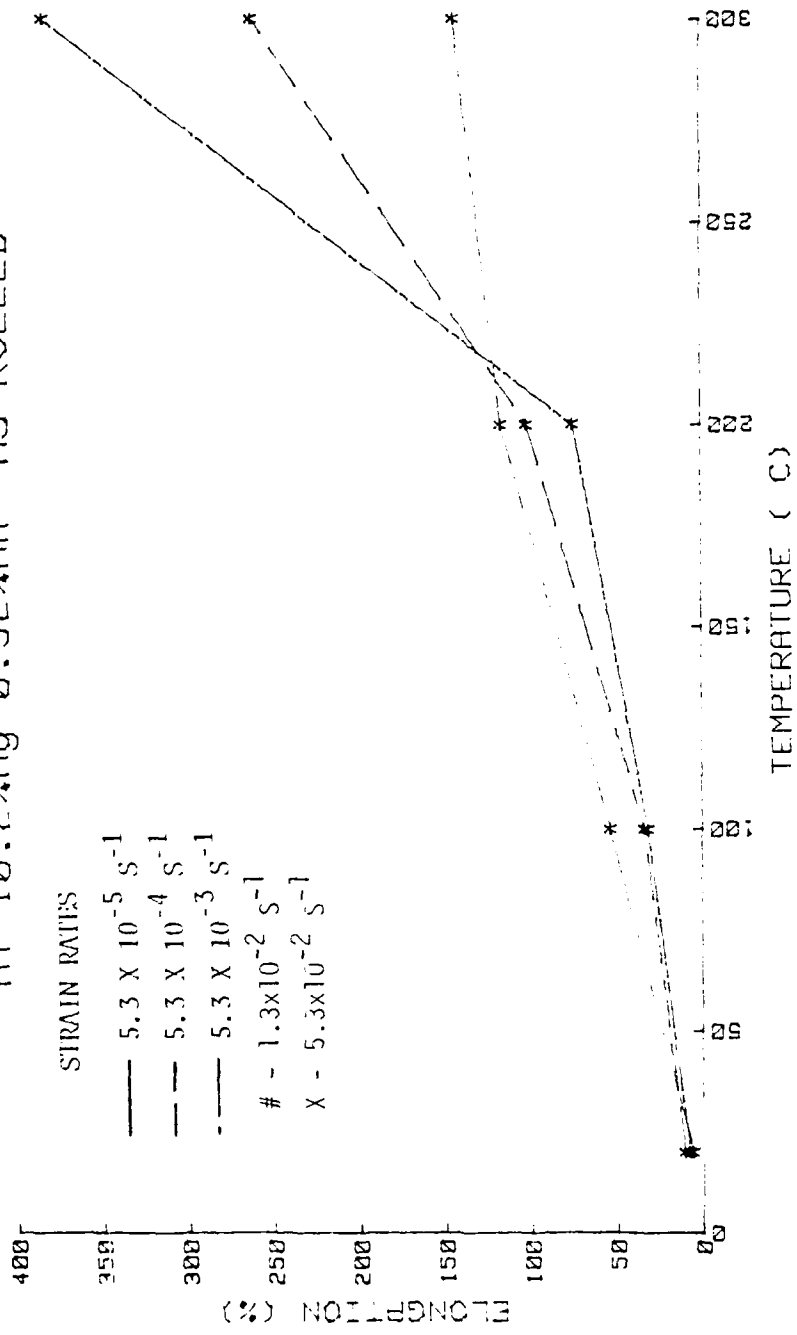
Al-10.2%Mg-.52%Mn - AS ROLLED



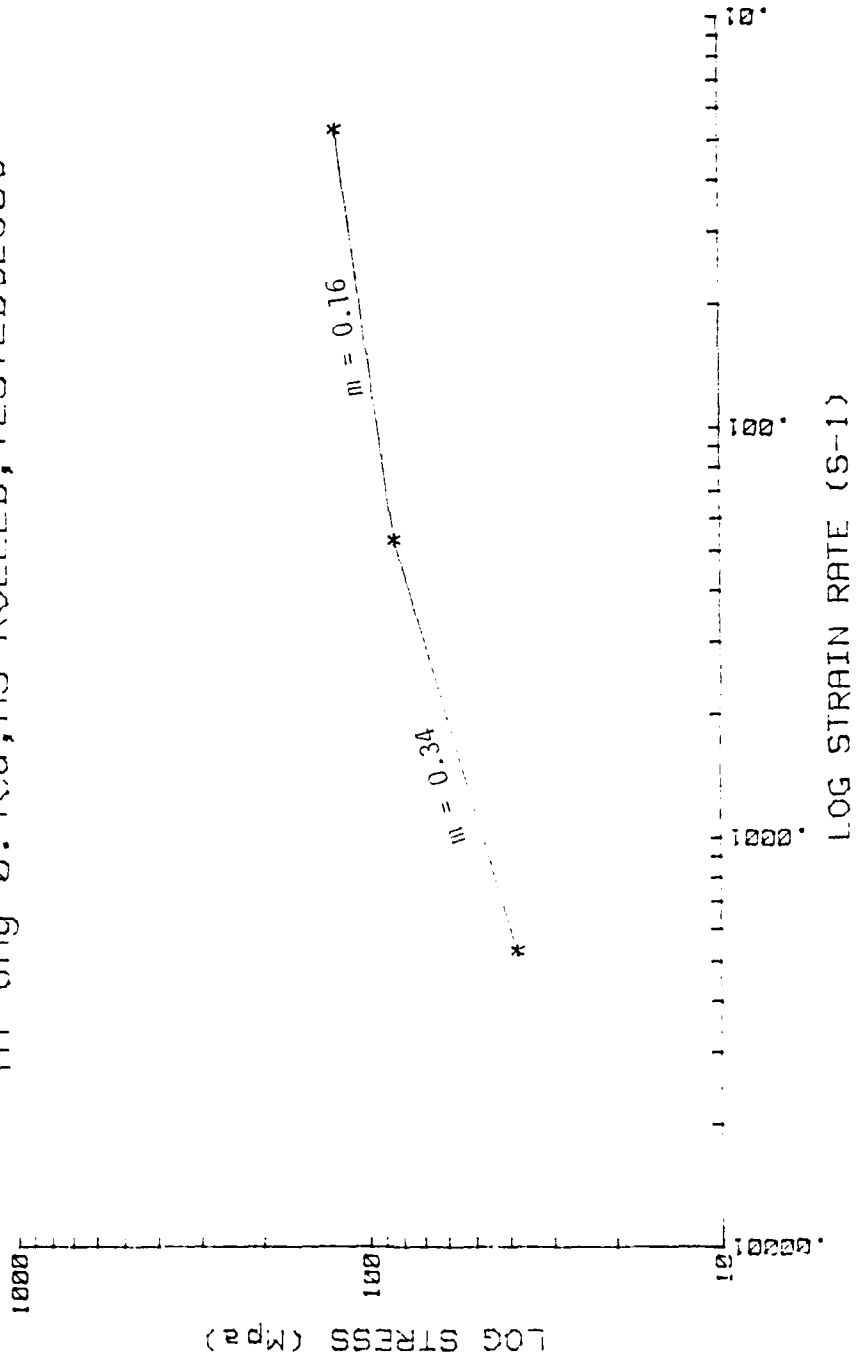
Al-10.2%Mg-.52%Mn - AS ROLLED



Al-10.2%Mg-0.52%Mn AS ROLLED

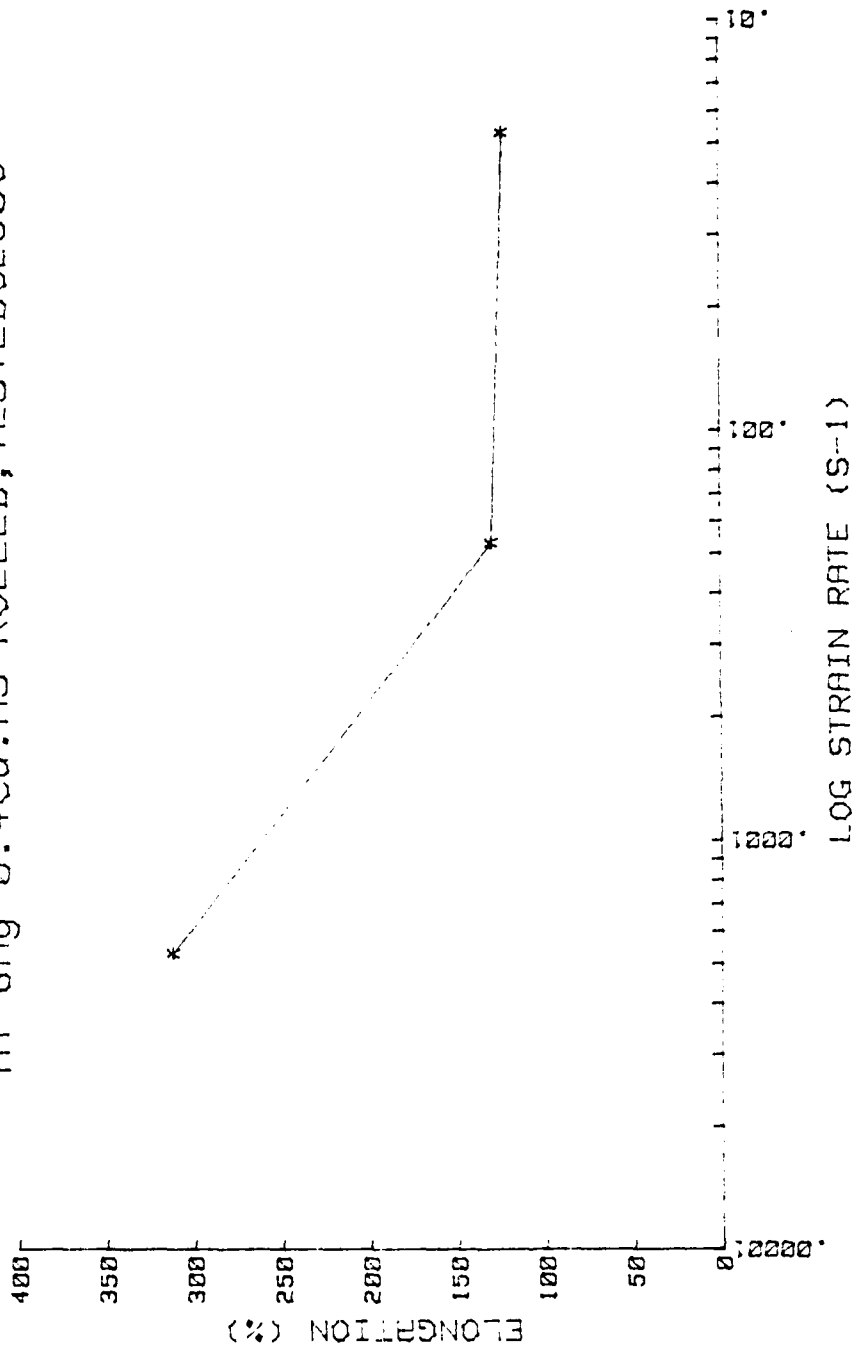


F11-8Mg-0.4Cu; NS ROLLED; TESTED @ 250C

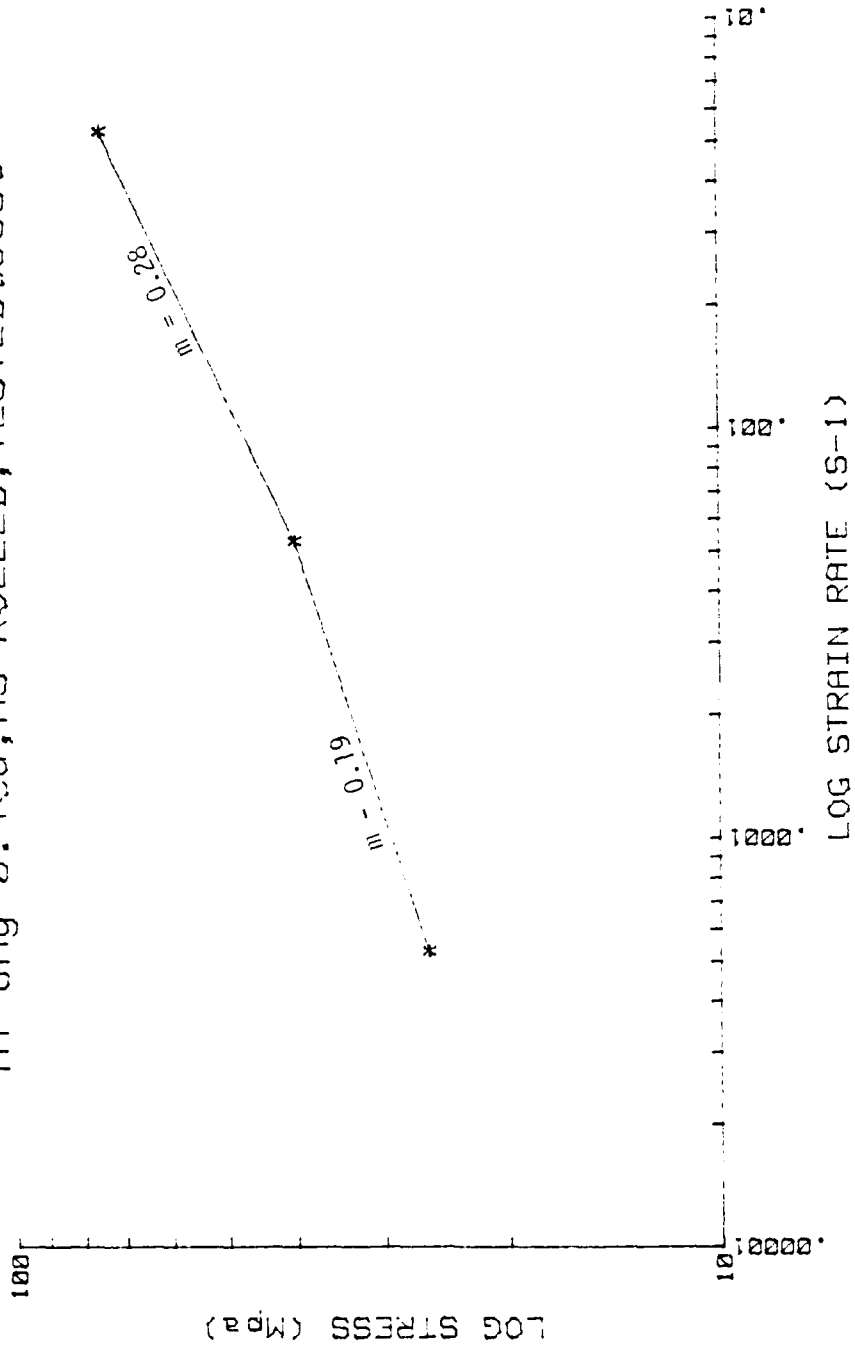


APPENDIX C

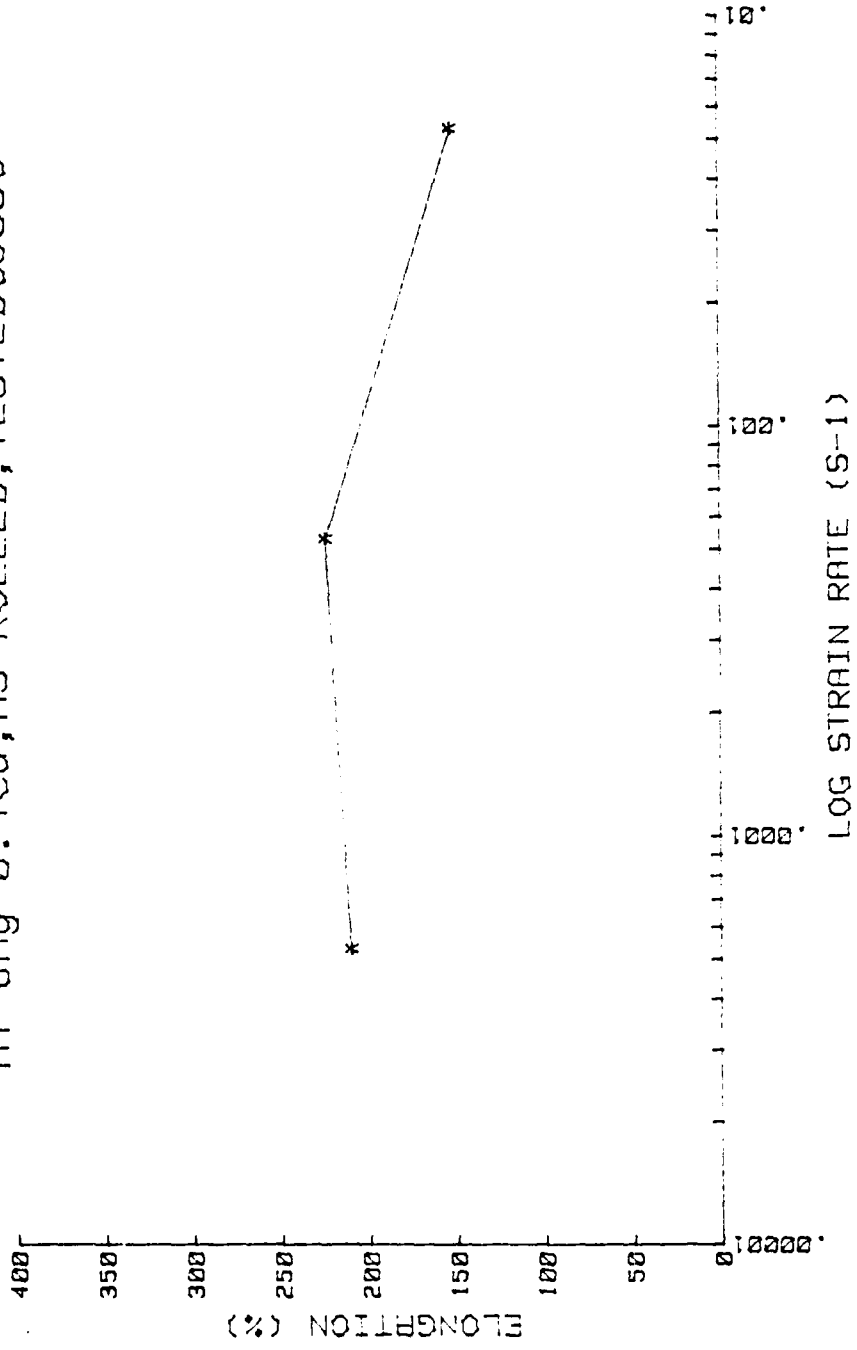
Al-8Mg-0.4Cu:AS ROLLED; TESTED @ 250C



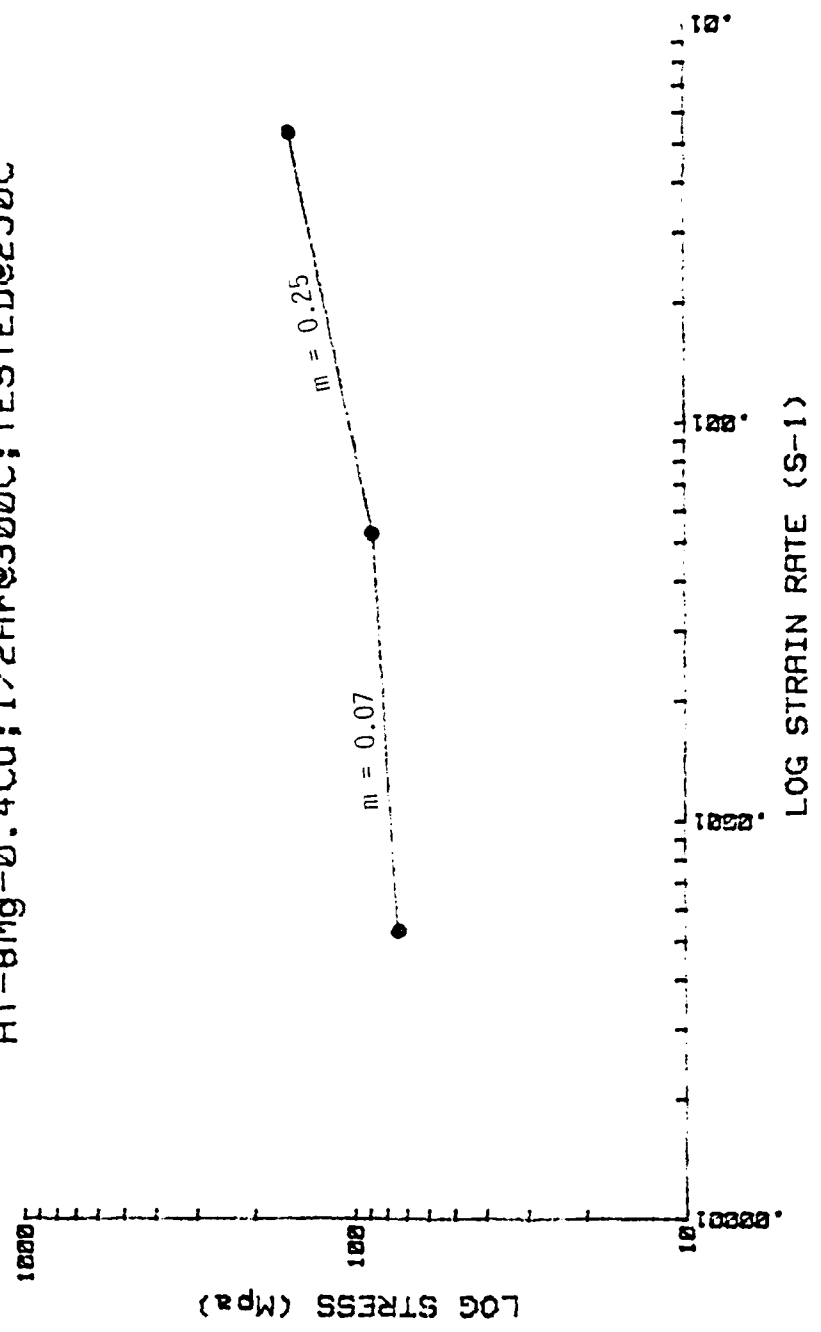
Al-8Mg-0.4Cu; AS ROLLED; TESTED @ 300C



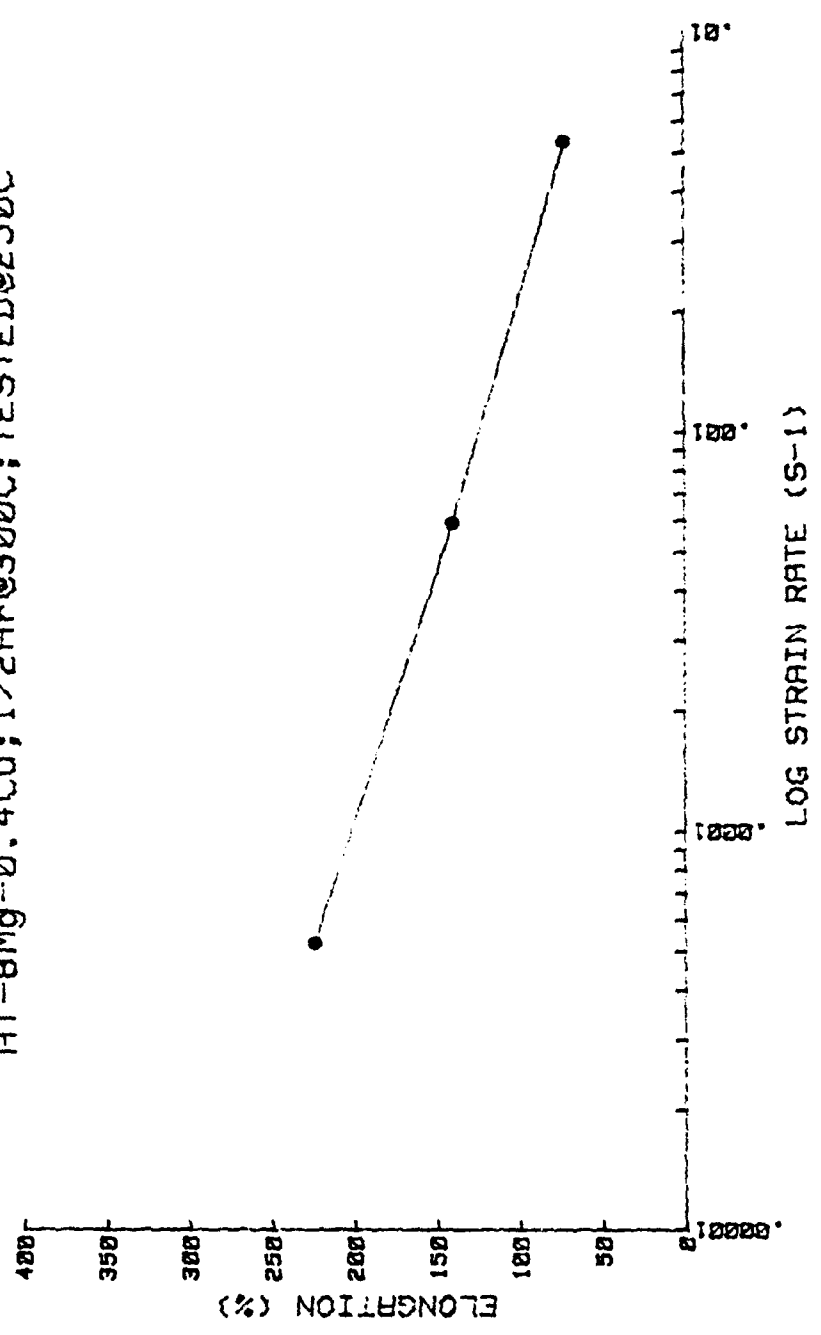
Al-8Mg-0.4Cu; AS ROLLED; TESTED @ 300C



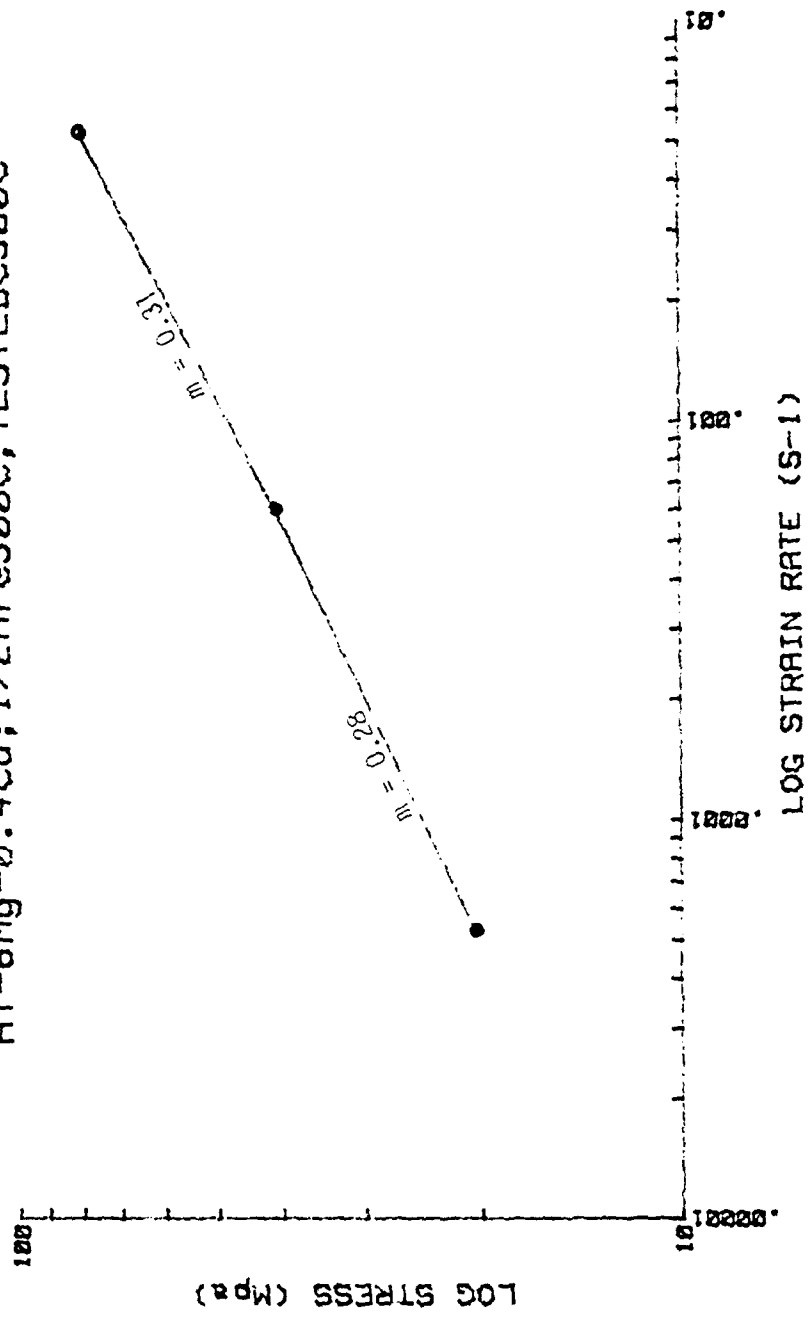
Al-8Mg-0.4Cu; 1/2HR@300C; TESTED@250C



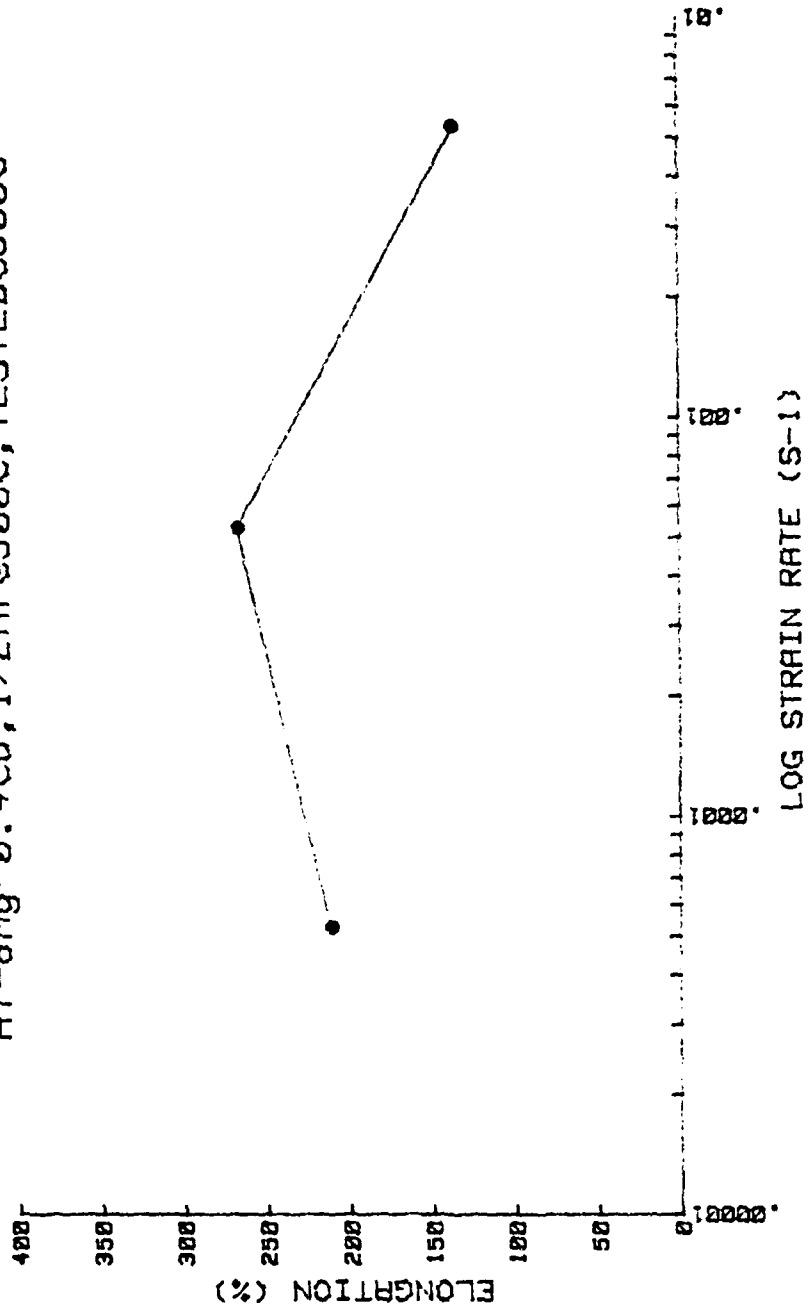
Al-8Mg-0.4Cu; 1/2Hr@300C; TESTED@250C



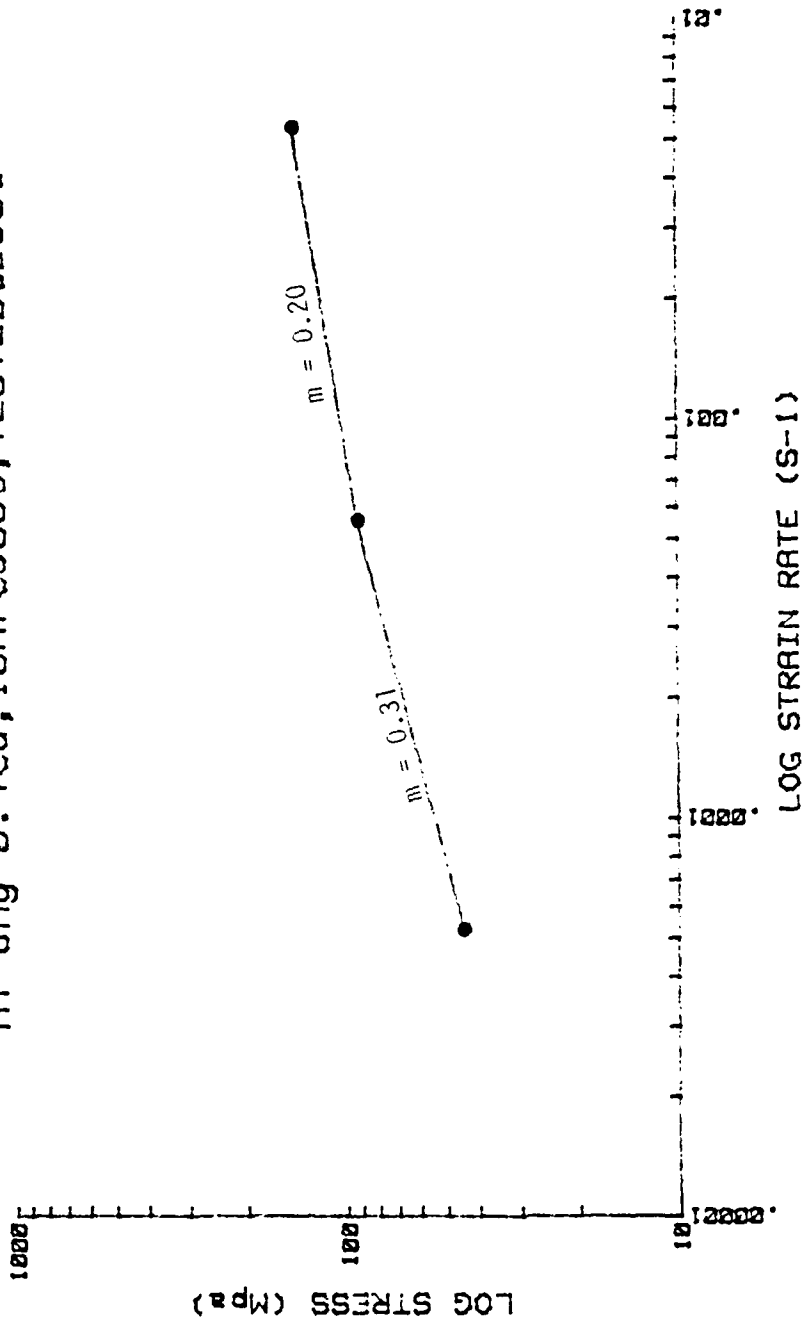
Al-8Mg-0.4Cu; 1/2Hr@300C; TESTED@300C



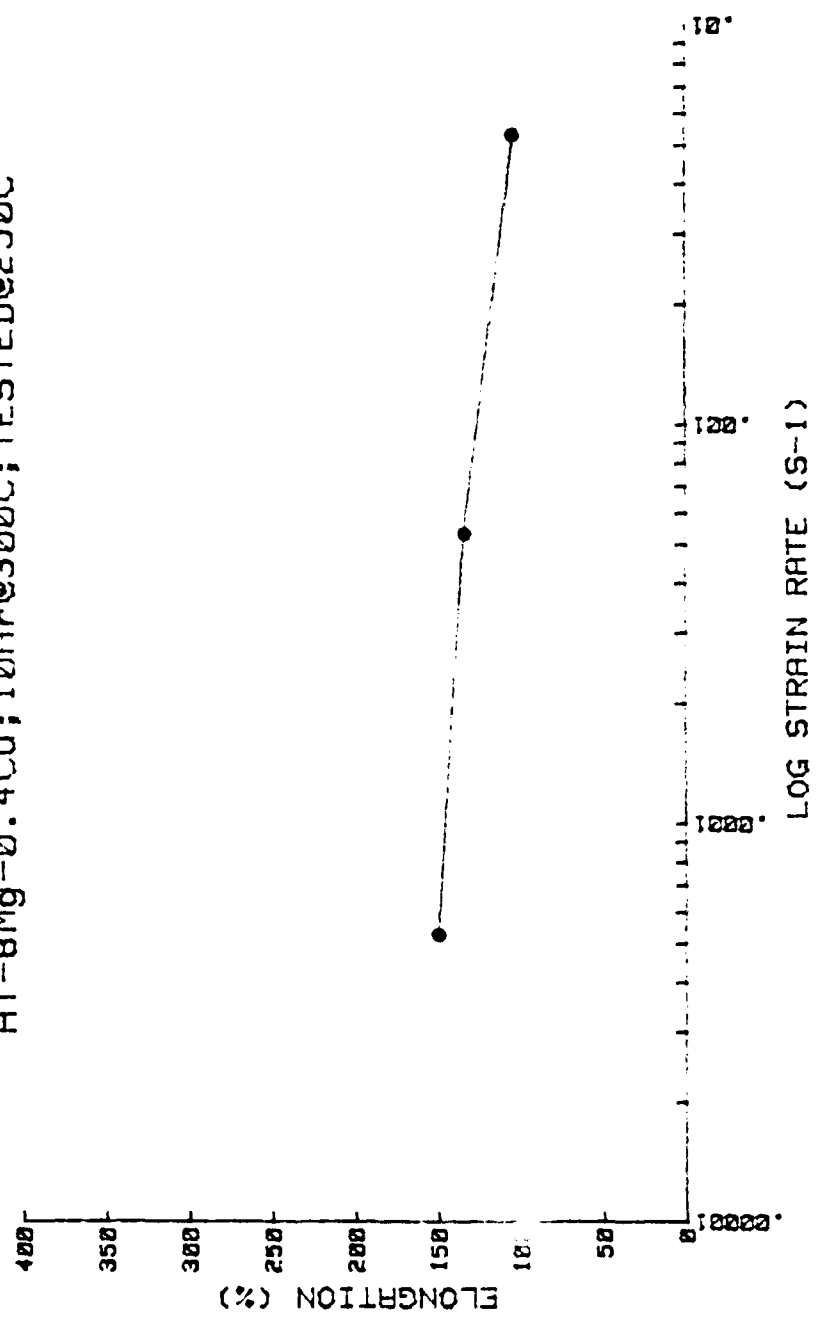
Al-8Mg-0.4Cu; 1/2Hr@300C; TESTED@300C



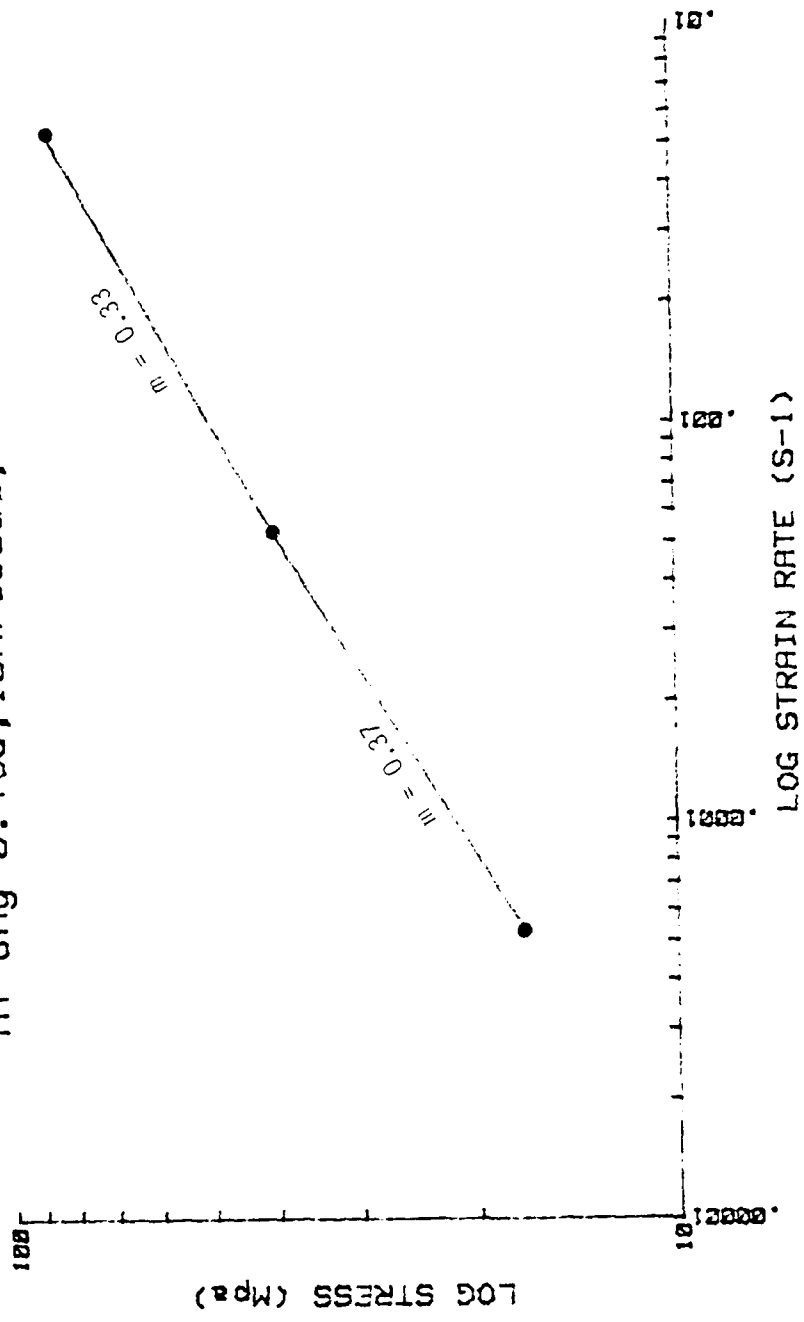
Al-8Mg-0.4Cu; 10Hr@300C; TESTED@250C



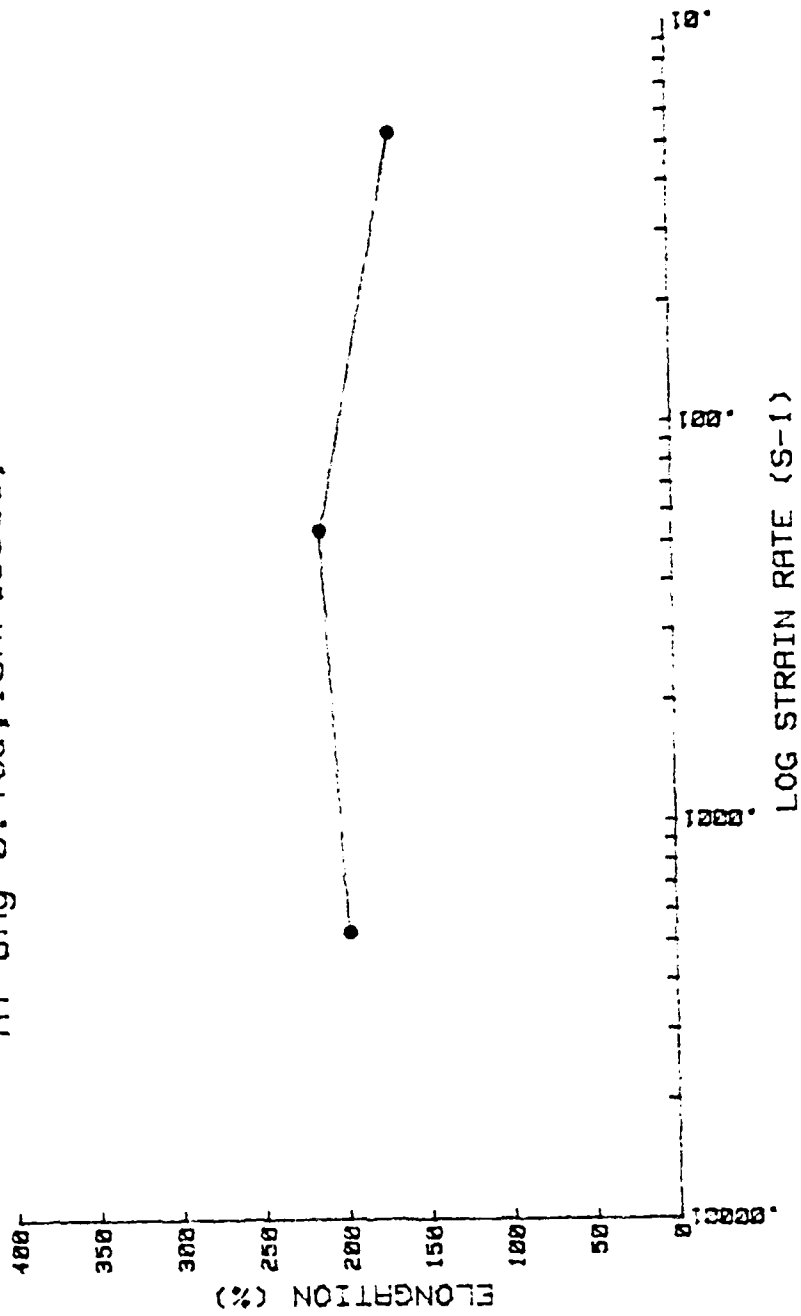
Al-8Mg-0.4Cu; 10Hr@300C; TESTED@250C



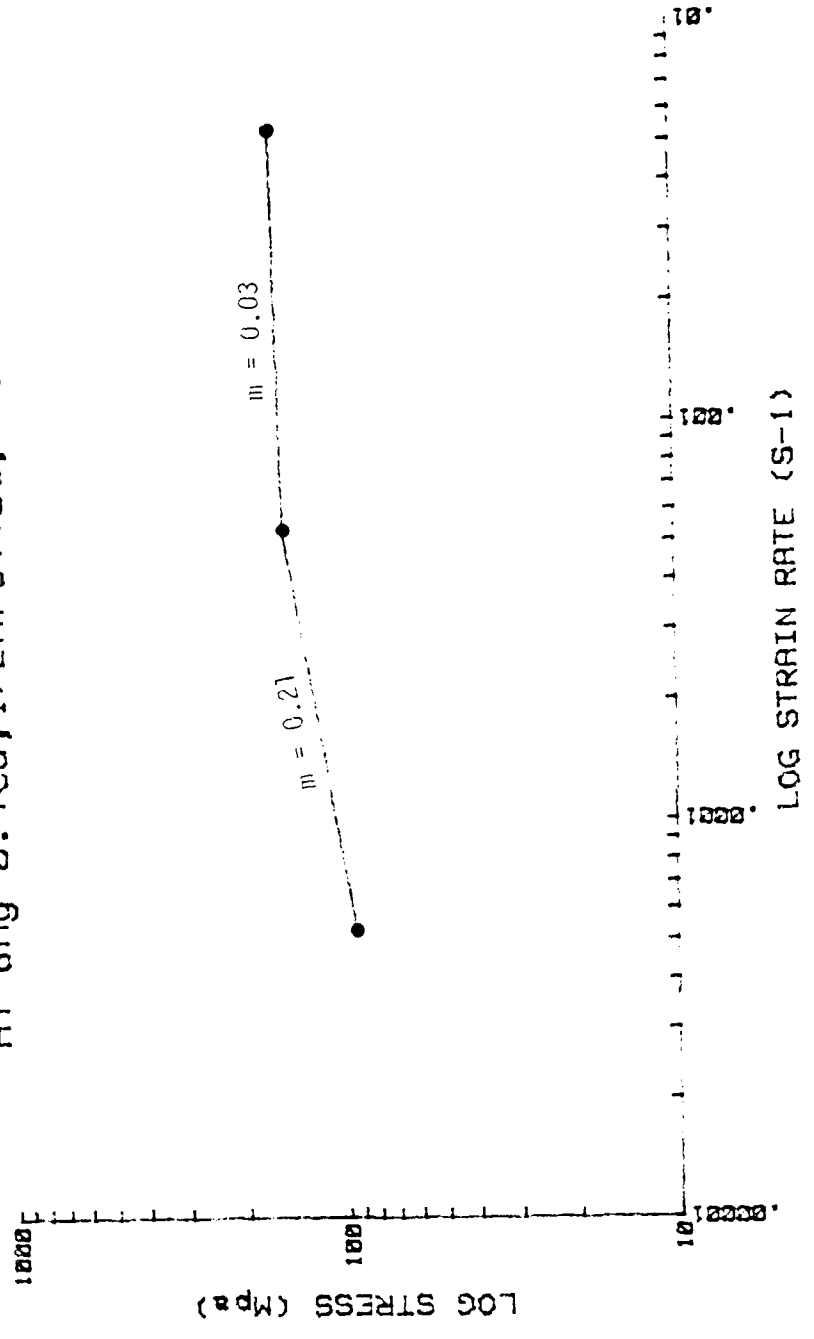
Al-8Mg-0.4Cu; 10Hr@300C; TESTED@300C



Al-8Mg-0.4Cu; 10Hr@300C; TESTED@300C



Al-8Mg-0.4Cu; 1/2Hr@440C; TESTED@250C



AD-A143 184

SUPERPLASTICITY IN THERMO-MECHANICALLY PROCESSED HIGH
MAGNESIUM ALUMINUM-MAGNESIUM ALLOYS(U) NAVAL
POSTGRADUATE SCHOOL MONTEREY CA J J BECKER MAR 84

212

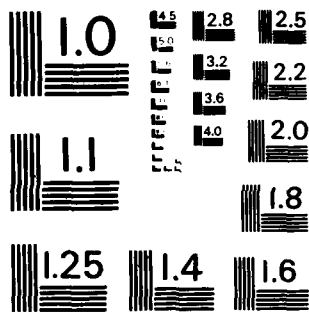
UNCLASSIFIED

F/G 11/8

NL

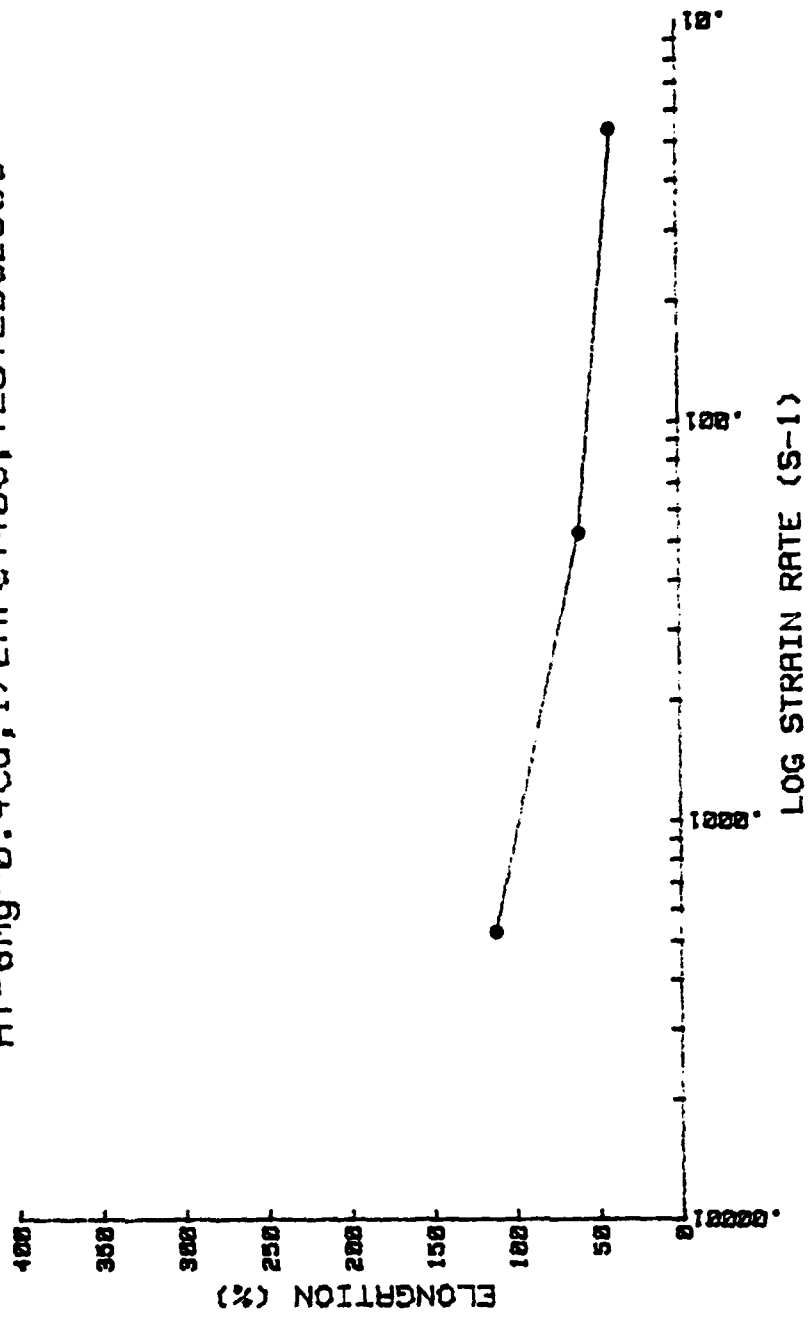


END
SERIALIZED
8 24
131

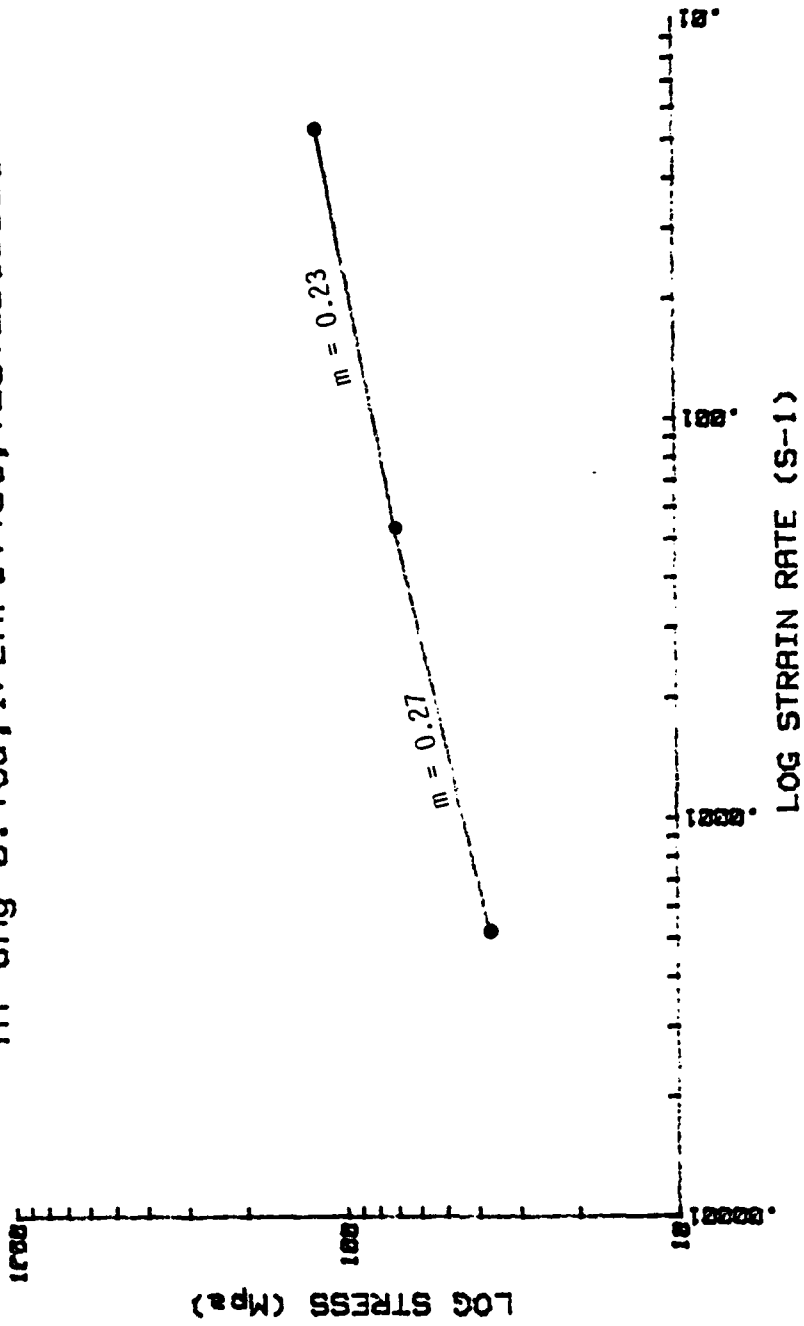


MICROCOPY RESOLUTION TEST CHART
NATIONAL BUREAU OF STANDARDS-1963-A

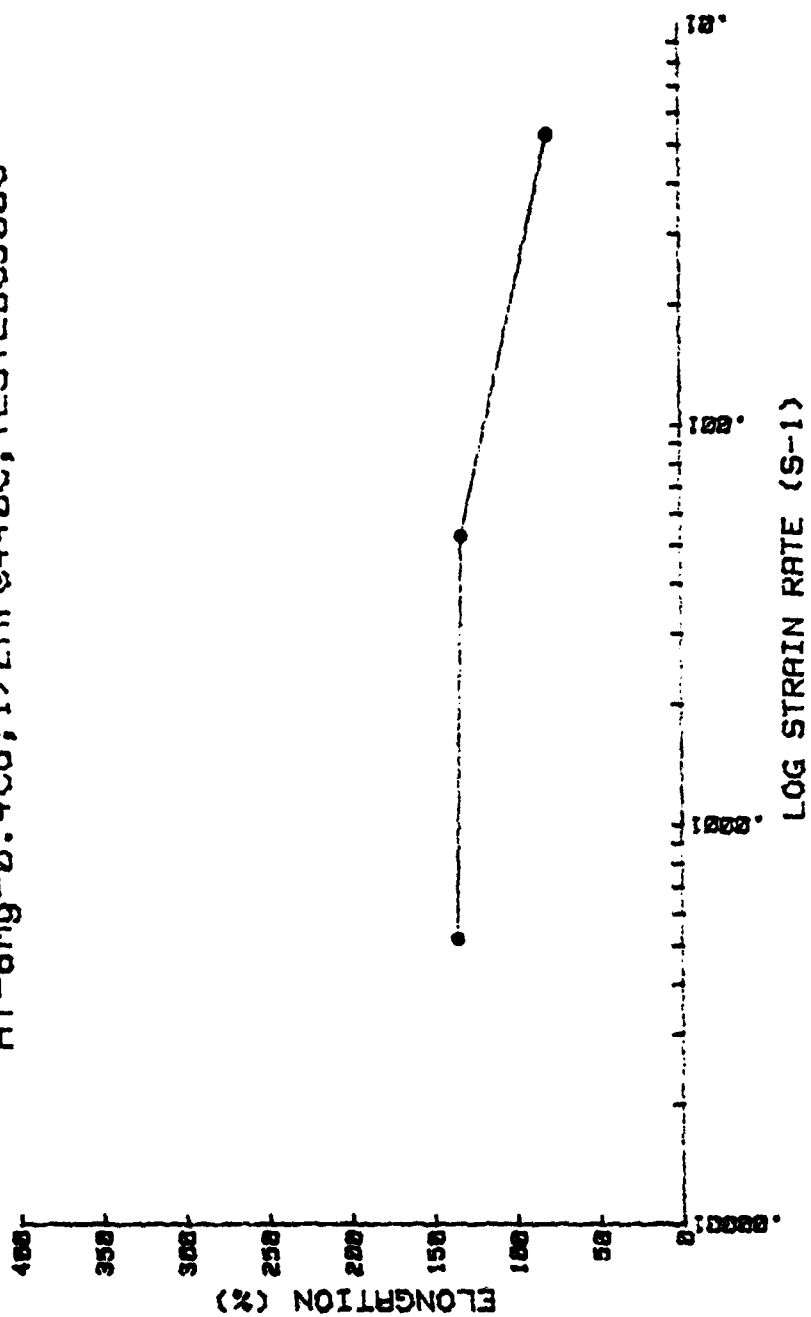
A1-8Mg-0.4Cu; 1/2Hr@440C; TESTED@250C



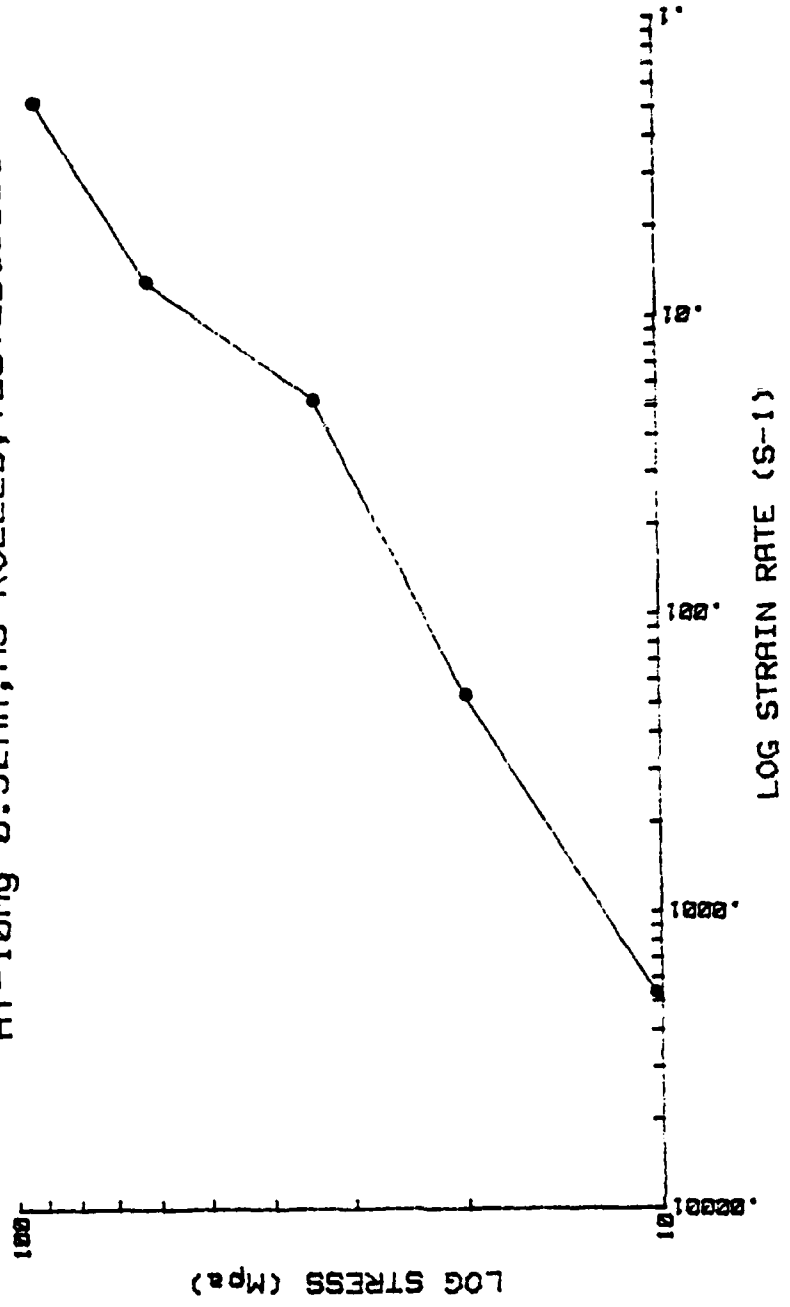
A1-8Mg-0.4Cu; 1/2Hr@440C; TESTED@300C



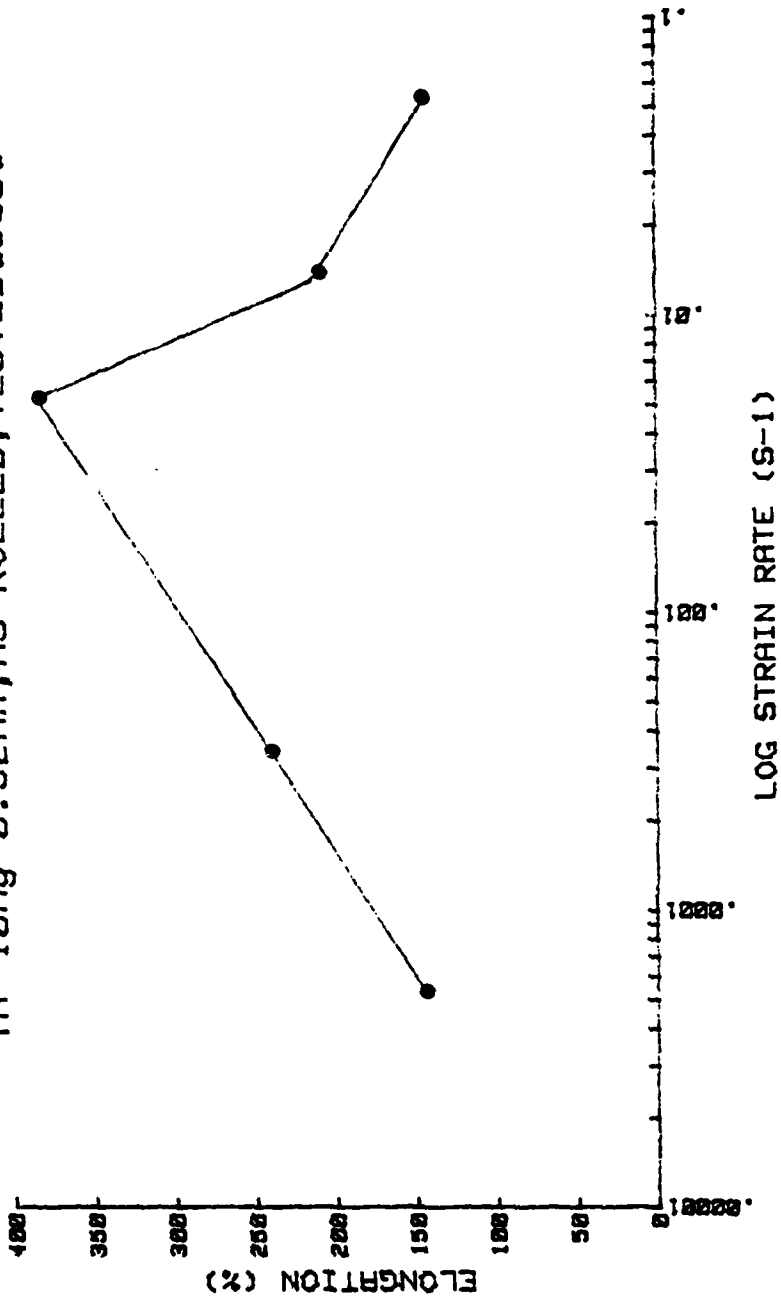
Al-8Mg-0.4Cu; 1/2Hr@440C; TESTED@300C



A1-10Mg-0.52Mn; AS ROLLED; TESTED @ 300C



AI-10Mg-0.52Mn; AS ROLLED; TESTED @ 300°C



INITIAL DISTRIBUTION LIST

	No. Copies
1. Defense Technical Information Center Cameron Station Alexandria, Virginia 22314	2
2. Library, Code 0142 Naval Postgraduate School Monterey, California 93943	2
3. Department Chairman, Code 69Mx Department of Mechanical Engineering Naval Postgraduate School Monterey, California 93943	1
4. Professor T. R. McNelley, Code 69Mc Department of Mechanical Engineering Naval Postgraduate School Monterey, California 93943	5
5. Mr. Richard Schmidt, Code AIR 320A Naval Air Systems Command Naval Air Systems Command Headquarters Washington, DC 20361	1
6. LCDR John J. Becker Supervisor of Shipbuilding, Conversion & Repair, USN Groton, Connecticut 06340	3